

AD-A054 290

SUNTECH INC MARCUS HOOK PA

F/G 11/8

INFRARED SPECTRA OF FLUID FILMS UNDER CONDITIONS OF INCIPIENT B--ETC(U)

DEC 77 J L LAUER

F49620-76-C-0042

UNCLASSIFIED

AFOSR-TR-78-0190

NL

1 of 2

AD
A054290



FOR FURTHER TRAINING

AD A 054290

INFRARED SPECTRA OF FLUID FILMS UNDER CONDITIONS OF INCIPIENT BEARING FAILURE

FINAL REPORT ON

F44620-74-C-0038 and F49620-76-C-0042

to the Air Force Office of Scientific Research

by

JAMES L. LAUER

Suntech, Inc., Subsidiary of Sun Company
(previously Sun Oil Company)
P.O.B. 1135, Marcus Hook, Pennsylvania, 19061

AD No. _____
DDC FILE COPY

DDC
MAY 22 1978

December 22, 1977

Approved for public release;
distribution unlimited.

UNCLASSIFIED

SECURITY CLASSIFICATION OF THIS PAGE (When Data Entered)

19 REPORT DOCUMENTATION PAGE		READ INSTRUCTIONS BEFORE COMPLETING FORM	
1. REPORT NUMBER 18 AFOSR-TR-78-0190	2. GOVT ACCESSION NO.	3. RECIPIENT'S CATALOG NUMBER 9	
4. TITLE (and Subtitle) INFRARED SPECTRA OF FLUID FILMS UNDER CONDITIONS OF INCIPIENT BEARING FAILURE		5. TYPE OF REPORT & PERIOD COVERED Final rept	
6. PERFORMING ORG. REPORT NUMBER		7. AUTHOR(s) James L. Lauer	
8. CONTRACT OR GRANT NUMBER(s) F49620-76-C-0042 F44620-74-C-0035		9. PERFORMING ORGANIZATION NAME AND ADDRESS Suntech, Inc. P. O. B. 1135 Marcus Hook, PA 19061	
10. PROGRAM ELEMENT, PROJECT, TASK AREA & WORK UNIT NUMBERS 61102F 2303A2 A2		11. CONTROLLING OFFICE NAME AND ADDRESS Air Force Office of Scientific Research/NC Bolling AFB DC 20332	
12. REPORT DATE 22 Dec 77		13. NUMBER OF PAGES 106	
14. MONITORING AGENCY NAME & ADDRESS (if different from Controlling Office) 12-112p.		15. SECURITY CLASS. (of this report) UNCLASSIFIED	
15a. DECLASSIFICATION/DOWNGRADING SCHEDULE			
16. DISTRIBUTION STATEMENT (of this Report) Approved for public release; distribution unlimited.			
17. DISTRIBUTION STATEMENT (of the abstract entered in Block 20, if different from Report)			
18. SUPPLEMENTARY NOTES Supersedes A050604 mc			
19. KEY WORDS (Continue on reverse side if necessary and identify by block number) Infrared Spectroscopy, Fourier Spectroscopy, Infrared Emission Spectroscopy, Elastohydrodynamics (EHD) Lubrication, High Pressures, Polyphenyl Ether (5P4E)			
20. ABSTRACT (Continue on reverse side if necessary and identify by block number) Emission Spectra were obtained from our operating E.H.D. contacts through a diamond window, using a specially built Fourier Infrared Emission Microinterferometer. These spectra were compared with similar statis spectra obtained in a high-pressure diamond anvil cell. As an example, 5P4E, polyphenyl ether fluid is discussed in detail. Changes in the spectrum with pressure and temperature under statis conditions allow inferences on these parameters under various dynamic conditions. The dynamic spectra differ markedly under polarization, an indication of molecular alignment.			

DD FORM 1 JAN 73 1473

EDITION OF NOV 65 IS OBSOLETE

UNCLASSIFIED

SECURITY CLASSIFICATION OF THIS PAGE (When Data Entered)

410 289

TABLE OF CONTENTS

	<u>Page</u>
ABSTRACT OF OBJECTIVES AND ACCOMPLISHMENTS	1
1. INTRODUCTION	4
2. EXPERIMENTAL APPROACH	6
2.1 Infrared Spectrophotometry of Thin Films	6
2.1.1 Infrared Emission Spectroscopy of Thin Films	6
2.1.1.1 Effects of Film Thickness and Non-Homogeneity, Boundary Surfaces	10
2.2 Laboratory Elastohydrodynamic Sliding Bearing and Infrared Emission Micro-Interferometer Entrance Optics for Dynamic Spectral Analysis of Lubricants	12
2.3 Infrared Fourier Interferometer	15
2.4 Infrared Emission Referencing System	19
2.5 EDH Contact Temperatures by I.R. Emission Spectroscopy	21
2.5.1 Elementary Analysis of Thermal Emission from Semi- transparent Films on Metallic Surfaces through Transparent Windows	22
2.5.2 Reduction of Emission Spectral Data to Temperatures	26
2.5.2.1 Ball Surface Temperatures	27
2.5.2.2 Fluid Film Temperature	27
2.6 Diamond Anvil Cell Pressures and Glass Transition under Pressure	29
3. RESULTS	
3.1 Emission Spectra with the Diamond Anvil Cell	32
3.2 Calibration and EHD Spectra of 5P-4E Polyphenyl Ether	33

TABLE OF CONTENTS (Continued)

	<u>Page</u>
3.3 Polarized EHD Emission Spectra of 5P-4E Polyphenyl Ether	35
3.4 EHD Film and Surface Temperatures for 5P-4E from Infrared Emission Spectral Data and Thermo-couple Measurements	36
3.5 Differences in Infrared Spectra of Fluids with Pressure	38
3.6 Polarization Studies of N-1 (Naphthenic) Fluid	38
3.7 Spectra Along the Conjunction Line	40
3.8 Friction Polymer Deposits	41
4. CONCLUSIONS	42
5. ACHIEVEMENTS DURING 1977	43
5.1 Apparatus	43
5.2 Data Collection	43
5.3 Data Analysis	43
5.4 Other Techniques	43
6. REFERENCES	44
7. TABLES	46
8. APPENDICES	52
8.1 Papers Published or Presented	52
8.2 Popular References to this Work	55
8.3 Patents	55
8.4 List of Mathematical Symbols	56
9. LIST OF FIGURES	57

COMPLETED PROJECT SUMMARY

1. TITLE: Infrared Spectra of Fluid Film Under Conditions of Incipient Bearing Failure
2. PRINCIPAL INVESTIGATOR: Dr. James L. Lauer
Suntech, Inc.
P. O. Box 1135
Marcus Hook, Pa. 19061

(Present Address): Department of Mechanical Engineering
Rensselaer Polytechnic Institute
Troy, N. Y. 12181
3. INCLUSIVE DATES: 1 January 1974 - 30 September 1977
4. CONTRACT NUMBER: AFOSR-F44620-74-C-0038
(1 January 1974 - 30 June 1976)
AFOSR-F49620-76-C-0042 (Continuation of above)
(1 July 1976 - 30 September 1977)
5. COSTS AND FLY SOURCE:

\$20,000 (Government) + \$ 9,213 (Sun Oil Co.) FY 73
\$40,000 (Government) + \$26,667 (Sun Oil Co.) FY 74
\$44,992 (Government) + \$29,995 (Sun Oil Co.) FY 75
\$57,406 (Government) + \$ 3,021 (Sun Oil Co.) FY 76
7. SENIOR RESEARCH PERSONNEL: Dr. James L. Lauer
Mr. Melvin E. Peterkin
7. JUNIOR RESEARCH TECHNICIAN: None
8. PUBLICATIONS: See pp. 52-55

9. INVENTIONS:

<u>Name of Inventor</u>	<u>Title of Invention</u>	<u>Patent Application Serial No.</u>	<u>Status</u>
J. L. Lauer/ M. A. Peterkin	Extremely High Pressure Measuring Device	S-75-G-121	Closed out, patentability questionable
"	Viscosity Measuring System	Serial 791,089	Filed on 2/27/76
"	System for Spectroscopic Analysis of a Chemical Stream	U.S.P. 3,997,786	Patent issued on Dec. 14, 1976
"	Emission Spectroscopic System having Compens- ation for Background Radiation	U.S.P. 4,009,962	Patent issued on March 1, 1977

10. ABSTRACT OF OBJECTIVES AND ACCOMPLISHMENTS: (see following page)

ABSTRACT OF OBJECTIVES AND ACCOMPLISHMENTS

Under conditions of high stress moving parts of machinery, such as bearings or gears, are prevented from self-destruction by the interposition of extremely thin films of lubricants. Since failure is unlikely to occur without warning, examination of the lubricant in operating bearings approaching failure appeared to be a procedure promising to provide clues on reasons for failure and thus to provide a basis for improved lubrication. The method of analysis chosen was infrared emission Fourier spectrophotometry, a relatively new procedure which is particularly well adapted to thin film analysis and which -- in contrast to absorption spectrophotometry -- requires only one window transparent to infrared radiation. The fluid film heated by internal friction during bearing operation takes the place of the source for the spectrophotometer.

This phase of the work was (1) to demonstrate that infrared emission spectrophotometry can be applied to bearing contact situations, (2) to provide background in the form of calibration spectra applicable to such situations, and (3) to show the potential of the method in specific instances relevant to the failure problem. Very substantial obstacles had to be overcome: (1) very weak radiant power passed through the window and most of it originating from the solid boundary surfaces rather than from the lubricant film; (2) different fluid and solid surface temperatures; (3) ignorance regarding expected lubricant spectral changes with pressure, temperature, shear rate, and fluid/glass transition. Accordingly much of the effort involved the development of appropriate hardware and background information.

Bearing failure is most likely to occur when the solid surfaces bounding the lubricant are elastically deformed under so-called elastohydrodynamic (EHD) lubrication. Curved surfaces are then flattened over the "Hertzian" contact region. Furthermore, sliding is more severe than rolling, hence a loaded bearing ball rotating, i.e., sliding, on a plate was adapted as a model to represent a bearing nearing failure. By making the plate a diamond window, some heat generated in the contact can be transmitted as radiation for spectroscopic analysis. Since diamond is transparent throughout most of the infrared spectrum, the examination of spectral changes even in the "fingerprint" infrared region (10-15 μm) and in the lattice region ($>15 \mu\text{m}$) is feasible. For calibration of the spectral information of the ball-on-plate apparatus a high-pressure diamond anvil cell was used as a "simulated contact". Its sample volume could be subjected to most of the conditions likely to prevail in a sliding EHD Hertzian contact (thickness $<2 \mu\text{m}$, open area 0.25 mm^2 , pressures 0-75 kbar, temperatures 0-200°C) except for shear. As typical fluids, an ester, polyphenyl ether (5P4E), a standard petroleum lubricant, and a so-called "traction" fluid were used. A Fourier infrared interferometer was adapted for all the spectroscopic work.

In the initial stages of the program, absorption spectra were obtained with the diamond cell under various temperatures and pressures. From the splitting of the $725\text{--}735\text{ cm}^{-1}$ CH rocking frequency band it was possible to infer crystallization at certain pressures and temperatures for the ester and the petroleum fluid. Entrance optics were built to convert the Fourier infrared interferometer into an emission micro-interferometer and it was possible to show the equivalence between absorption and emission spectra at the same temperature and pressure. This achievement constitutes a major breakthrough; for while infrared emission spectra of thin layers of organic material on metal substrates have been obtained by previous investigators, spectra from contained volumes as small as Hertzian contacts and at average temperatures as low as $30\text{--}50^\circ\text{C}$ very nearly represent the limit of today's instrumental capability.

A model ball-on-plate apparatus was then built for the same interferometer and entrance optics. The window was located at the bottom of a cup containing the test fluid. A loaded bearing ball rotated about a horizontal axis while sliding over the window provided the bearing contact. The apparatus was located above the interferometer entrance optics. Precise alignment of the contact region on the optic axis and in the focal plane of the entrance optics was essential and was achieved. Indeed it was possible to obtain "dynamic" infrared spectra from the fluids under various conditions prevailing in the Hertzian area.

The analysis of the spectra gave some surprising results. It was possible to deduce both ball surface and fluid film temperatures from the spectra. When temperature differences were plotted against shear rate, the data for all the fluids fell on practically the same curve, which showed a peak corresponding to an intermediate shear rate. The traction fluid reached the highest temperature difference under equal conditions. However, the polyphenyl ether would reach the highest absolute temperature at high shear rates -- just prior to bearing failure. At the same time its spectrum would change, indicating decomposition. Another observation was an intensity change with shear rate of one band, which could be related to polarization of the emitted radiation. The mechanism for it might well be stream birefringence, although other explanations have not yet been excluded. For example, glassification and strain polarization (photoelastic effect) could be a mechanism which, moreover, is in agreement with recent theories by other investigators. The extent of this polarization could, conversely, be used as a measure of lubricant stress prior to failure.

Some of the spectra obtained in a diamond anvil cell for calibration purposes showed very significant changes with pressure. Absorption bands would shift and disappear possibly indicating molecular changes or, perhaps, changes in the distribution of isomers.

A separate but related achievement was the design and construction of apparatus to determine pressure and state of material in the diamond anvil cell from the peak frequency and width of the fluorescence band of ruby crystals contained within the sample. In contrast to earlier opinion considering traction as caused by glassy particles in the contact zone, the traction fluid tested needed higher pressures to be converted into the glassy state than the other fluids and must therefore function by a different mechanism.

Work was started toward a reliable determination of the state of the fluid (liquid or glassy) from the dynamic infrared spectra.

1. INTRODUCTION

Under conditions of high stress, moving parts of machinery such as bearings and gears, are prevented from self-destruction by the interposition of extremely thin films of lubricants. When these films are no longer capable of separating the metal surfaces, their contact is likely to cause failure of the machinery. Advanced technology requires lubricants to withstand even higher temperatures and pressures without undergoing deterioration.

Lubricant stability has been investigated by many procedures at very high temperatures and pressures -- outside of operating machinery. Much work has also been directed at compositional changes of lubricants as a result of prolonged times of use in operating machinery. However, essentially no work has dealt with the behavior of lubricants in their working environment. This study by infrared emission spectrophotometry is believed to be the first aimed at analyzing the lubricant film itself. It therefore can include: (i) shear as a variable, (ii) prevailing temperature and pressure distributions in contact zones, and (iii) chemical and physical conditions in different regions of the contact zone.

Infrared emission Fourier spectrophotometry is, in principle, particularly well adapted to thin film analysis and requires only one window (preferably diamond) transparent to infrared radiation. Under extreme conditions -- those most conducive to failure in elastohydrodynamic (EHD) sliding lubrication -- lubricant films are only about 0.2 μm thick and typically 350 μm in diameter and, on the average, at about 80°C as a result of internal friction. Yet their infrared radiation transmitted through a diamond window is adequate for spectral analysis. Composition changes, phase changes, orientation of molecules in the conjunction region, adsorption of fluids on solid boundary surfaces, as well as fluid and solid surface temperatures can be deduced from adequate infrared spectral information.

This phase of the program, a one-man effort for four years (1 January 1974 to 1 October 1977) was devoted to: (i) design and construction of the appropriate interfaces -- notably a rotating ball-on-diamond-plate -- to obtain infrared spectra from EHD films, (ii) demonstration of the feasibility of infrared Fourier emission infrared spectroscopy from bearing contacts, and (iii) gathering of spectral information and analyses from a few selected lubrication systems. For calibration of the spectral information of the ball-on-plate apparatus, absorption and emission spectra were obtained with a high-pressure diamond anvil cell. Its sample volume could be subjected to typical EHD temperatures and pressures, but, of course, not to shear.

A related, parallel program of work of about equal size was supported by NASA - Lewis under Contract No. NAS3-19758. It was more applied in nature and concerned specific lubricating systems of their selection. However, inevitably, some parts of that work are pertinent to this contract as well and are therefore briefly included here.

The work is to be continued and expanded with superior facilities after the Principal Investigator's move to Rensselaer Polytechnic Institute.

Because many of the results have already been published, this report is limited to the essentials of apparatus and procedures and to previously unpublished data. For this reason, our work on 5P4E polyphenyl ether is presented in detail here while the reader is referred to our publications (especially items 18 to 25 in our List of Publications) for the results on the other fluids. The 5P4E results are an excellent illustration of the potential of our capabilities.

2. EXPERIMENTAL APPROACH

2.1 Infrared Spectrophotometry of Thin Films

The thickness of the typical liquid lubricant film under the extreme conditions of elastohydrodynamic (EHD) lubrication is of the order of tenths of micrometers. Only the very strongest infrared absorption bands are measurable through parallel windows by the usual transmission methods under these conditions and then only with difficulty. Hence, transmission methods were not considered as promising even if parallel windows could be installed in a bearing. Reflection at the windows can cause significant losses unless reduced by various devices such as the use of index matching materials or Brewster angle incidence. Conversely, these reflection losses have been made the measurement objective in procedures such as total internal reflection (TIR), attenuated total reflection (ATR), ellipsometry, and the use of evanescent waves and guided waves. These methods are, of course, particularly adapted to measuring losses (absorptions) in surfaces and coatings. Thus, for example, frustrated multiple internal reflection infrared spectroscopy (FMIR) has been used to study boundary lubricating surface films by a Battelle group. As the name of the method indicates, multiple reflections are essential to increase the effective absorption length along the window (or transmitting plate)/fluid interface and it is therefore necessary to have this interface reasonably long; say, one centimeter. This length cannot be significantly reduced by closer spacing of the reflections, since the angle of radiation incidence must invariably exceed the critical angle. Hence, it would be difficult to apply reflection methods to EHD contact regions which are typically only 10-500 μm in diameter (ball/plate). Indeed, cylinder/plate contacts could be studied by reflections along their long dimension, and they have been considered by us for the future, but the emission methods described below appeared more promising to us for an initial stage.

2.1.1 Infrared Emission Spectroscopy of Thin Films

Infrared emission spectroscopy of thin, partially absorbing films or "dielectric layers" has been studied and used by workers in the fields of glass and minerals technology, surface coatings, and the like. The extreme potential sensitivity of the method has been noted. Hordvik¹ (Rome Air Development Center) recently stated that "the use of a material's emissivity to measure absorption is probably the technique with the greatest potential for measuring low loss and, at the same time, get spectral information."

2.1.1 (Cont'd)

To see why this claim has been made, let us first consider a thin film layer at thermal equilibrium and bounded by the same transparent surfaces on both sides. Then, as McMahon² has shown for the case of unidirectional emission normal to the surfaces, the emissivity of the outwardly emerging radiation is given by

$$E = \frac{(1 - R)(1 - T)}{1 - RT} \quad (1)$$

where $E(\lambda, t)$, $R(\lambda, t)$, and $T(\lambda, t)$ are all functions of λ and t , the wavelength and temperature, R and T being the reflectivity and transmissivity respectively. Simple algebraic manipulation brings Eq. (1) into the form:

$$E + R + T = 1 + ERT + RT$$

which reduces to

$$E + R + T = 1 \quad (2)$$

since E , R , and T are, by definition, all less than unity and thus their products small compared to unity. Eq. (2) is an extended form of Kirchhoff's law and can be verified thermodynamically. It means that "all radiation impinging on a semi-transparent body in a uniformly heated enclosure must, at equilibrium, be equal to the sum of emission, reflection, and transmission in order to maintain a constant temperature."

By Lambert's law,

$$T = e^{-kh} \quad (3)$$

where $k(\lambda, t)$ is the spectral absorption coefficient and h the film thickness.

Since the reflectance of most samples with discrete emission spectra is low, Eq. (1) approximates to

$$E \approx 1 - T = A(\lambda, t) \quad (4)$$

2.1.1 (Cont'd)

where $A(\lambda, t)$ is the absorptivity, which is not to be confused with the absorption coefficient k . Substitution of T from Eq. (3) gives

$$E \approx 1 - (1 - kh + \frac{1}{2} k^2 h^2 \dots) \approx kh \quad (kh \leq 1) \quad (5)$$

In chemical analysis it is customary to express the transmissivity by the Beer-Lambert law

$$T = 10^{-\epsilon ch} \quad (6)$$

where T is now defined as the experimental transmittance, $\epsilon(\lambda, t)$ is the molar extinction coefficient of the material and c the molar concentration of the solute. Clearly, from Eq. (6) and Eq. (3)

$$k = \epsilon \ln 10 = 2.303 \epsilon c \quad (7)$$

To complicate the algebra still further, but to be consistent with the pertinent literature, it is necessary to introduce the absolute band intensity of an absorption band

$$I_{\text{band}} = \frac{1}{m h} \int_{\text{band}} k(f) df \quad (8)$$

where f is the frequency, i.e., the wave number in cm^{-1} times the velocity of light (3×10^{10} cm/sec) and m is the number of molecules of the absorbing species per unit volume. Accordingly

$$m = 6.02 \times 10^{23} D/M \quad (9)$$

where D is the density in g/cm^3 and M is the molecular weight. For a typical fluid ($M = 300$, $D=1$), we have

$$m \sim 2 \times 10^{21}$$

For a rectangular band, 10 cm^{-1} wide, and a fluid layer thickness of $0.1 \text{ } \mu\text{m}$ thickness, Eq. (8) can be approximated by

$$\begin{aligned} I_{\text{band}} &= \frac{1}{2 \times 10^{21}} \cdot \frac{1}{10^{-5}} \cdot k \cdot 10 \cdot 3 \times 10^{10} \\ &= \frac{3 \times 10^{11}}{2 \times 10^{16}} k \approx 10^{-5} k \end{aligned}$$

2.1.1 (Cont'd)

The literature³(Table I) lists values for the most intense bands as (I_{band}) as lying between 10^{-9} and 10^{-6} so that k would be bracketed as follows:

$$10^{-4} < k < 10^{-1}$$

According to Table II, also from Hordvik's paper, the lower limit is "routinely" possible by emittance, though generally not by transmission. Since these requirements are for the "pure" lubricant and our interest lies in new species and transformations, it is apparent that a one-percent constituent should be determinable, if the infrared band is on the strong side.

The preceding discussion was kept in general terms. However, a thin dielectric film--assuming thermal equilibrium for the moment--radiates with a wavelength or wavenumber distribution corresponding, at least roughly, to a Planck radiation distribution. Another way of looking at the situation is to regard the lubricant film as a coating on the metal surface in a bearing, increasing its thermal emissivity at wavelengths corresponding to infrared absorption and not affecting it at those where the film is transparent. Since the emissivity at a spectral location is, in effect, a proportion of the blackbody emission, its measurement depends strongly on the blackbody emission at that location. Radiant energy is the quantity measured.

An important question is, "is the best region accessible to emission measurements at actual operating temperatures." If the average temperature in the oil film in the conjunction region is near 350° K, then the spectral energy emitted per unit fractional change in wavelength is a maximum when

$$(\lambda t)_{\text{max}} = 0.3670 \text{ cm K} \quad (10)$$

For $t = 350^{\circ}$ K, the wavelength for maximum energy is therefore $10.5 \text{ } \mu\text{m}$, or, in terms of wavenumber

$$\left(\frac{\nu}{t} \right)_{\text{max}} = 2.725 (\text{cm K})^{-1} \quad (11)$$

and the wavenumber for maximum energy is 954 cm^{-1} .

2.1.1 (Cont'd)

It should perhaps be pointed out why the constant of Eq. (10) is not Wien's displacement constant of $0.2898 \text{ cm}^{\circ}\text{K}$. The reason is that the value of the constant depends on the definition of intensity in terms of wavelength or wavenumber. In Fourier spectroscopy wavenumber is the usual primary unit. Since energy is measured, Eq. (10) would seem to be more directly applicable. In any case then, other things being equal, i.e., for example a linear wavelength response by the detector, the spectral region near 950 cm^{-1} is most useful in infrared emission spectroscopy of fluids at around 100° C . Fig. 1 shows that spectral radiance falls off quite a bit toward higher frequencies. The fall-off is even worse when the absorption of the diamond windows is taken into account. A spectrum of one of our Type IIA (the most transparent diamond in the infrared) windows is shown in Fig. 2. Since diamond is really the only window material transparent in the mid- and far-infrared and capable of withstanding the pressures encountered in lubricating contacts, the relative emission band intensities of Fig. 3, band intensities which have been adjusted for changes of Planck emission and diamond absorption, constitute real experimental limitations. Thus the carbonyl band near 1700 cm^{-1} , which is usually considered to be among the most intense bands, is more difficult to measure by emission than the C-H aromatic frequency near 700 cm^{-1} . Clearly the most energetic band for our purposes is the C-F band near 1000 cm^{-1} .

Fortunately these restrictions are not serious for the present work. The all-important characteristic infrared vibration bands near $10 \text{ }\mu\text{m}$ and above are all readily available to our measurements. The greater signal/noise ratio of the new solid-state detectors will make it possible to extend the effective wavelength range in the near future.

2.1.1.1 Effects of Film Thickness and Non-Homogeneity. Boundary Surfaces

Practically all the spectroscopic work on infrared emission spectra reported in the literature assumed temperature, pressure, and composition homogeneity through the sample. Thus Fabbri and Baraldi⁴ recorded emission spectra of solids on a metal support and related them to absorption spectra by assuming the sample to be an optically homogeneous plate. Steger and Rasmus⁵ corrected the analysis of Fabbri and Baraldi for absorption and reflection along the lines of Eqs. (1)-(6), but still assumed equal temperatures of sample and support. Even with these corrections, distorted bandshapes are likely to result unless Eq. (5) holds. In other words, infrared emission spectroscopy is particularly well suited only to thin films ($kh \leq 1$).

2.1.1.1 (Cont'd)

While most of our lubricant films are indeed "thin" in this sense, the limit of thinness is approached occasionally, as will be seen, so that the following rudimentary analysis may be pertinent.

Fig. 4 illustrates what happens to a strong emission band as the film gets thicker. Since strong emission bands are also strongly absorbed, self-absorption will flatten their peaks as the blackbody limit is approached. This effect will tend to equalize differences between emission peaks even for films of uniform temperature. However, if the temperature is also non-uniform and lower near the window through which the radiation is monitored (our situation), the weaker excitation in the cooler region can cause a decrease of intensity near the band center, the so-called self-reversal, which often makes a band appear as a well-resolved doublet. When several strong film bands are close enough together, their self-absorption can produce sufficient broadening to give the appearance of blackbody radiation containing "absorption" bands at the normal band frequencies; in other words, the self-reversal has the appearance of absorption.

The film "blackbody" radiation can be differentiated from the graybody radiation of the bounding surfaces by the radiant flux intensity in frequency regions where the film is definitely transparent. When this graybody radiation containing film absorption bands is observed, it is a sign that the bounding surface temperature is higher than the film temperature and the film is thick enough for appreciable absorption. Under certain conditions a band can just disappear. Then the blackbody background temperature equals the so-called reversal temperature, where the populations of the two states corresponding to this band are related by a Boltzmann distribution.

Polarization and unequal boundaries introduce other effects into thin film infrared emission spectroscopy, which will be discussed after the apparatus of our study of high-stress lubrication has been described.

The changes of band shape, band reversals, and the polarization phenomena can provide very useful information on the state of a lubricant film in a bearing, which is additional to that of the basic infrared emission spectrum. Since the theory is rather difficult and different interpretations are sometimes possible, stress was put on empirical correlations based on calibration experiments. It proved to be easy to allow for these additional measurements and others in the apparatus design described below. Indeed the work performed so far has strengthened our belief in infrared emission spectrophotometry as an ideal tool for the study of elastohydrodynamic lubricant films.

2.2 Laboratory Elastohydrodynamic Sliding Bearing and Infrared Emission Micro-Interferometer Entrance Optics for Dynamic Spectral Analysis of Lubricants

The conjunction region of the ball-on-plate sliding contact used for infrared emission spectrophotometry is shown schematically in Fig. 5. A loaded steel ball (diameter 0.0286 m) is rotated in a fluid and made to slide over a diamond window. A contact region is formed in the fluid layer between the elastically flattened ball and the diamond surface. Typical layer thicknesses are $0.2\text{ }\mu\text{m}$ for customary fluid viscosities and fluid temperatures under typical loads and linear sliding velocities. These thicknesses were calculated for most of this work from correlations between fluid properties, thicknesses and loads established by other workers. However, recently we were able to apply optical interferometry through the diamond window and photograph the interference pattern (distorted Newton's rings) through a microscope while the system was operating. The reflectivity of the diamond surface is high enough to produce sufficient contrast without the metallization other workers⁶ found necessary when working with sapphire.

The loading of the ball was accomplished initially by placing a platform over it to whose lower surface three small bearing balls were rigidly attached at the apices of an equilateral triangle, and by hinging the platform at one end and hanging weights on the other. It proved helpful to insert small sapphire pads into the small bearing balls at the contact points, so as to increase the areas of sliding contact between the rotating large ball and the three small holding balls. Fluid pulled up by the large ball rotating in the fluid cup was providing lubrication at these three support points. Unfortunately the friction and frequent starvation condition at these positions produced frequent failures with some fluids. Furthermore it was not possible to relate the current of the dc motor driving the ball to the traction at the diamond (EHD) contact. For these reasons a different support for the loading platform was designed, built, and put into service early in 1977. It substitutes two one-inch diameter rollers (standard SKF or Barden roller ball bearings) for the three point contacts. These rollers bear down on the ball in the same plane as the EHD contact, at angles about 30° with the vertical. The friction at the rollers is small compared to that at the EHD contact with the diamond and no failure has been experienced after many months of operation. To prevent the ball from moving an additional point contact is provided by a set screw along the horizontal axis of ball rotation and opposite to the attachment of the driving shaft.

Fig. 6 shows the apparatus in some detail (except for the loading platform). By locating the ball/diamond plate contact at the bottom of a cup filled with fluid it is possible to introduce the transmitted radiation into the infrared interferometer over the shortest possible distance. It also almost insures flooded conditions

2.2 (Cont'd)

at the EHD contact point. On the other hand, it causes interactions between the fluid flow in the cup (reservoir) and in the contact zone. Thus the only practical way to remove the heat generated in the contact was to insert an aluminum coil containing cooling water into the cup itself. The water is pumped from a large reservoir kept at constant temperature. For calibration purposes (stationary test ball) the entire assembly can be heated by circulating warm water through the coil. Then the fluid in the cup functions merely as a heat transfer medium.

The test ball is rotated about a horizontal axis by a motor and a drive shaft provided with a universal joint and a sleeve allowing for the correction of small misalignments. It is absolutely essential that the axis run "true"; otherwise, strong vibrations are set up in the contact, which seriously interfere with the spectroscopy. Vibrations pose a problem in any case, because of the high sensitivity required of the radiation detector. To keep them minimal, the mechanical set up is located on a table mounted on vibration-dampers and not physically in direct contact with the interferometer-spectrometer.

The shaft attached to the test ball is used only for torque transmission, not for locating the ball and keeping it in place. The rollers or upper contact points and the set-screw opposite to the shaft are serving this purpose. At the bottom of the reservoir cup, the plate containing the diamond is adjustable by set-screws allowing for the tangential alignment between ball and diamond. This condition is obtained when the Newton rings made visible in reflected light by a reflecting microscope are centered. In the presence of fluid in the cup and appropriate irradiation these Newton rings also determine the film thickness. The entire cup assembly can also be moved along the x and y directions on the table to bring the EHD contact point on the optic axis of the lens. The legs of the table are adjustable for height to bring the contact region in focus.

The optical arrangement shown in Fig. 6, consisting of the all-reflecting microscope objective lens (Beck lens), 45 degree mirror to change the direction of the infrared radiation from vertically downward to horizontal, chopper, and collimator has recently been changed in certain important respects. In the old arrangement, the radiation emitted by the chopper blade provided the reference, the detector reading the difference between the source radiation and the chopper blade radiation. The effective aperture of the collimator could be altered by insertion of "restrictors." The graybody radiation of the ball was balanced by the "restricted" graybody radiation of the blade in the phase-sensitive amplifier (lock-in amplifier) tuned to the chopper frequency. This arrangement did not leave much freedom

2.2 (Cont'd)

for adjustment and was unworkable when the frequency range of the interferometer was extended: Since the blade could not be heated appreciably, its radiation could not be matched to the ball's radiation from the contact region.

The new set-up of Fig. 7 obviates these difficulties. The heat radiation transmitted through the diamond window is periodically interrupted by the reflecting blades (tines) of a tuning fork, which are located above the Beck lens. A pair of small plates is also attached to the same tuning fork tines in such a way that the reference heat source (a thermoelectric cooler/heater, operable in either mode) is covered when the reflecting blades are in the open (apart) position. Since the lower surfaces of the upper blades are reflecting, radiation from the reference source and radiation from the contact source enter the Beck lens alternately. The amplifier detects only the difference between the power of the source radiation and that of the reference radiation and amplifies it.

The referencing procedure is very important to this work. Without it the signal would be swamped by graybody radiation from the ball's surface and the film spectrum would be lost in the noise. An aperture stop inside the interferometer limits the field of view of the Beck lens and, thus, the portion of the conjunction region (Hertzian area) investigated. When no signal is detected, the radiant power from that portion equals that of the reference. When the source is only the ball heated to a known temperature, the reference heater voltage required to match the reference radiation to that of the ball provides a calibration mark. This match is hardly disturbed when a fluid film is present between the ball and the diamond window, since the radiation of the thin film is emitted only at selected frequencies. However, at these frequencies the film's emission spectrum becomes visible. These emission spectra will be discussed later.

By moving the field of view of the Beck lens along the direction of fluid flow through the contact region, it is possible to obtain spectra from fluid volumes subjected to a history of temperatures and pressures. By varying the ball speed, exposure times are varied, and changes of the corresponding infrared spectra can be correlated with changes of fluid composition.

At least three temperatures in the fluid cup were continuously monitored during every experiment: (a) the temperature at the diamond window by a thermocouple touching it within the mounting cement, (b) the temperature at the ball by a thermocouple loosely touching it, and (c) the temperature at a relatively quiescent location within the fluid. The constancy of these temperatures to better than 2.0 °C during a spectral scan (about 20-25 minutes) was essential.

2.2 (Cont'd)

Because of the extremely high thermal conductivity of the diamond window (a specially ground 4 mm diameter, 2 mm thick disc of natural Type II A diamond chosen for near perfect infrared transparency and oriented so as to minimize stress in the direction of sliding), the temperature recorded at (a) was assumed to be equal to--or at least closely parallel to--the fluid inlet temperature at the Hertzian contact. Changes of rotational speed or load were reflected instantly by changes of this temperature. Temperature (b) rather than temperature (c) was chosen as the best measure of the bulk fluid temperature because the many temperature gradients and currents in the main body of the cup made precise relocation of the thermocouple at (c) impossible.

The largest readily available stainless steel ball (440 C, diameter 0.0572 m) was chosen initially so as to provide a large Hertzian contact region for analysis. With the help of SKF (Sweden), larger and smoother balls were obtained (440 C, diameter 0.680 m) which were gold-plated by a special process. The roughness of these balls is less than 100 Å. The gold-plating reduced the graybody surface radiation considerably and allowed much better film spectra to be obtained. These balls could be used with the three-point loading platform only, because the platform using the rollers is not readily adaptable to the larger ball diameter. On the other hand, the recently received ceramic (aluminum oxide) balls are almost of the same size as the steel balls and can be used with either loading platform. These balls are also gold-plated. Their different physical properties, especially thermal conductivity and hardness, give rise to different film temperatures and spectra.

2.3 Infrared Fourier Interferometer

The intensity of the radiation emitted from the (EHD) contact region and transmitted by the diamond window is too low for analysis by an ordinary dispersive spectrometer. The amount of heat generated in the lubricant by viscous friction may be large per unit volume, as Winer⁷ has shown, but the total is small. It should be realized that a measurement of total radiation for the purpose of temperature determination is considerably easier--though by no means easy--than a spectral analysis of this radiation. Winer and his students have been able to obtain temperatures for ten separate regions along the conjunction line of both sliding and rolling contacts, using radiation passed through sapphire windows; why should there be so much difficulty in obtaining spectra from a third of the contact region or even from the entire region? The answer lies, of course, primarily in the necessity for the splitting of the total radiation into the some 500 elements necessary for even a rudimentary spectral analysis.

2.3 (Cont'd)

Immediately the most sensitive spectrometer is called for and this today is the Fourier spectrometer or interferometer, which has been quoted ⁸ to offer sensitivities at least two orders of magnitude greater than those of dispersive instruments. However, Fourier spectrometers are much more readily adapted to the far infrared than to the near infrared. Their instrumental problems are much greater the higher the frequency. Hence, even though near infrared detectors exist that are one to two orders of magnitude more sensitive than mid-or far infrared detectors and that are thus able to compensate for the lower radiance of low-temperature fluid films in the near infrared than in the far infrared, instrumental difficulties remain in the near infrared spectral region. In addition, the near infrared is often less informative to the spectroscopist than the mid- or far infrared. These considerations are, of course, of no significance for radiation temperature measurements and for these the near infrared is the region of choice.

It might appear surprising that it should be easier to build an interferometer for the far infrared, a region of inherently low energy, than for the nearer infrared. However, the longer wavelength makes the optics less critical--a good detector is the main requirement. Before the start of this project we had just completed the extension of our Beckman-RIIC Model FS-720 Far Infrared Interferometer from 400 cm^{-1} to 1000 cm^{-1} by substitution of a thinner Mylar beamsplitter and by halving of the mirror travel distance between readings (from 4 μm to 2 μm or from 8 μm to 4 μm in terms of optical retardation). This was accomplished by new circuitry for the Moiré comb monitoring system so that zero crossings would trigger for both positive and negative slopes on the photocell potential/comb displacement curve (Fig. 8). This system served us well and many of the results discussed below were taken in this way.

Further increase of the frequency range was not possible with the Mylar beamsplitter, for it was difficult to obtain even thinner film (less than 8 gauge or 2.5 μm thick) and, even more importantly, because of the strong absorption bands of Mylar in the high frequency region. A new beamsplitter consisting of a 0.55 μm thick layer of germanium evaporated on a disc of KCl, three inches in diameter and one-quarter inches thick and covered by a similar KCl disc, was therefore made and installed in place of the Mylar film. The installation of this "sandwich" and the subsequent alignment was a major task, but it was nevertheless easier than thought possible. The sandwich was mounted in a holder originally designed for Mylar film; this holder is therefore interchangeable with the other beamsplitter holders and the flexibility of the instrument is therefore increased, not decreased. In contrast to

2.3 (Cont'd)

Mylar film, germanium is barely transparent to visible light. The "barely" is just it, for a He/Ne laser beam is transmitted (less than 0.1 percent) by the germanium layer, but just enough for viewing by the accommodated eye in absolute darkness. Yet this beam made the optical alignment possible by eye (minor adjustments were made on the basis of instrumental measurements).

With the new beamsplitter went a new solid-state Golay detector of greater sensitivity and new electronic circuitry. As already mentioned, a new chopper and reference source had to be installed.

The new beamsplitter is effective over the 2 to 15 μm region or from 600 to 4000 cm^{-1} . However, to make use of this capability the Moiré system had to be further improved. This was done by providing for triggering pulses not only at the zero crossings but at peaks and valleys as well and further for pulses half-way between zero crossings and peaks or valleys. Fig. 9 is a schematic diagram of the circuitry built for us by Klinetics, Inc., of Swarthmore, Pennsylvania. The key to success is the initial filtering of the Moiré signal; the sine wave produced is smooth enough to permit differentiation, making it possible to detect peaks and valleys as zero crossings. The in-between points are found by cutting the time intervals in half. This procedure is not strictly correct, since the whole purpose of the Moiré system is to provide pulses at equal distances of mirror travel and not at equal times. Anyone familiar with Michelson interferometry is aware of the sheer impossibility of driving a mirror at an exactly constant rate. Nevertheless our ultimate division by two in terms of time works very well, because (i) the amplitudes are read exactly--only the time interval is interpolated and (ii) the interval is small enough to be constant within our present limits of error. Hence we succeeded in reducing the retardation interval from 8 μm originally to 1 μm now or the mirror travel distance interval from 4 to 0.5 μm .

We believe our present Moiré measuring system is about the ultimate for this type of design and we are very proud of it. Further extensions will require a laser reference system. Such a system is nothing more than a version of Michelson's set-up for measuring the standard meter in terms of the cadmium line; the He/Ne laser takes the place of the cadmium arc and the traveling mirror moves together with the moving mirror of the infrared interferometer. The interference maxima corresponding to the 0.6 μm wavelength of the laser will take the place of the transmission maxima of the Moiré combs, but with a spacing even smaller than what we are now able to get by laboriously dividing

2.3 (Cont'd)

the Moiré spacings electronically. The smaller spacing will then be used primarily for noise removal (oversampling readings during mirror travel), since no further extensions of the wavelength range are needed. All the optical and electronic parts for this apparatus improvement are already in our possession and partially assembled.

Fig. 10 shows a polystyrene film absorption spectrum taken with our instrumentation (single beam) and a standard reference spectrum. It should be appreciated that the source was only a 1-mm diameter portion of a hotplate kept at 100°C at the focus of our 15x Beck lens (cf. Fig. 7) and the mirror travel was exactly the same as that used in all our EHD contact spectra. Hence the resolution was only about 5 cm^{-1} , since only a limited number of points per run can reasonably be recorded. It will be noticed that the correspondence of the band frequencies is within the expected limits over the entire frequency range covered. The optics are therefore adequate and the spectral positions and shapes are believable.

The slow-scanning feature of our instrumentation became an even slower-scanning feature every time the reading interval was decreased. The present scanning rate of about one micrometer per second requires 1000 seconds or about 20 minutes per run for a mirror travel distance of one millimeter from the central burst. Because of zero-filling the resolution is effectively 5 cm^{-1} , which is adequate. Even if the time per run could be doubled--and this was tried--the effective resolution in a dynamic experiment is not improved because of the virtual impossibility of maintaining constant operating conditions for this length of time.

The slow scanning rate is partly compensated by the signal integration between readings--the noise is reduced. However, the principal reasons for the slowness are (i) the Golay detector, essentially a gas-filled bag whose expansion with temperature rise provides the output signal, and (ii) the paper-tape interface for the digital signal output. Improvements are underway for pushing both of these limits further out. A mercury-cadmium-telluride photoconductive detector (HCT detector) is much faster, less subject to microphonics (vibrations), and even inherently somewhat more sensitive.* Its installation is approaching completion. A complete dedicated microcomputer system (Texas Instruments #990/4) is on order, which will allow signal storage on a disc at a much faster rate and the completed recording of a spectrum in minutes. (Our present method of computation makes use of time-sharing on a Honeywell #635 Processing System; the turn-around time can be as long as one hour per spectrum.) The new system will permit us to accumulate spectra at a 10 to 20 times faster rate than now.

*Fig. 11 compares the detectivity of various infrared detectors. It is based on a recent article by Levinstein.⁹

2.3 (Cont'd)

While a commercial fast-scanning interferometer is being considered for further work, the inherent advantages of the present method to the spectroscopy of the weak signals emitted by EHD contacts should be remembered. Above all the use of a chopper (not used in fast-scanning instruments) permits immediate removal of the graybody radiation by referencing and a temperature calibration. The use of long time constants with weak signals helps reduce the noise. The potentially longer mirror travel of the slow-scanning instrument makes for higher resolution. Real-time computations may become possible. Furthermore our three- to four-inch optics (depending on the beamsplitter) can gather considerably more radiation than the (usually) one-inch optics of a fast-scanning instrument. Our scanning time of 20 minutes per spectrum is about equal to the time required to obtain the number of spectra needed for the same signal/noise ratio with a fast-scanning instrument.

We therefore believe that the improvements already underway will improve future work very considerably. However, the potential advantages of a new commercial Fourier spectrometer interfaced with our microscope and EHD apparatus can also be substantial.

2.4 Infrared Emission Referencing System

In Section 2.2 the referencing system was briefly discussed as part of the entrance optics. Since the referencing or the removal of the bulk of the graybody emission spectrum from the EHD contact region spectra is very important both for the recording of meaningful emission spectra from the lubricant film and for estimates of the prevailing temperatures, a more detailed discussion of the experimental situation is warranted.

The slow-scanning interferometer requires the use of a radiation chopper as does the Golay pneumatic detector, with which all our work to date has been done. An Ithaco Model 391A lock-in amplifier is tuned to the 12 Hz chopper frequency and phase-locked in such a way that only the difference between the signals alternately falling on the detector, viz., the EHD contact radiation and the reference radiation reflected by the closed chopper blades (Fig. 7) are recorded. The reference source can be heated or cooled--a stream of cooled gas onto the opposite (heated) side is necessary to remove heat when the cooling mode is used--by varying the supply voltage or current until the center burst of the interferogram, which is the analog output signal, is barely standing out over the noise output. Under these conditions the modulation of the interferogram is optimized as the dynamic range required has been reduced.

2.4 (Cont'd)

When this procedure is followed, some very good emission spectra can be obtained and the reference potential can become a measure of average contact temperature after suitable calibrations. However, there can be problems which must be recognized.

For example, Fig. 12 shows three different emission spectra obtained from the same 2.5 μm thick Mylar film backed by aluminum at the same temperature. The only difference in the experimental conditions was the reference voltage. The interpretation of the various bands--the 730 cm^{-1} band was chosen for this experiment because it is strong and isolated--is not difficult once it is realized that the Fourier transformation of the output signal furnishes only an absolute value of the difference between source and reference signals. Furthermore, our spectral plots are always normalized to the peak for the frequency range calculated, but since the normalization factor (GUA = greatest unnormalized amplitude) is always recorded, different spectra can be compared. Now, in the first instance of Fig. 12 the exitance of the reference was below the graybody background of the signal, in the second case it was above the graybody background but below the peak emittance, and in the third case it was above the background and above the peak emittance. The results are an emission peak in the first case, multiple peaks in the second, and an absorption peak in the third case.

Since the frequency range calculated and plotted for most of our spectra is narrow, the background emission can be considered horizontal with very little error. Our interferograms ("over-sampled," as already stated) are numerically filtered prior to the "Fast Fourier Transformation (FFT)" by convolution with the apodized Connes filter¹⁰, resulting in a much smaller "filtered interferogram" containing only the information pertaining to the desired frequency range and less noise. By adding or subtracting the Fourier transform of a rectangle, i.e., a flat background, in the spectrum to the filtered interferogram, the reference exitance can be effectively lowered or raised in the spectrum after the Fourier transformation is performed. The height of this rectangle that must thus be added to convert the multiple peak spectrum of Fig. 12(A) into the proper emission spectrum of Fig. 12 can be correlated to the experimental reference potential change. The Fourier transform of a rectangle is the well-known $(\sin x)/x$ function¹¹, which has a sharp peak at the center and much weaker modulations symmetrically around it. It turns out that in our case these modulations are so small compared to the center peak that they can be effectively ignored and the "reference relocation" can be performed by adding successively larger values to the center burst of the filtered interferogram until the structure of the normalized spectrum no longer changes.

2.4 (Cont'd)

This numerical manipulation is now an easy routine incorporated into our software, which can be related to the ball surface temperature in the conjunction region by combining the minimum "K-Unit" added with the reference potential. This procedure must be repeated for every narrow wavenumber interval considered. For large intervals the background level is no longer flat and more sophisticated manipulations based on the basic radiation law and the instrumental factors are needed. In practice, two or three small frequency intervals turned out to be simpler to handle than one large one with many uninformative gaps.

2.5 EDH Contact Temperatures by I.R. Emission Spectroscopy

Temperatures are inevitably included in any spectral study of operating bearing contacts. The best way to learn the influence of temperature on the spectra appeared to be the development of procedures for obtaining temperatures from the recorded spectra themselves. The comparison of these temperatures with those of other workers (Crook¹², Winer¹³) was helpful in giving us confidence in our data.

In our early work one-third by volume of poly-alpha-methylstyrene was mixed with the fluids studied--too much to qualify merely as an additive--to provide two strong infrared emission bands, one near 700 cm^{-1} and one near 750 cm^{-1} , which are characteristic of monosubstituted aromatic hydrocarbons. The different properties in the bearing contact of the various fluids could then be deduced from the same spectral bands, so that their calibration for temperature, for example, would apply to all fluid mixtures. In particular, the 700 cm^{-1} was used for fluid temperature estimates, since this band was hardly overlapped, influenced by physical state or by polarized infrared radiation. Although most of the procedures used were reported previously under our NASA contract, their essentials are repeated here because (i) their development was carried out under this AFOSR contract and (ii) the temperatures reported below for neat fluids were calculated mostly in this way.

It should be pointed out at the start that our temperature estimates are averages over most of the Hertzian contact region, i.e., the area where the ball is elastically deformed under the load. Although some spatial division of the region was done by an iris diaphragm in the image plane of the interferometer ahead of the detector, essentially all our values are lower than those obtained by Winer and his students¹³ for small regions of the contact.

2.5 (Cont'd)

Furthermore, the temperatures represent vertical averages as well, i.e., over the film thickness. As will be shown later, some of our spectra clearly suggest the existence of a temperature gradient across the film of lubricant. Such a gradient is not unexpected, since most of the theories postulate heat generation by viscous friction in the lubricant stressed in a bearing contact and much of the heat is conducted to the bounding surfaces.

2.5.1 Elementary Analysis of Thermal Emission from Semitransparent Films on Metallic Surfaces through Transparent Windows

In all the work reported on infrared emission spectroscopy from thin layers of materials on metal surfaces equality of the temperatures of the layer and the metal was assumed. Low¹⁴, for example, studied the emission spectra of oleic acid spread on aluminum in this way. Inverted peaks in his spectra are indicative of a temperature gradient through his thicker films, but these were considered artifacts to be avoided. In EHD contact regions, the fluid film temperature must be assumed, under steady operating conditions, to be always different from the surface temperature of the sliding ball and from the temperature of the diamond window as well. McMahon's widely quoted equations of his paper on "Thermal Radiation from Partially Transparent Reflecting Bodies"² apply to thick (wavelengths small compared to thickness) slabs with equal boundary conditions on both surfaces. Our situation is that of thin radiating films bounded by different materials at different temperatures. A separate analysis of our case is therefore required.

If an accepted mathematical model of the EHD situation were available for a few standard fluids, the spectra of these fluids could be employed for apparatus calibrations and a calculation of fluid temperatures from their spectra would be simple. Such a model is still lacking, although excellent effort in this direction is underway. Our approach has, therefore, been to use fluid emission spectra obtained with the diamond anvil cell under static conditions for calibration. The physical differences between a real EHD contact and one simulated with the diamond cell do, however, require a model to map static into dynamic data. The main difficulties are (a) the absence of shear under static conditions, (b) the near impossibility of producing fluid films statically as thin as those sheared ($0.1\text{--}0.5\text{ }\mu\text{m}$), (c) providing for equivalent film boundaries (diamond vs. metal), and (d) different heat transfer characteristics. The following sections will describe a model approaching these requirements. It is based on the radiation transfer theories developed by the astrophysicists for estimating temperatures in stellar atmospheres. However, drastic simplifications had to be made.

2.5.1 (Cont'd)

Since our Hertzian contact consists essentially of a flat plate of dielectric, the fluid, sandwiched between a flat metal surface (the flattened portion of a ball surface) and a diamond window, the schematic diagram of Fig. 5 will represent the situation. Following a more detailed analysis made by Viskanta, Hommert, and Groninger¹⁵ of a similar situation encountered with a heated glass sheet, the starting equation is the steady-state radiative transfer equation for a plane layer of a nonscattering, semitransparent dielectric (the fluid film in our case) in local thermodynamic equilibrium. With azimuthal symmetry and--for the moment--restriction to one-dimensional radiation transfer and one spectral frequency, this equation is

$$\frac{dI(y)}{dy} = -k[n^2 I_B(t) - I(y)] \quad (12)$$

where $I(y)$, k , n , and I_B are respectively the monochromatic intensity (radiance), spectral absorption coefficient*, index of refraction, and Planck blackbody function at absolute temperature t , all at wavenumber ν . It is convenient to separate $I(y)$ into two contributions: the intensity in the forward direction (increasing negative y), $I^+(y)$, and that in the negative direction, $I^-(y)$. By solving Eq. (12) in the standard way, using the appropriate boundary conditions, the outwardly emerging intensity at wavenumber ν turns out to be proportional to

$$\begin{aligned} I^+(0) &= A + B, \text{ with} \\ A &= (1-R_1) (1-R_1 R_2 T^2)^{-1} (1-R_2) T B_M \quad \text{and} \\ B &= (1-R_1) (1-R_1 R_2 T^2)^{-1} (1-T) (1+R_2 T) B_F \end{aligned} \quad (13)$$

where R_1 and R_2 are the reflectivities* at the two boundaries, $T = \exp(-kh)$ is the transmissivity through the fluid, h is the fluid film thickness, B_M and B_F are $I_B(t_M)$ and $I_B(t_F)$, i.e., the Planck radiation functions evaluated for the metal surface and average film temperatures respectively. Equation (2) corresponds to Eq. (18) of the article by Viskanta, Hommert, and Groninger.¹⁴

It is evident that Eq. (13) could have been derived from first principles without formally solving Eq. (12), for A is evidently the radiant intensity emerging from the fluid as a result of radiation from the metal surface, which is transmitted through the two interfaces and attenuated on its way and B is the radiant intensity of sources

*assumed to be independent of temperature

2.5.1 (Cont'd)

$$\frac{B_M}{B_F} = \frac{\frac{C_2}{\lambda^5 T_F^4} - 1}{\frac{C_2}{\lambda^5 T_M^4} - 1} \quad (17)$$

for $B_M/B_F \ll 1$, $(1-R_2) B_M/B_F$ is neglected in Eq. (16).

Here T_F and T_M are the absolute film and metal surface temperatures, λ is the absorption band wavelength in meters and $C_2 = 0.014388$ mK, the universal radiation constant. The baseline band intensity is proportional to

$$I^+_{\text{eff}} = E_F^{\text{eff}} B_F \quad (18)$$

In the high pressure diamond anvil cell, schematically shown in Fig. 13, the fluid film is sandwiched between two diamond windows and the entire setup is isothermal. The outwardly emerging intensity is proportional to

$$I^+(0) = \frac{(1-R_1)(1-T)}{1-R_1 T} B_F = E_D B_F \quad (19)$$

an equation readily derived from Eq. (13) by setting $B_M = 0$ and $R_1 = R_2$.

A calibration of band intensity in the diamond cell versus temperature (it is not necessary to compute B_F explicitly) for a fluid layer of known thickness will thus yield E_D , from which E_F^{eff} can be calculated when R_2 , B_M/B_F , and h are known (say from separate experiments). Once E_F^{eff} is known, the temperature of the EHD film can be determined from the corresponding emission band intensity of an EHD film.

2.5.1 (Cont'd)

The effect of the front diamond window on the emission of the fluid film has been assumed to amount to an attenuation factor equal for both the diamond cell and the contact film so that calibration takes care of it automatically. If the reflected portion of the emerging radiation at the front diamond surface returns into the fluid and re-emerges to a significant extent, this argument may not be strictly true. However, the difference due to this assumption will be much less than our various experimental errors. It also seems unlikely that thermal radiation from the fluid film could be coherent enough to cause significant interference phenomena; none were observed in our work.

Perhaps the neglect (in the work reported here) of the last term in Eq. (16), viz., $(1-R_2)B_M/B_F$, in temperature calculations is a more serious error than the foregoing. It can be accounted for computationally by a loop-type correcting procedure, since knowledge of B_M/B_F must precede the determination of B_F from Eq. (18). Omitting the term is equivalent to assuming $(1-R_2)B_M/B_F$ small compared to $1+R_2T$. Typically for $R_2 = 0.72$, $T = 0.5$, $t_M = 50^\circ\text{C}$, and $t_F = 80^\circ\text{C}$, this amounts to an E_F^{eff} that is 16 percent too small. Our present radiometrically deduced temperatures could thus be too low, especially for thick films absorbing considerable radiation (small T). This problem will be attended to later, when better film thickness values (h) and calibration data will be available to us.

2.5.2 Reduction of Emission Spectral Data to Temperatures

The procedures for obtaining film and ball surface temperatures will now be detailed. The film temperatures were based on the intensities of the 700 cm^{-1} band of polymethylstyrene. The ball surface temperatures were based on the spectral responses at 660 and 810 cm^{-1} . At these frequencies the fluids have no infrared bands so that the responses are entirely graybody.

For the following discussions, two definitions are needed:

(i) Spectral response, r , is defined at a wavenumber, ν , as the fraction of the maximum signal--assigned a value of unity--(which almost invariably occurred at the same frequency recorded between 630 and 930 cm^{-1}) multiplied by (a) the greatest unnormalized amplitude computed in our standard way, and (b) the amplifier gain factor.

(ii) Band strength, P , is defined as the baseline band area measured in a spectrum in units of spectral response times wavenumber.

2.5.2 (Cont'd)

The procedure of drawing baselines is admittedly arbitrary, but with consistent criteria it is quite reproducible. In our case, we drew average lines on both sides of the band to be measured in such a way that they would meet near the wavenumber of the band peak. Often a shoulder in the band contour indicated the location of the baseline quite naturally.

2.5.2.1 Ball Surface Temperatures

Simple calibration experiments are sufficient to determine the ball surface temperatures from the spectra in all cases. All that was needed experimentally was to record spectra under our standard conditions for the stationary ball while the fluid in the cup was kept at a constant elevated temperature by circulating warm water through the coil. Curves of spectral response vs. temperature for different reference settings were drawn.

From these curves and corresponding spectral responses for the EHD runs, ball surface temperature could be estimated to within $\pm 2^\circ\text{C}$.

2.5.2.2 Fluid Film Temperature

An attempt was made to obtain the necessary calibrations from contact region spectra at zero rotational speed in a way analogous to the calibrations for the ball temperature. For this purpose the ball was held in the fluid-filled cup in such a way above the diamond window as to just make contact. Under these conditions the film thickness was taken as the distance between the circumference of the ball and its tangent, the flat plate formed by the diamond window, averaged over the diameter of the instrument's field of view. However, this idea failed when it proved to be impossible to locate the ball at the precise tangent position. Accordingly a high-pressure diamond anvil cell was aligned in place of the ball/plate apparatus and emission spectra were recorded under known conditions.

To record the pressure in the cell the ruby chip method originally developed by Block, Piermarini, and their co-workers¹⁶ at the National Bureau of Standards was used. (We developed a simple spectrometer for this purpose, which is described in our Paper No. 21). Spacer thickness proved to be a problem, for no suitable metal sheet of thickness equivalent to that of an EHD film is commercially available.

2.5.2.2 (Cont'd)

Dilution with an inert solvent was used for some of our test fluids as a substitute for thinner gaskets, but unpredictable interactions between solvent and solute can make this procedure highly suspect. For this reason we needed thinner gasket material. While it is possible to etch certain metals thinner by using HF/HNO₃, we were able to obtain some 6 μ m, 3 μ m and 2 μ m tantalum sheet and used this for certain of the test fluid runs. It is not easy to handle this material but it can be accomplished with reasonable effort.

With the diamond cell infrared bandstrengths can be obtained as a function of temperature by exactly the same interferometer setup as that used for the EHD spectra. For example, in the work with the poly-alpha-methylstyrene diluent, the 700 cm⁻¹ base lineband areas were measured and found to be a function of temperature according to the empirical equation

$$P_{700}^D = ae^{bt} \quad (20)$$

where a and b are empirical constants (a = 0.2627, b = 0.0668) and t is the temperature. It turned out, as expected, that the plots were almost independent of restrictor size. Absorption spectra were also obtained under analogous conditions and a mean absorption coefficient of $k = 2000 \text{ cm}^{-1}$ was determined for the 700 cm⁻¹ band area. The emissivity for the diamond cell was calculated according to Eq. (19), using a reflectivity of $R_1 = 0.04432$ for the diamond/fluid interface. This value was computed from the Fresnel equation¹⁷ for normal incidence using $n = 2.23$ for the refractive index of diamond at 700 cm⁻¹ and $n = 1.5$ for the mean refractive index of the fluids in the temperature range considered.

Emissivities for the fluid films in the contact region were calculated by Eq. (16) for the same polymethylstyrene band at 700 cm⁻¹ for a range of thicknesses h. For the reflectivity of the metal/fluid interface Winer's value of $R_1 = 0.72$ was chosen while the same value of $R_1 = 0.04432$ was used for the diamond/fluid interface as before for the diamond cell. A table of E_f/E versus h was computed. With the help of this table E_f/E_D values corresponding to any experimental film thickness could be found which, when divided into the experimental bandstrengths P_{700} , would yield P_{700}^D bandstrengths, i.e., bandstrengths for the diamond cell equivalent to those observed from the contact region. The empirical equation, Eq. (20) in the tabular form was then used to calculate average film temperatures.

2.5.2.2 (Cont'd)

It should be noted that the h used in Eq. (20) was only one-third of the actual (computed) film thickness when polymethylstyrene diluent was present in a dilution of one-third. Furthermore, it was noted that changes in R_1 even as great of a factor of two would not affect the ratio E_f/E_d very much. Thus temperature variations and even anomalous dispersion of refractive index would not seem to be important with the diluent.

These procedures will be illustrated in Section 3.3 discussing our work on polyphenyl ether fluid.

2.6 Diamond Anvil Cell Pressures and Glass Transitions Under Pressure

In order to obtain background spectral information for our dynamic infrared spectra the diamond anvil cell turned out to be an essential tool. With it infrared absorption or emission spectra could be obtained at various known temperatures and pressures. Fortunately for us, Block, Piermarini, and their co-workers¹⁶ at the National Bureau of Standards had just published their work on the ruby fluorescence method for pressure measurement. Crystals of ruby are immersed in the liquid sample. As the pressure is raised by squeezing the two diamond anvils against each other, the wavelength of the main ruby fluorescence peak is increased by 0.365 Å/kbar. Temperature also increases the peak's wavelength at the rate of 0.068 Å/°C. Both the pressure and the temperature shifts are linear over a very wide range and independent of each other. "Glass" transition temperatures--or pressures at given temperatures--can also be deduced from the ruby fluorescence spectrum. As the liquid becomes so viscous that pressure in the sample volume is no longer equal throughout but is different in the center and near the edges, for example because of elastic deformation of the diamonds, different ruby crystals dispersed in the liquid are at different pressures, thus giving rise to a broadening of the fluorescence band.

The NBS procedure is now generally used in high-pressure work on liquids. Our problem in adopting it was the lack of a high resolution spectrometer. Our solution was a tilting filter spectrometer, making use of the change of transmission of a narrow-band interference filter with angle of incidence. This instrument worked very well for us. By measuring the time rate of change of fluorescence bandwidth, from a large initial width to a much smaller one after standing for hours or days, the viscosity of liquids at elevated temperatures and pressures could also be determined. In principle, this procedure is similar to the rate of fall measurement of a spherical particle developed by Block, et al. Our spectrometer design was published and a patent for the viscosity determination was applied for (see Appendix).

2.6 (Cont'd)

Recently we found that the glass transition pressures obtained in this way for some fluids were higher than literature values. Microscopic examination of the pressurized sample between crossed polaroid sheets showed a cellular structure. The cell bodies transmitted light, but the boundaries were black. Fig. 14 contains a schematic sketch of such a material under an intermediate pressure, estimated at about 4 kbar. As the pressure was further increased, most of the boundaries disappeared and the transparent material became colored. Sometimes a black cross appeared in the center. This behavior occurred whether ruby chips were present or absent in the sample.

It would appear--work is needed to substantiate this idea--that light transmission through the sample between crossed polaroids becomes appreciable before the ruby fluorescence band is noticeably broadened. At this point the material has been converted from a liquid into platelets of crystals or glass, rotating the plane of polarization. The cell "boundaries" remain black under crossed polaroids because of "phase contrast" or because they contain "fluid". In the presence of some additives, the boundaries are thicker. At still higher pressures these platelets fuse together and the thickness of these platelets becomes different enough in different regions of the sample space to produce interference colors. In other words, the situation becomes similar to that observed with uniaxial crystals under the polarizing microscope. The reason for the higher pressure needed to produce appreciable fluorescence band broadening with the ruby chips is the potential movement of the separate platelets around these chips, which equalize the pressure. Note that the pressure in the diamond cell is non-uniform for solids.

We believe that this explanation of our observations--if confirmed--can be of practical significance in lubrication. The small platelets--glassy, crystalline, or liquid crystal, if you will--can be the lubricant under intermediate pressure conditions. Additives are squeezed out from solution as their solubility is decreased by pressure. This factor is sometimes overlooked.

Light transmission between crossed polaroids seems to be a better criterion of crystal or "strained" glass formation from a fluid than broadening of the fluorescence spectrum of dispersed ruby chips. It would be a simple matter to build a system based on these phenomena to determine the transition points quantitatively.

In the preceding section the need for extra thin gaskets for infrared spectroscopy was discussed. The tantalum gaskets solved that problem, but introduced another one: How does one get ruby chips thin enough to fit into the gasket hole, small enough in cross-section so as not to block much of the sample volume, and yet fluorescing with sufficient strength to provide good fluorescence peaks for measurement? Really we have not yet solved

2.6 (Cont'd)

this problem in a practical way. Perhaps Klaeboe's cyclohexanol¹⁸ is then a more practical pressure indicator (OH shift in the infrared spectrum) than ruby, despite the evident drawbacks. Perhaps the observations just described can become the basis of a new procedure.

3. RESULTS

3.1 Emission Spectra with the Diamond Anvil Cell

The first question at the beginning of this work was, of course, whether emission spectra of thin films could be obtained at all when these films were confined between windows or between one window and a metal surface. As a matter of fact, recent literature is conflicting for thin films merely on metal surfaces. Indeed, these films are much thinner than those encountered in bearing situations, being absorbed layers. However, since such layers are also of interest to us, mention of them here is pertinent.

Thus in one and the same issue of *Spectrochimica Acta*, Baumgarten¹⁹ stated that "it seems to be impossible to investigate adsorbed species on a metal mirror using emission techniques," and Blanke and Overend²⁰ described their emission spectra of stearate films on a gold substrate. The work of Greenler²¹ on reflection techniques is also important here. Greenler pointed to the role played by the direction of the vibrating molecular dipole causing infrared absorption. Baumgarten gave interference in the film as a reason for impossibility of emission spectroscopy; evidently it is possible to avoid these difficulties.

Keeping these and other potential troubles in mind, we were therefore very pleased when we were able to get our spectra of Fig. 15, showing the almost perfect agreement between emission and absorption for the Sun Traction Fluid. This particular figure has been widely quoted and it made its way into a book on "Spectroscopic Techniques." The point is that the diamond cell is perhaps the ideal tool for infrared emission spectroscopy. The sample volume is very small and almost buried in a bulky metal holder, the bulk being necessary for holding high pressures. This bulk insures temperature uniformity of the sample and the diamond windows, being infrared-transparent and therefore non-radiating and the best heat conductors known, insure temperature uniformity within the sample. Self-absorption phenomena, which can totally obliterate spectral features, are therefore absent. For these reasons infrared emission spectroscopy of fluids in the diamond cell is one of the most sensitive instrumental methods of analysis--a realization that came to us as a spin-off from this work.

An analysis of the various factors involved in quantitative accuracy was made and will be published soon. For example, the angular field of view and polarization by reflection at the interfaces were taken into account. For the purpose of calibration most of them are not very important since empirical data would be relied on.

3.2 Calibration and EHD Spectra of 5P-4E Polyphenyl Ether

As was stated in the Introduction, the work under the AFOSR contract was more concerned with establishing the methods than the collection of lots of data, since our parallel NASA contract was more clearly designed for that. However, some fluids were studied as part of this contract and 5P-4E was studied most extensively since (i) it is a characteristic and useful "advanced" lubricant of high temperature stability, (ii) it readily fails under certain operating conditions, thus falling clearly within the scope and title of this project, (iii) it has been studied by other investigators and hence has data available for comparison, and--importantly for our work--it has an exceedingly intense infrared spectrum owing to its highly aromatic character. Table III lists some of its pertinent properties.

Fig. 16 shows an emission spectrum of our 5P-4E fluid (trade name OS-124) in the diamond cell at low pressure. The most important features in the frequency region shown are the aromatic band at $\sim 690\text{ cm}^{-1}$, corresponding to the 700 cm^{-1} band of poly-alpha-methylstyrene previously mentioned and a doublet between 750 and 780 cm^{-1} , which reflects the mono- and disubstituted character of the five phenyl groups in the molecule. The sample temperature was only 41°C , only 16°C above room temperature, yet the spectrum certainly stands out rather clearly. Fig. 17 is a duplicate spectrum, where the temperature was just one degree higher, but the reference radiation was increased (restrictor 1.5 inch diameter instead of 0.75 inch). The greatest unnormalized amplitude thus decreased from 0.102×10^6 to 0.933×10^5 . As can be seen, the difference between the two spectra are slight, showing good reproducibility. Fig. 18 was taken under the same conditions as the preceding spectrum, except that the temperature was raised to 52.5°C . The small wiggles have now disappeared, only a trace of a shoulder is left of the 750 cm^{-1} band and the (combined) 780 cm^{-1} band is now just as high as the 688 cm^{-1} band. Both main bands are also broader. The reason for the equalization of band heights was given in Section 2.1.1.1; in simple terms, both bands now peak at maximum emissivity so that increased intensity can only contribute to greater width. This situation is analogous to totally absorbing absorption bands; their depth will be the same. At still higher temperatures the spectrum no longer showed discrete emission bands, just a continuous "blackbody" curve. Clearly, both the emission of 5P-4E and the overall radiation increase with temperature.

By diluting the 5P-4E 10:1 with pentaerythritol tetraheptanoate ester it was possible to obtain emission spectra at even higher temperature, e.g., Fig. 19 shows the spectrum at 72°C . Note that the bands have not changed essentially, except for intensity.

3.2 (Cont'd)

These diamond cell emission spectra contain emission from the fluid, partial reabsorption within the fluid, and hopefully very little emission from the gasket between the diamonds and the cell body. The field of view of the objective lens was set in the same way as for the dynamic EHD experiments and the reference was set similarly, so that the diamond cell spectra (band intensities) could be used as temperature calibration for the dynamic spectra. A flat metal plate held a very short but known distance away from the diamond window in the EHD experimental apparatus could provide a more realistic film for emission spectra calibration than the diamond cell. Its temperature would be that prevailing in the cup. However, the diamond cell could also provide information on spectral changes with temperature and pressure as will be shown in Section 3.5, while the flat plate method was valid only at ambient pressure.

Dynamic spectra from the EHD contact region were obtained at various loads, ball speeds, and bath temperatures, for at least three conditions of every variable. The significance of these variables in terms of Hertzian pressures and linear velocities are given in Table 4. Fig. 20 was our first 5P-4E spectrum from the Hertzian contact region. The 690, 750, and 780 cm^{-1} peaks are clearly present (the 730 cm^{-1} absorption band is due to the Mylar beamsplitter). At this low speed and load the spectrum was very similar to the diamond cell spectrum of Fig. 17. The greatest unnormalized amplitude (GUA) for Fig. 20 was 0.89×10^5 . When only the ball speed was increased from 240 to 360 RPM, the GUA (Fig. 21) changed only slightly to 0.94×10^5 and the 690 cm^{-1} band hardly changed. However, the 750/780 cm^{-1} doublet shifted very strongly toward higher frequencies and changed substantially in appearance. The peak strength of the doublet also decreased in relation to the 690 cm^{-1} peak. There is no doubt that the wave-number scale remained properly in place, for the Mylar absorption band did not shift in frequency. Further increase of rotational speed to 480 RPM left the GUA again essentially unchanged (0.95×10^5), but this time the strength of the 690 cm^{-1} band was increased and the 750/780 cm^{-1} doublet became an even weaker triplet.

The preceding three dynamic spectra were taken at an intermediate fluid reservoir temperature to start with (cooling bath temperature at 36°C). The corresponding series at lower fluid reservoir temperature (Figs. 22, 23, and 24) show total and partial inversion of the 690 cm^{-1} peak, similar to that observed for Mylar at different reference levels (Fig. 12). Evidently the reference radiation energy exceeded the graybody

3.2 (Cont'd)

radiation energy from the contact. The greater resolution of the 450/480 cm^{-1} doublet and the shift of these bands and the 690 cm^{-1} band toward higher wavenumbers is especially pronounced in Fig. 24.

The contrast of the preceding series of spectra with those of Figs. 25, 26, and 27 (high cooling bath temperature, high load, and varying ball speeds) is interesting. There is now hardly any change in the spectra with speed and the doublet is reduced to a plateau.

3.3 Polarized EHD Emission Spectra of 5P-4E Polyphenyl Ether

The spectra described in the preceding section showed that the 690 cm^{-1} aromatic band was--except for intensity--rather little affected by changes of ball speed or Hertzian pressure, but the 750/780 cm^{-1} doublet was rather significantly affected. The 690 cm^{-1} band is therefore well-suited for comparisons of film temperature, just as the 700 cm^{-1} band of poly-alpha-methylstyrene, which we used in this way for our earlier work on fluids diluted one-third with this "infrared indicator." One possible reason for the changes in the appearance of the 750/780 cm^{-1} doublet is solidification of the fluid or of some of its components, another is a change of molecular orientation, be it due to solidification as a crystal, as a strained glass, or as an adsorbate. Winer²² has shown that 5P-4E is likely to be a glass under many of these operating conditions.

We therefore picked out one set of operating conditions and obtained EHD spectra without polarizer, with a polarizer oriented with its plane of vibration of the electric vector parallel to the EHD conjunction line and with its plane of vibration oriented at right angles to the conjunction line. As this work was done with the old setup, i.e., the Mylar beamsplitter which itself is a polarizer of 75 percent efficiency (our recent work with the germanium beamsplitter does not have this bias), the data are not the best. However, if the Mylar beamsplitter was indeed acting as an analyzer of polarized infrared radiation, the results of these experiments should confirm it.

Fig. 28 is the base spectrum (no polarizer) for these operating conditions (480 RPM, 11 Kg load, an intermediate fluid reservoir temperature). The 690 cm^{-1} band was partly intersected by the reference level; hence the "ditches" on both sides of it

3.3 (Cont'd)

and predominantly on the high-frequency side. The $750/780\text{ cm}^{-1}$ doublet is clearly shown. Fig. 29 is the corresponding spectrum with the polarizer in the conjunction line position. Now the $750/780\text{ cm}^{-1}$ doublet is much better resolved. Fig. 30 corresponds to the polarizer set at right angles to the conjunction line. Since this orientation is also at right angles to the polarization plane set by the Mylar film, the intensity of this spectrum is much weaker and the "ditches" relatively stronger (note that the ordinate scale goes negative). Nevertheless one can see that the form of the 690 cm^{-1} emission band is essentially the same as before, but of the $750/780$ doublet only the first component is standing out; the other is barely a shoulder. Now the resolution of this doublet is cut down. Some in-between positions, i.e., between the in-line 12 o'clock and the crossed 3 o'clock position of the polarizer, were also run. For example, Fig. 31 and Fig. 32 represent the 11 o'clock and the 2 o'clock positions. These spectra are almost identical; now the 780 cm^{-1} component of the doublet is standing out alone. From these spectra one could conclude the plane of the molecular alignment is not in the 12 o'clock position.

There is clearly much more to be learned from polarization spectra. The orientation of the 750 and 780 cm^{-1} band are different. If the bands belong to different species, conditions may promote one or the other.

3.4 EHD Film and Surface Temperatures for 5P-4E from Infrared Emission Spectral Data and Thermocouple Measurements

During every experiment in which an emission spectrum was recorded (taking about 15 minutes), at least the temperatures next to the diamond window, the ball surface, and in a quiescent region of the fluid reservoir were also recorded. An example of such a record is shown in Fig. 33 for a run with OS-124. Note that the temperature increase at the diamond is essentially instantaneous when the speed is increased, then all the temperatures reach a level value. Spectral recording did not begin until level values were reached.

Table 5 gives the temperature data and film thicknesses obtained by optical interferometry for series of runs. The temperatures have been defined as t_f (average fluid film from spectrum), t_d (diamond), t_m (ball metal surface from radiation), and t_b (fluid near ball). Various temperature differences are also shown. Some of the fluid film temperatures (all of them obtained from the 690 cm^{-1} peak strength) turned out to be exceedingly high. We believe they are realistic for shortly

3.4 (Cont'd)

after these runs the ball became scored and the fluid contained black particles (failure). Ferrographic analysis carried out by Mr. William R. Jones, Jr. at NASA-Lewis showed the usual metal particles. Our own x-ray analysis showed the presence of iron carbide.

Perhaps the various temperature plots can provide more insight into the mechanism by which failure had occurred. The behavior of Hertzian film thickness and the difference of temperature between fluid and metal surface as the load is increased is shown in Fig. 34 for three constant speeds on three plots corresponding to cooling bath temperatures of 30, 18, and 0°C, the lowest temperature being at the bottom. As the load is increased, film thickness is decreased and temperature increased as expected. This is, of course, as it should be. However, the sharpness of the break in the curves at a given load for every speed and the subsequent constancy of thickness while the temperature is shooting up was, at first sight, rather surprising. It did not occur for any of the fluids we had studied previously. The temperature difference at the breaks is highest for the lowest cooling bath temperature, yet the "limiting" film thickness was about 0.5 μm in all of the three groups of plots.

It thus looks that once the film thickness has been reduced below the limiting value by increase of load, decrease of speed, or increase in initial fluid temperature, further changes of these parameters in the same direction will lead to catastrophic increase of film temperature with respect to metal surface temperature.

The polarized infrared emission spectra of Figs. 31, 32, and 33 were not taken under condition of this minimum film thickness. Unfortunately, polarized spectra under different conditions were not collected, primarily because the lower spectral intensity did not then permit further reduction by polarization. Our present experimental conditions would permit the recording of these spectra. Balls of different asperity heights should also be investigated.

Other plots, e.g., shear rate (speed divided by film thickness) against the various temperatures and temperature differences could be easily obtained from the data of Table V. They would convey the same message: Avoid the critical film thickness.

These data from OS-124 have not been published before. However, similar data have been reported for other fluids in our NASA reports (see publications list), which refer to work done with the poly-alpha-methylstyrene diluent.

3.5 Differences in Infrared Spectra of Fluids with Pressure

The following high (10 kbar) and low pressure (1 kbar) spectra were obtained at room temperature with the diamond cell and are reported here for the first time:

(i) Fig. 35, N-1, a standard naphthe fluid studied by other investigators. The changes in the $700\text{--}1200\text{ cm}^{-1}$ region are rather striking. Their study is not yet complete, but a change of rotational isomer concentration is a possible cause. These changes are pronounced enough to allow inferences on pressure in dynamic spectra.

(ii) Fig. 36, Synthetic paraffin. At high pressure most features weaken or disappear (note, in particular, the 720 cm^{-1} band).

(iii) Fig. 37, OS-124, 5P-4E polyphenyl ether. Only very small changes occur in the spectra.

(iv) Fig. 38, Krytox, fluoro-ether. At high pressure bands broaden and a satellite band at 1210 cm^{-1} disappears.

Other similar spectral data will be reported in our NASA report.

3.6 Polarization Studies of N-1 (Naphthenic) Fluid

Figure 39 shows an emission spectrum from the contact zone obtained when a typical naphthenic fluid (N-1) (base oil, no additives) was sheared between the rotating ball and the diamond plate. The experimental conditions provided a linear surface sliding velocity of about 0.6 meters per second, a contact pressure of about 6 kbar and an average film thickness of about $0.1\text{ }\mu\text{m}$ over the Hertzian area, i.e., the conjunction region where the ball surface is flattened by elastic compression. The temperature in the bulk of the fluid was maintained near 30°C . Three emission peaks, near 1320 , 1430 and 1490 cm^{-1} , and a shoulder near 1450 cm^{-1} are evident in the $1300\text{--}1500\text{ cm}^{-1}$ region. The standard absorption spectrum of the fluid over this region showed maxima at 1315 , 1350 , and 1450 cm^{-1} , of which the last one was by far the strongest. For a number of reasons relative intensities of emission peaks can be different from those of the corresponding absorption peaks: (1) these emission spectra are uncorrected, single beam spectra (though normalized for maximum ordinate spread), (ii) thermal radiation drops with increased wave-number in this region according to the Planck curve for the prevailing

3.6 (Cont'd)

temperature, and (iii) diamond windows adsorb some radiation. However, the apparent split of the 1450 cm^{-1} band is not produced by any of these reasons but is due to self-absorption caused by a temperature gradient through the fluid layer.

It could be argued that the dip at 1450 cm^{-1} is not reabsorption of infrared emission originating within the oil film, but simply an absorption band produced by fluid absorption of radiation emitted by the ball surface. To counter this argument, the radiant intensity was measured at several wavenumbers in parts of the spectrum where the fluid is totally transparent. This radiation is the graybody radiation from the ball surface. By a calibration procedure it was possible to determine from the Planck radiation laws that the ball surface temperature was significantly less than that of the film (determined by calibration of emission band intensities). The temperature measured with the thermocouple whose junction was attached to the edge of the diamond window was also below that of the fluid film. From these results we deduced that the region of maximum temperature is in the fluid film itself.

When a polarizing disc was introduced into the radiation path, just ahead of the detector with its plane perpendicular to the optic axis and the plane of polarization was set parallel to the direction of the conjunction line between the ball and the diamond plate, the spectrum of Figure 40 was obtained. All the experimental conditions remained the same. The vertical scale of the plot was normalized as before, resulting in a scale-expansion ratio of about two with respect to the spectrum of Figure 39. It should be pointed out that the interferometer with the germanium beamsplitter does not favor one direction of polarization over any other to any appreciable extent and that the geometry under static conditions is circularly symmetrical throughout. Except for relative intensities there is little difference between the spectrum of Figure 39 and that of Figure 40. Reabsorption of the 1450 cm^{-1} peak still takes place and there also appears reabsorption on the high wavenumber side of the band.

When the polarizing disc was turned 90 degrees about the optic axis of the interferometer, the spectrum of Figure 41 was obtained. Now the peak of an emission band is found at 1450 cm^{-1} and this peak is surrounded by valleys on each side. Thus the band is mainly a re-absorption band, but the peak is strong enough to show through as emission.

Similar polarization phenomena were found with the same oil under different operating conditions. Other fluids would -- or would not -- exhibit polarization phenomena. Since the 1450 cm^{-1} band is ascribable to hydrogen bending vibrations whose dipole moment maintains a definite angle with respect to the molecular axis, these results are indicative of molecular alignment. Aside from their inherent scientific interest, they may be of considerable practical significance, for they point to changes of fluid behavior and properties under various operating conditions.

3.7 Spectra Along the Conjunction Line

Figure 42 shows an emission spectrum of the central portion of the conjunction region of a low-load (10 kg, about 0.6 kbar), high speed (*480 RPM, about 1.5 m/sec.), low temperature (cooling bath temperature 15°C) run with a mono-substituted aromatic fluid. The three principal infrared bands are marked. They are clearly emission peaks, though there is also some reabsorption ("bands sit in their own trough"). Since the film temperature is highest in this region, reabsorption is minimized, although even here (film thickness estimated as $\sim 0.2\text{ }\mu\text{m}$) the temperature gradient is unmistakable. A computer program will be employed to fit this spectrum to a gradient in such a way as to make the "troughs" disappear. Clearly, then, the EHD film is not isothermal and a proper film temperature profile through the EHD region should include both x, y, and z directions.

Figure 43 corresponds to the same conditions, except that the region looked at was slightly displaced towards the exit region. The 690 cm^{-1} aromatic band is standing out a little more over its background and its peak is displaced toward lower frequency, both observations being in line with somewhat higher temperatures. The $757/775\text{ cm}^{-1}$ doublet has fused into one band.

Figure 44 is the spectrum when the observed region was displaced toward the inlet side. The cooler temperature is indicated by the reabsorption of the 690 cm^{-1} peak, higher wavenumbers, and the (asymmetric) split of the $745/775\text{ cm}^{-1}$ doublet.

Figure 45 corresponds to Figure 42, but at twice the load. Now the 690 cm^{-1} band is much broadened and the 745 cm^{-1} band shows evidence of peak reabsorption, while the 775 cm^{-1} partner of the doublet is much enhanced.

The relative intensities of these three bands, and especially of the doublet's components might well correspond to solidification. This possibility will be further investigated.

3.8 Friction Polymer Deposits

In some instances a "friction" polymer was deposited on the diamond surface, showing a characteristic wake-like pattern. The deposit appeared to be white, very strongly attached to the diamond -- it had to be removed by scraping -- and exceedingly thin. Figure 46 is an example of the one formed after a number of runs with a naphthenic fluid containing tricresyl phosphate. No such deposit was formed without the additive. The deposition of this material had some effect on the spectra prior to its detection, but no definitive spectrum of the polymer itself could be recorded with the effort spent. Traction and lubrication properties also changed as the polymer was deposited.

4. CONCLUSIONS

The work has shown that infrared emission spectroscopy is a useful approach for following lubricant failure in bearings under elastohydrodynamic lubrication. Extended studies of polyphenyl ether (5P4E) in particular have shown large rises in the difference between fluid film and metal surface temperatures and significant spectral changes prior to failure. The temperature of the fluid films are not uniform, which is manifested by the shape of spectral emission lines.

Polarization phenomena have been demonstrated, indicating an alignment of the fluid molecules. This alignment could be due to glassification and stresses in the glass (photoelastic effect), crystallization, or to flow polarization. In either case the viscosity of lubricant would be different from the value extrapolated to the temperature and pressure conditions prevailing in an elastohydrodynamic contact.

The development of the method constituted a large proportion of this effort. Further work will apply it to many situations of critical value to Air Force lubrication problems.

5. ACHIEVEMENTS DURING 1977

5.1 Apparatus

a. Smoother (than the previously used steel balls) gold-plated steel and ceramic balls were obtained and a special rig made for them and installed. Their reduced surface radiation will improve the quality of lubricant emission spectra.

b. Reduced field of view spectra were obtained from the Hertzian area (Section 3.7). However, this work was done by reduction of the iris diaphragm rather than by installation of a different objective lens (for reasons of time).

c. A new radiation chopper (tuning fork) was installed and used to great advantage (Figure 7). It made the polarization measurements possible in conjunction with the new beamsplitter.

d. A germanium beamsplitter helped extend the range of our spectrometer to 2 μm .

5.2 Data Collection

The polyphenyl ether and polarization data presented constitute our main achievements. More detail is given in the body of the report.

5.3 Data Analysis

Most interesting are the 5P4E polyphenyl ether data of Sections 3.2, 3.3, and 3.4.

5.4 Other Techniques

Debris from the 5P4E polyphenylether experiments was analyzed microscopically, by x-rays, and ferrographically (at NASA-Lewis) (Section 3.4). Attempts were made to analyze friction polymer deposits.

6. REFERENCES

1. Hordvik, A., "Measurement Techniques for Small Absorption Coefficients: Recent Advances," Applied Optics, 16, 2827-83 (1977)
2. McMahon, H. O., "Thermal Radiation from Partially Transparent Reflecting Bodies," J. Opt. Soc. Am., 40, 376-80 (1950)
3. Gribov, L. A., Intensity Theory for Infrared Spectra of Polyatomic Molecules." Consultants Bureau, New York 1964, pp. 103-110.
4. Fabbri, G., and Baraldi, P., "Infrared Emission Spectra of Solids," Applied Spectroscopy, 26, 593 (1972)
5. Steger, E., and Rasmus, D., "Comments on "Infrared Emission Spectra of Solids" by G. Fabbri and P. Baraldi," Applied Spectroscopy, 28, 376-377 (1974)
6. Stejskal, E. O., and Cameron, A., "Optical Interferometry Study of Film Formation in Lubrication of Sliding and/or Rolling Contacts," NASA CR-120842, MRC-SL-345, April 1972
7. Jakobsen, J., Sanborn, D. M., and Winer, W. O., "Simulation of Severe Shear Conditions in Lubrication," Symposium on Viscometry and its Application to Automotive Lubricants, Collected and Collated by McKay, R., McMillan, M. L., and Selby, T. W., Presented at SAE National Automotive Meeting, Detroit, Michigan, May 14-18, 1973, Published by SAE, Two Pennsylvania Plaza, New York, New York, 10001, pp. 59-67.
8. Bell, R. J., "Introductory Fourier Transform Spectroscopy." Academic Press, New York, 1972. Chapter II.
9. Levinstein, H., "Infrared Detectors," Physics Today, 30, No. 11, 23-28, November 1977
10. Connes, J., and Nozal, V., "Mathematical Filtering in Spectroscopy by the Fourier Transformation," J. Phys. Radium, 22, 359 (1961)
11. Bracewell, R., "The Fourier Transform and Its Applications," McGraw-Hill Book Company, New York, 1965.

6. REFERENCES
(Continued)

12. Crook, A. W., "A Theoretical Discussion of Friction and Temperature in the Oil Film (Part III of "Lubrication of Rollers")." Phil. Trans. Roy. Soc. A., 254, 237 (1961)
13. Turchina, V., Sanborn, D. M., and Winer, W. O., "Temperature Measurements in Sliding Elastohydrodynamic Point Contacts," Trans. ASME, Journal of Lubrication Technology, Series F, Vol. 96, No. 3, 464-471, July 1974
14. Low, M. J. D., and Coleman, I., "The Measurement of Infra-red Emission Spectra Using Multiple-Scan Interferometry," Spectrochim. Acta, 22, 369-76 (1966)
15. Viskanta, R., Hommert, P. J. and Groninger, G. L., "Spectral Remote Sensing of Temperature Distribution in Semitransparent Solids Heated by an External Radiation Source," Applied Optics, 14, No. 2, 428-37 (February 1975)
16. Barnett, J. D., Block, S., and Piermarini, G. J., "An Optical Fluorescence System for Quantitative Pressure Measurement in the Diamond Anvil Cell," Rev. of Scientific Instruments, 44, 1-9 (1973)
17. Born, M., and Wolf, E., "Principles of Optics." Pergamon Press, Oxford, 1964
18. Christian, S. D., Grundnes, J., and Klaboe, P., "High Pressure Infrared Studies of Liquids with the Diamond Anvil Cell," Applied Spectroscopy, 30, 227-229 (1976).
19. Baumgarten, E., "Investigation on Infrared Emission Spectroscopy, especially of Thin Layers," Spectrochim. Acta, 32A 865-870 (1976)
20. Blanke, J. F., and Overend, J., "Infrared Spectroscopy of Surface Species; Emission Spectra from a Semi-Blackbody," Spectrochim. Acta, 32A, 1383-1386 (1976)
21. Greenler, R. G., "Infrared Study of Absorbed Molecules on Metal Surfaces by Reflection Techniques," J. Chem. Physics, 44, 310-315
22. Alsaad, M., Bair, S., Sanborn, D. M., and Winer, W. O., "Glass Transition in Lubricants: Its Relation to Elastohydrodynamic Lubrication (EHD)," Bulletin of the Japan Petroleum Institute Vol. 19, No. 1, 1-16 (May 1977)

7. TABLES

- I. Absolute Intensities* of Characteristic Infrared Absorption Bands**
- II. State-of-the-Art Sensitivities for Thin Layer Absorptions* (Absorption Coefficient k)
- III. Some Properties of 5-Phenyl-4-Ether (Five-ring Polyphenyl Ether)
- IV. (a) Mechanical Constants of Ball and Window
(b) Operating Parameters
- V. 5P-4E Runs Data

Table I

Absolute Intensities* of Characteristic Infrared Absorption Bands**

<u>Functional Group</u>	<u>Wave Number*</u>	<u>Intensity (in $\text{cm}^2/\text{molecule-sec}$)</u>
C - N	2250	3×10^{-8}
C = O	1700	100×10^{-8}
S - H	2570	1.7×10^{-8}
O - H	3600	30×10^{-8}
NH ₂	3400	10×10^{-8}
- CH	2900	40×10^{-8}
- CH	1460	6×10^{-8}
- CH	1370	2.5×10^{-8}
- CH ₂	720	0.6×10^{-8}
C - Cl	730	10×10^{-8}
C - Cl	1300	5×10^{-8}
C - Br	950	3×10^{-8}
C - Br	1300	6×10^{-8}
C - F	1050	50×10^{-8}
C - I	880	4×10^{-8}
C - I	1250	12×10^{-8}
CH (arom)	673	44×10^{-8}
CH (arom)	1500	6×10^{-8}
CH (olef)	950	40×10^{-8}
CH (olef)	1440	10×10^{-8}

* These are averages (for comparison only) for different molecules in solution or in the gaseous state.

**According to Gribov, L.A., Intensity Theory for Infrared Spectrum of Polyatomic Molecules. Consultants Bureau, New York, 1964.

Table II

State-of-the-Art Sensitivities for Thin Layer Absorptions*
(Absorption Coefficient k)

<u>Method</u>	<u>Routine</u>	<u>Possible</u>
Transmission	$10^{-3} - 10^{-4}$	10^{-5}
Emittance	$10^{-4} - 10^{-5}$	$10^{-6} - 10^{-7}$
Thermocouple calorimetry	$10^{-4} - 10^{-5}$	10^{-6}
Photoacoustic calorimetry	$10^{-4} - 10^{-5}$	10^{-6}

*According to Hordvik, A., Applied Optics, 16, 2827-83 (1977).

TABLE III

SOME PROPERTIES OF 5-PHENYL-4-ETHER (FIVE-RING POLYPHENYL ETHER)

Molecular Weight: $C_{30}H_{22}O_4$, 446	
Glass Transition Temperature at Ambient Pressure by DTA:	-23°C
Viscosity at 37.8°C, m^2/s	363×10^{-6}
at 98.9°C, m^2/s	13.1×10^{-6}
Density at 22.2°C, Kg/m^3	1.205×10^3
at 37.8°C, Kg/m^3	1.19×10^3
Flash Point, °C	288
Pour Point, °C	4.4

Source: Monsanto Chemical Company

TABLE IV

(a) MECHANICAL CONSTANTS OF BALL AND WINDOW

	Young's Modulus(E) N/m ²	Poisson's Ratio(σ)	RADIUS m
Ba11 (440C Steel)	0.200×10^{12}	0.29	0.0286
Diamond	1.05×10^{12}	0.177	∞
Reduced Elastic Modulus	0.364×10^{12}	---	---

$$\left(\frac{2}{E_1} = \frac{1 - \sigma_1^2}{E_1} + \frac{1 - \sigma_2^2}{E_2} \right)$$

(b) OPERATING PARAMETERS

Loads	Hertzian Radius		Average Hertzian Pressure N/m ²	Maximum Hertzian Pressure N/m ²
	Kg	N		
11.0	107.9	2.334×10^{-4}	6.301×10^8	0.9451×10^9
19.5	191.2	2.825×10^{-4}	7.626×10^8	1.1439×10^9
28.5	279.4	3.206×10^{-4}	8.654×10^8	1.2980×10^9

TABLE V
5P-4E RUNS DATA

Load KG	Speed RPM	Aperture (inches)	t _B °C	t _D °C	GUA x 10 ⁵	h μm	t _M °C	t _F °C	Δt ₁ [*]	Δt ₂ [*]	Δt ₃ [*]	Δt ₄ [*]
Bath Temperature 0°C												
11	240	0.75	31.0	34.0	0.340	1.40	35.5	47	13.0	1.5	3.0	11.5
	240	1.0	31.0	34.0	0.333	1.40	35.2	47	13.0	1.2	3.0	11.8
	360	1.0	31.5	34.5	0.603	1.74	38.0	46	11.5	3.5	3.0	8.0
	480	1.0	33.0	36.5	0.656	1.80	37.8	50	13.5	1.3	3.5	12.2
19.5	240	1.0	36.5	41.5	0.987	0.87	39.2	60	18.5	-2.3	5.0	20.8
	360	1.0	39.5	46.0	1.520	0.87	43.0	77	31.0	-3.0	6.5	34.0
	480	1.0	44.0	50.0	1.860	0.84	44.5	146	96.0	-5.5	6.0	101.5
	240	1.0	43.0	49.0	2.130	0.57	46.5	220	171.0	-2.5	6.0	173.5
28.5	360	1.5	47.5	50.5	1.100**	0.69	54.0	86	35.5	3.5	3.0	32.0
	480	1.5	52.0	53.5	1.540**	0.70	65.0	107	53.5	11.5	1.5	42.0
	240	1.0	36.5	39.0	0.889	1.02	39.0	52	13.0	0.0	2.5	13.0
	240	1.0	36.5	39.0	1.090	1.01	39.5	56	17.0	+0.5	2.5	16.5
19.5	240	1.0	34.0	36.5	0.890	1.17	39.0	51	14.5	2.5	2.5	12.0
	360	1.0	35.0	38.0	0.938	1.37	39.0	50	12.0	1.0	3.0	11.0
	480	1.0	36.0	39.0	0.953	1.54	38.5	54	15.0	-0.5	3.0	15.5
	240	1.0	38.5	43.5	1.640	0.77	43.5	63	19.5	0.0	5.0	19.5
28.5	360	1.5	43.0	50.5	1.800	0.69	46.5	65	14.5	-4.0	7.5	18.5
	480	1.5	43.0	45.0	2.668	1.09	51.0	87	42.0	6.0	2.0	36.0
	240	1.5	44.0	49.0	0.945**	0.57	52.0	102	53.0	3.0	5.0	50.0
	360	1.5	48.0	53.0	1.432**	0.60	60.0	129	76.0	7.0	5.0	69.0
11	480	1.5	52.5	54.5	1.863**	0.67	68.0	147	92.5	13.5	2.0	79.0
	240	1.5	38.5	40.0	1.240	0.94	45.5	47	7.0	5.5	1.5	1.5
	360	1.5	40.5	41.0	1.890	1.14	47.5	58	17.0	6.5	0.5	10.5
	480	1.5	41.0	42.5	2.190	1.26	49.5	56	13.5	7.0	1.5	6.5
19.5	240	1.5	43.5	46.5	0.709	0.66	49.5	67	20.5	3.0	3.0	17.5
	360	1.5	46.0	50.5	3.230	0.69	56.0	78	27.5	5.5	4.5	12.0
	480	1.5	48.5	52.0	1.45**	0.76	62.5	75	23.0	10.5	3.5	12.5
	240	1.5	47.5	52.0	1.39**	0.49	61.0	138	86.0	9.0	4.5	67.0
28.5	360	1.5	50.5	59.0	1.87**	0.46	68.0	220	161.0	9.0	8.5	152.0
	480	1.5	52.0	55.0	2.030**	0.66	72.0	170	115.0	17.0	3.0	98.0

*These temperature differences are defined: $\Delta t_1 = t_F - t_D$ $\Delta t_2 = t_M - t_D$ $\Delta t_3 = t_D - t_B$ $\Delta t_4 = t_P - t_M$

h = Film thickness

**Sensitivity = 30 dB, multiplied by 3

8. APPENDICES

8.1 Papers Published or Presented

1. Low Temperature and High Pressure Far Infrared Spectra of Condensed Phases: Mono- and Dimethylcyclohexanes. Applied Spectroscopy, 28, No. 1, 41-46 (1974).
2. Prepared Discussion of Paper: Temperature Measurements in Sliding Elastohydrodynamic Point Contacts by V. Turchina, D. M. Sanborn, and W. O. Winer at ASME/ASLE Joint Conference, Atlanta, October 13-17, 1973.
3. Infrared Spectrographic Analysis of Lubricants in Concentrated Contacts. Invited talk presented at Gordon Research Conference on Friction, Lubrication, and Wear, Colby College, New Hampshire, June 13, 1973.
4. Infrared Emission Spectra of Liquids in a High Pressure Diamond Cell with the Beckman-RIIC FS-720 Interferometer. The Transform, No. 3 p. 22-25, September 1974 (R. J. Jakobsen, Editor, Battelle Memorial Institute, 505 King Avenue, Columbus, Ohio 43201).
5. Analysis of Infrared Spectra of Fluid Films in Simulated EHD Contacts. Paper No. 74-Lub.-34. Presented at and Preprinted for the ASME/ASLE Joint Lubrication Conference, Montreal, Canada, October 8-10, 1974. Published in ASME Transactions, Journal of Lubrication in Technology, Vol. 97, Series F, No. 2, p. 145-150 (April 1975).
6. The Ruby Fluorescence Spectrum Method of Determining Pressure and Phase of Fluids Contained in a Diamond Anvil Cell. Paper No. 49. Presented at the 1975 Pittsburgh Conference on Analytical Chemistry and Applied Spectroscopy, Cleveland, Ohio, March 3, 1975, and abstracted in the official program of the conference.
7. Infrared Emission Spectra of Fluid Films by Fourier Transform Spectroscopy (I). Paper No. 182F. Ibid. March 4, 1975.
8. Infrared Emission Spectra of Fluid Films by Fourier Transform Spectroscopy (II). Paper No. 363. Ibid. March 6, 1975.
9. Study to Define Behavior of Liquid Lubricants in an Elastohydrodynamic Contact. NASA CR-134671, October 17, 1974. Prepared for National Aeronautics and Space Administration, NASA Lewis Research Center, Cleveland, Ohio. 95 pages \$3.00 (Unclassified).

8.1 Cont'd

10. Infrared Emission Spectra of Liquids in a Diamond Anvil Cell by Interferometry. *Applied Spectroscopy*, 29, 78 (January 1975).
11. Infrared Emission Spectra of Elastohydrodynamic Contacts, ASME Paper No. 75-LUB-10. Presented at and preprinted for the ASME/ASLE Joint Lubrication Conference in Miami Beach, Florida, October 21-23, 1975. Published in *Journal of Lubrication Technology*, Vol. 98, No. 2, April 1976.
12. Infrared Emission Spectra of Fluid Films in Bearing Contacts by Fourier Transform Spectroscopy, Paper No. 75. Presented at the 22nd Spectroscopy Symposium, Spectroscopy Society of Canada, Montreal, October 26-29, 1975.
13. Infrared Emission Spectra of Fluid Films, *American Laboratory*, Vol. 7, No. 11, pp. 27-33 (November 1975).
14. Infrared Emission Spectra of Lubricants in Operating Bearings, Presented at the 10th Middle Atlantic Regional ACS Meeting at the Marriott Hotel, Philadelphia, on February 26, 1976.
15. Infrared Emission Spectra from Lubricant Films in Operating Bearings by Fourier Methods. Paper No. 333. Presented at the 27th Pittsburgh Conference on Analytical Chemistry and Applied Spectroscopy, Cleveland, Ohio, March 1-5, 1976.
16. Analysis of Infrared Spectra of Elastohydrodynamic Lubricant Films. Presented at the American Chemical Society National Centennial Meeting, Symposium on Lubricant Properties in Thin Lubricating Films. April 6, 1976, and to be published in an ACS Journal.
17. "High Pressure Infrared Interferometry," Chapter 5 in "Fourier Transform IR: Application to Chemical Systems" (J. R. Ferraro and L. J. Basile, editors). Academic Press, N. Y., pp. 169-213, to be published in January 1978.
18. Infrared Emission Spectra from Operating Elastohydrodynamic Sliding Contacts. NASA CR-134973, Final Report on Contract No. NAS 3-18531. 87 pp. March 8, 1976.

8.1 Cont'd

19. Traction and Lubricant Film Temperature as Related to the Glass Transition Temperature and Solidification. Preprint No. 77-AM-1A-3. Presented at the 32nd Annual Meeting in Montreal, Quebec, Canada, May 9-12, 1977.
20. Glass Transition Pressures of Fluids from the Bandwidths and Frequencies of the Fluorescence Spectrum of Ruby. Paper No. 261. Presented at 3rd Annual FACSS Meeting (Federation of Analytical Chemistry and Spectroscopy Societies), Philadelphia Civic Center, November 15-19, 1976.
21. Glass Transition and Fluid Pressure Determinations from the Fluorescence Spectrum of Ruby. Canadian J. of Spectroscopy 21, 153-158 (September, October 1976).
22. Differential Infrared Fourier Emission Microspectrometer for Lubrication Studies. Paper No. M.B.3. Presented at the 1977 International Conference on Fourier Transform Infrared Spectroscopy, University of South Carolina, Columbia, S.C., June 20-24, 1977.
23. Infrared Fourier Transform Emission Microspectrometer. Paper No. 17. Presented at the 28th Pittsburgh Conference, Cleveland Convention Center, February 28 - March 4, 1977.
24. Polarized Infrared Emission Spectrophotometry with a Micro-interferometer. American Laboratory, Vol. 9, 29-40 (November 1977).
25. Polarized Infrared Emission Spectra from Operating Bearings. Paper No. 592. Invited for presentation in the Coblenz Symposium at the 29th Pittsburgh Conference, Session on Application of Fourier Transform Infrared Spectroscopy, Little Theater, Cleveland Convention Center, March 2, 1978.

8.2 Popular References to this Work

1. "The Diamond Cell Stimulates High-Pressure Research," by S. Clark and G. Piermarini, Physics Today, 44-55 (September 1976).
2. "The Strange World of Superpressure," by Joan Steen Wilentz, Popular Science, p. 80 (February 1977)
3. "Applications of Fourier Transform Spectroscopy," Chapter 3 by R. J. Bell in Spectrometric Techniques, Vol. 1, p. 123, (George A. Vanasse, editor), Academic Press, N. Y., 1977.

8.3 Patents

1. Invention Disclosure, S-76G036, "Viscosity Measuring System," for early filing with the U. S. Patent Office. Submitted on February 27, 1976.
2. U.S.P. 4,009,962 (March 1, 1977). An Emission Spectroscopic System Having Compensation for Background Radiation.
3. U.S.P. 3,399,786 (December 14, 1976). System for Spectroscopic Analysis of a Chemical Stream.

8.4 List of Mathematical Symbols

A	parameter defined in Eq. (13)
A'	parameter defined in Eq. (14)
$A(\lambda, G)$	absorptivity
a	empirical constant defined by Eq. (20)
B	parameter defined in Eq. (13)
B_F	Planck radiation function of fluid film at its temperature
B_M	Planck radiation function of metal surface at its temperature
b	empirical constant defined by Eq. (20)
c	molar concentration of solute
D	density
$E(\lambda, t)$	emissivity
E_D	emissivity of fluid in the diamond cell
$E_F(\text{eff})$	effective film emissivity defined by Eq. (16)
f	frequency
h	film thickness
I_B	Planck blackbody function
I_{band}	absolute band intensity
$I^+(\text{eff})$	effective intensity defined by Eq. (15)
$I(y)$	monochromatic intensity, radiance
$I^+(y)$	monochromatic intensity in the forward and
$I^-(y)$	backward direction
$k(\lambda, t)$	spectral absorption coefficient
m	number of molecules of absorbing species per unit volume
P	band strength
P_{700}	band strength of fluid in diamond cell at 700 cm^{-1}
$R_D(\lambda, t)$	reflectivity
R_1, R_2	reflectivities at film boundaries
$r(\nu)$	spectral response at wavenumber ν
$T(\lambda, t)$	transmissivity
t	temperature
t_f	film temperature
t_m	metal surface temperature
y	coordinate along the optic axis
$\epsilon(\lambda, t)$	molar extinction coefficient
λ	wavelength
ν	wavenumber

9. LIST OF FIGURES

1. Blackbody Spectral Radiance
2. Infrared Transmittance of a Type II-A Diamond Window (thickness 2 mm; not corrected for reflectance)
3. Spectral Radiance of Infrared Group Bands Corrected for Planck Emission and Diamond Absorption
4. Emission Band Profiles of Increasing Intensity
5. Schematic of Ball/Plate Sliding Contact Illustrating Temperatures of Table V
6. New Micro-Interferometer Entrance Arrangement
7. Laboratory EHD Sliding Contact and Infrared Emission Micro-Interferometer Entrance Arrangement
8. Triggering Positions for Moire' Combs Photodetector Signal
9. Schematic of Moire' Combs Triggering Circuitry
10. Wavenumber Calibration of Interferometer in Terms of Standard Polystyrene Spectrum (Note that the standard absorption spectrum is referenced, i.e., double-beam, whereas the interferometer spectrum is single beam. The interferometer source temperature was only 100°C and the source diameter only 1mm)
11. Comparison of Detertivities of Infrared Detectors
12. Mylar (Polyethylene Terephthalate) Film Emission Spectrum Obtained with Different Voltages in the Reference Circuit
- 12A. An Original and Its Numerically Rereferenced Emission Spectrum of Mylar (Polyethylene Terephthalate) Film
13. Schematic of Diamond Anvil Cell
14. Cellular Structure Observed under the Microscope with a Lubricant under Medium High Pressure between Crossed Polarizers
15. Comparison of an Emission and an Absorption Spectrum of a Fluid Containing Monosubstituted Aromatic Hydrocarbons (the spectra were taken in a diamond anvil cell at 165°C and at 3 kbar pressure)

9. LIST OF FIGURES (Cont'd)

16. Emission Spectrum of Polyphenyl Ether (5P4E or OS-124) in the Diamond Cell at Low Pressure (~ 2 kbar) and at 41°C (Aperture 1 inch)
17. Emission Spectrum of Polyphenyl Ether (5P4E or OS-124) in the Diamond Cell at Low Pressure (~ 2 kbar) and at 42°C (Aperture 1.5 inch)
18. Emission Spectrum of Polyphenyl Ether (5P4E or OS-124) in the Diamond Cell at Low Pressure (~ 2 kbar) and at 52.5°C (Aperture 1.5 inch)
19. Emission Spectrum of Polyphenyl Ether (5P4E or OS-124) in the Diamond Cell at Low Pressure (~ 2 kbar) and at 52.5°C Diluted 10:1 with pentaerthritol ester in the diamond cell at low pressure (~ 2 kbar) and at 72°C)
20. Emission Spectrum from an Operating EHD Bearing Contact (Lubricant: OS-124, 240 rpm, 11 KG, Bath Temperature 36.5°C)
21. Emission Spectrum from an Operating EHD Bearing Contact (Lubricant: OS-124, 360 rpm, 11 KG, Bath Temperature 36.5°C)
22. Emission Spectrum from an Operating EHD Bearing Contact (Lubricant: OS-124, 240 rpm, 11 KG, Bath Temperature 31°C)
23. Emission Spectrum from an Operating EHD Bearing Contact (Lubricant: OS-124, 360 rpm, 11 KG, Bath Temperature 31°C)
24. Emission Spectrum from an Operating EHD Bearing Contact (Lubricant: OS-124, 480 rpm, 11 KG, Bath Temperature 31°C)
25. Emission Spectrum from an Operating EHD Bearing Contact (Lubricant: OS-124, 240 rpm, 28.5 KG, Bath Temperature 47.5°C)
26. Emission Spectrum from an Operating EHD Bearing Contact (Lubricant: OS-124, 360 rpm, 28.5 KG, Bath Temperature 50.5°C)
27. Emission Spectrum from an Operating EHD Bearing Contact (Lubricant: OS-124, 480 rpm, 28.5 KG, Bath Temperature 52°C)
28. Emission Spectrum from an Operating EHD Bearing Contact (Lubricant: OS-124, 480 rpm, 11 KG, and no polarizer)
29. Emission Spectrum from an Operating EHD Bearing Contact (Lubricant: OS-124, 480 rpm, 11 KG, and polarizer horizontal)

9. LIST OF FIGURES (Cont'd)

30. Emission Spectrum from an Operating EHD Bearing Contact
(Lubricant: OS-124, 480 rpm, 11 KG, and polarizer horizontal)
31. Emission Spectrum from an Operating EHD Bearing Contact
(Lubricant: OS-124, 480 rpm, 11 KG, and polarizer in 1 o'clock position)
32. Emission Spectrum from an Operating EHD Bearing Contact
(Lubricant: OS-124, 480 rpm, 11 KG, and polarizer in the 2 o'clock position)
33. Temperature Record for OS-124 Polyphenyl Ether
34. Constant Speed Characteristics for OS-124 at Varying Loads and Temperatures
35. Comparison of Low and High Pressure Spectra of N-1 Naphthenic Fluid in the Diamond Cell at Ambient Temperature
36. Comparison of Low and High Pressure Spectra of XRM Synthetic Paraffin in the Diamond Cell at Ambient Temperature
37. Comparison of Low and High Pressure Spectra of 5P4E Polyphenyl Ether in the Diamond Cell at Ambient Temperature
38. Comparison of Low and High Pressure Spectra of Krytox in the Diamond Cell at Ambient Temperature
39. Emission Spectrum of N-1 Hydrocarbon Lubricant from an EHD Operating Bearing Contact Showing Peak Inversion, No polarization used
40. Emission Spectrum of N-1 Hydrocarbon Lubricant from an EHD Operating Bearing Contact Showing Peak Inversion, Polarization used in the Vertical (Conjunction Line) Position
41. Emission Spectrum of N-1 Hydrocarbon Lubricant from an EHD Operating Bearing Contact Showing Peak Inversion, Polarization used in the Horizontal (across Conjunction Line) Position
42. Emission Spectrum from the Central Portion of the Hertzian Contact of an Operating Bearing for a Substituted Aromatic Fluid

9. LIST OF FIGURES (Cont'd)

43. Emission Spectrum from the Exit Portion of the Hertzian Contact of an Operating Bearing for a Substituted Aromatic Fluid
44. Emission Spectrum from the Inlet Portion of the Hertzian Contact of an Operating Bearing for a Substituted Aromatic Fluid
45. Emission Spectrum from the Central Portion of the Hertzian Contact of an Operating Bearing for a Substituted Aromatic Fluid
46. Photomicrograph of Friction Polymer

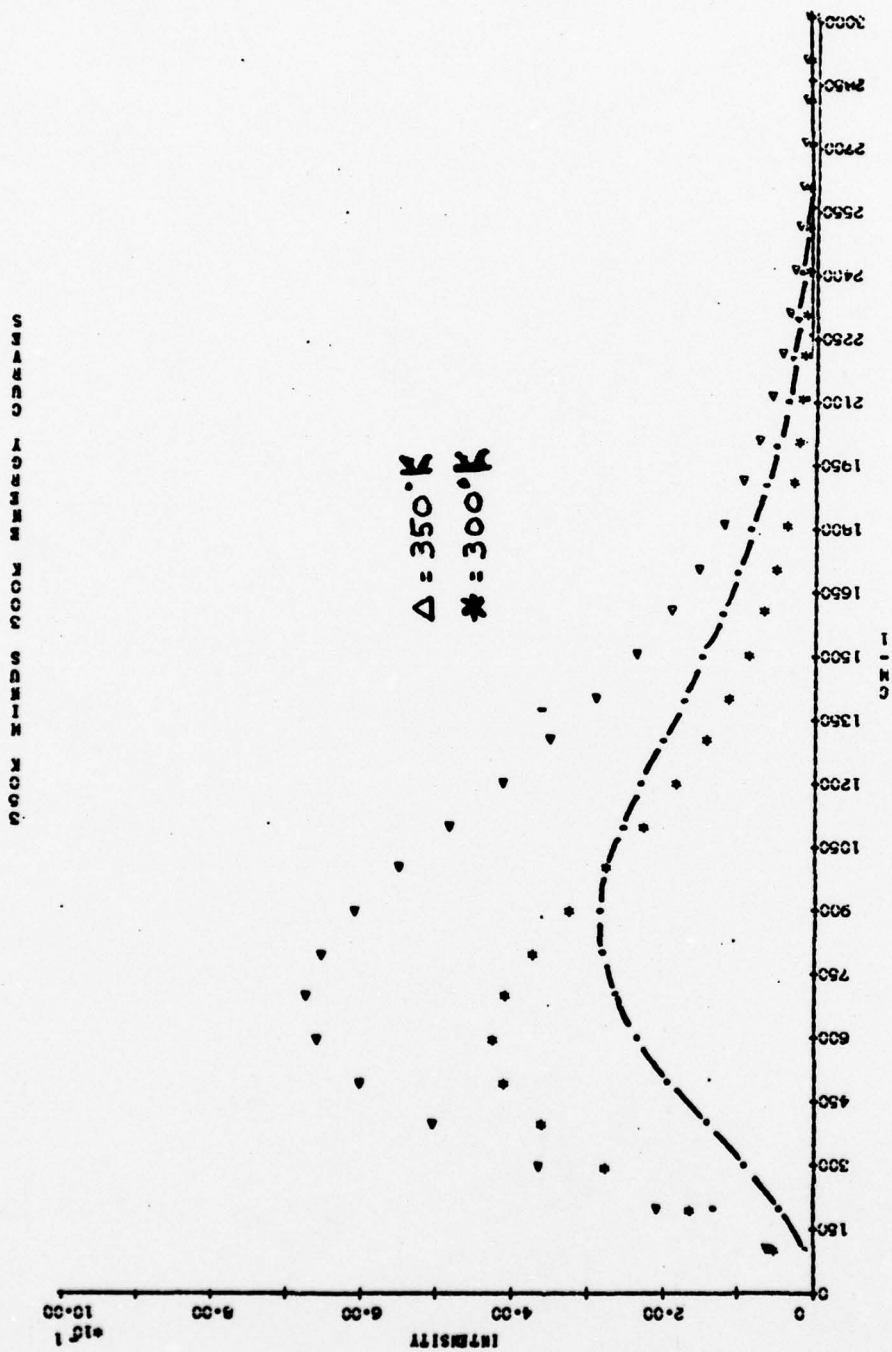


FIGURE 1
Blackbody Spectral Radiance

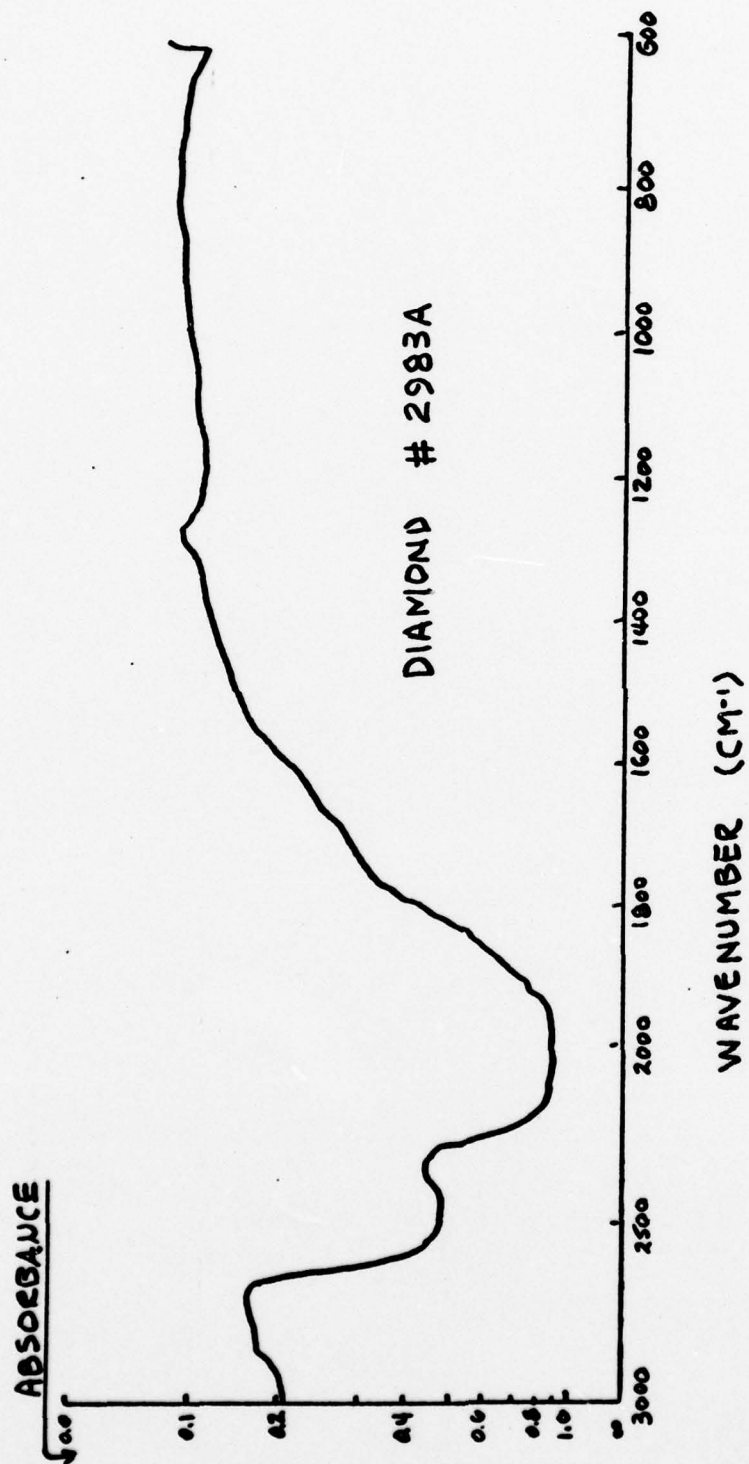
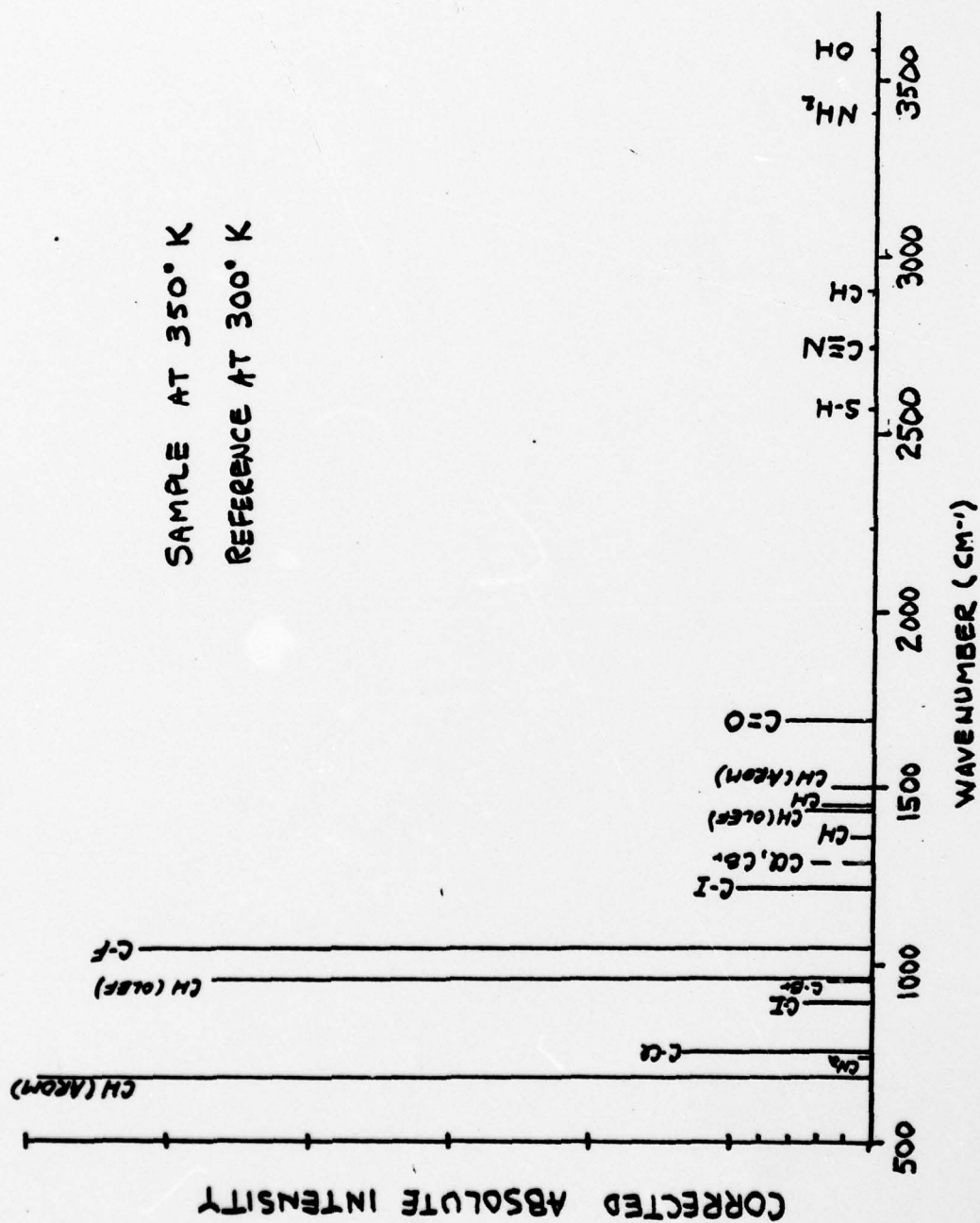


FIGURE 2

Infrared Transmittance of a Type II-A Diamond Window
(thickness 2 mm; not corrected for reflectance)

FIGURE 3

Spectral Radiance of Infrared Group
Bands Corrected for Planck Emission and Diamond Absorption



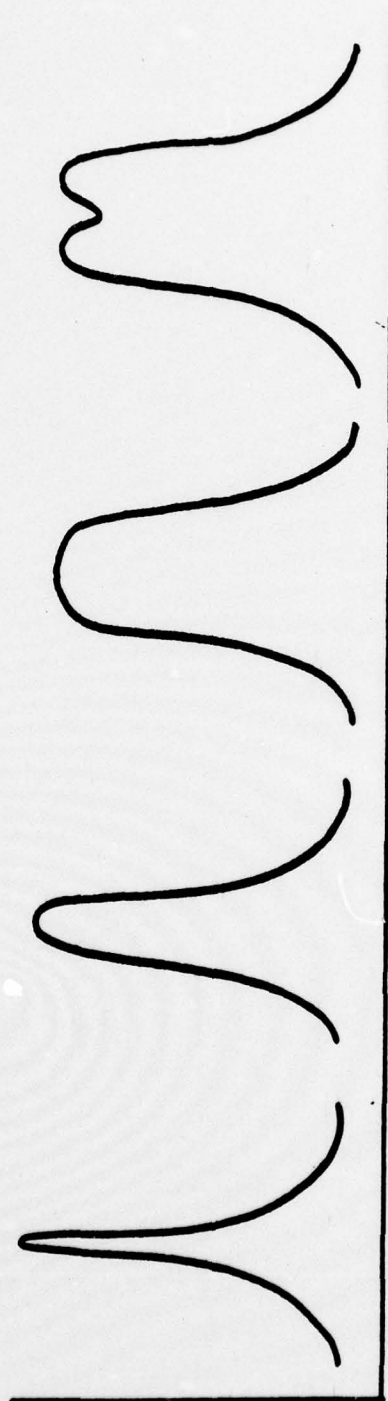


FIGURE 4
Emission Band Profiles of Increasing Intensity

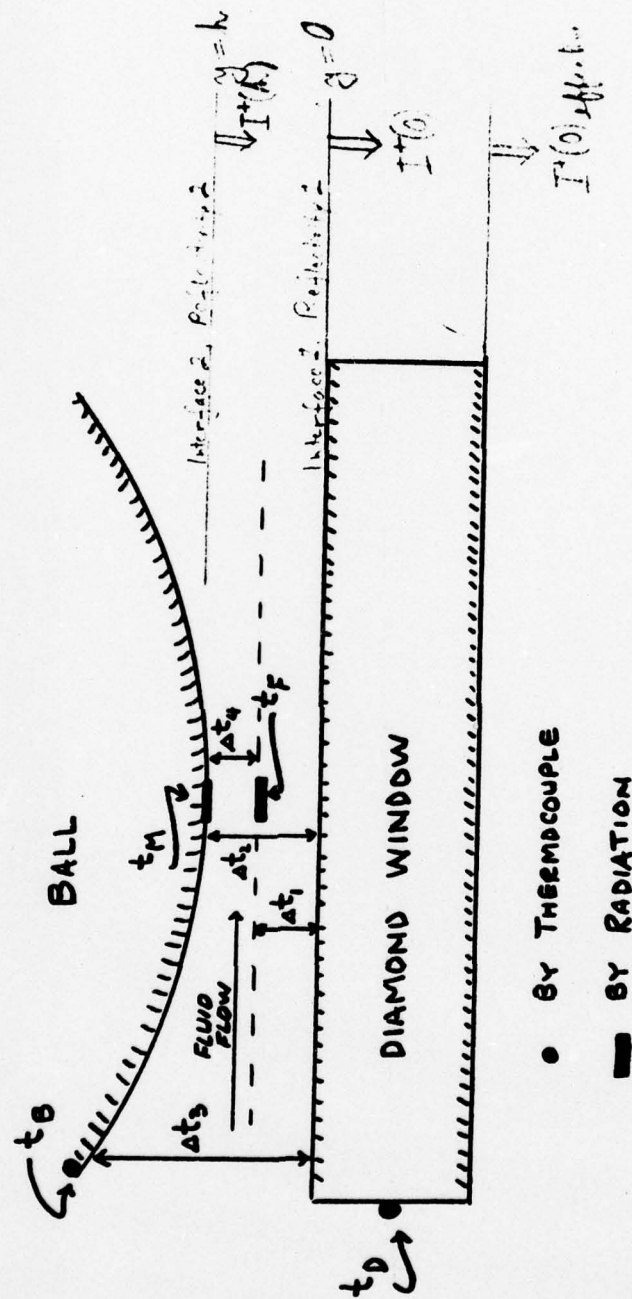
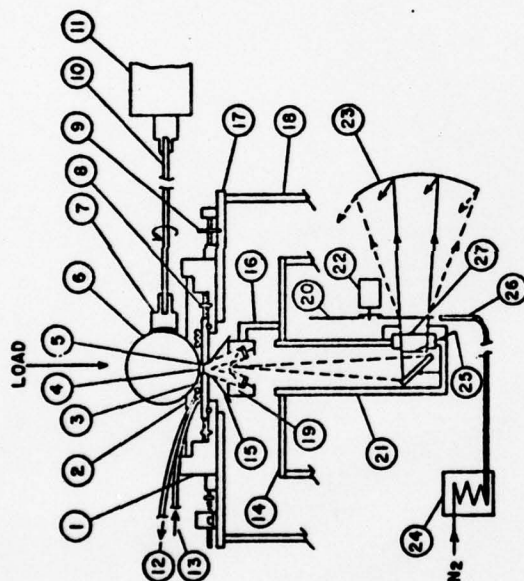


FIGURE 5

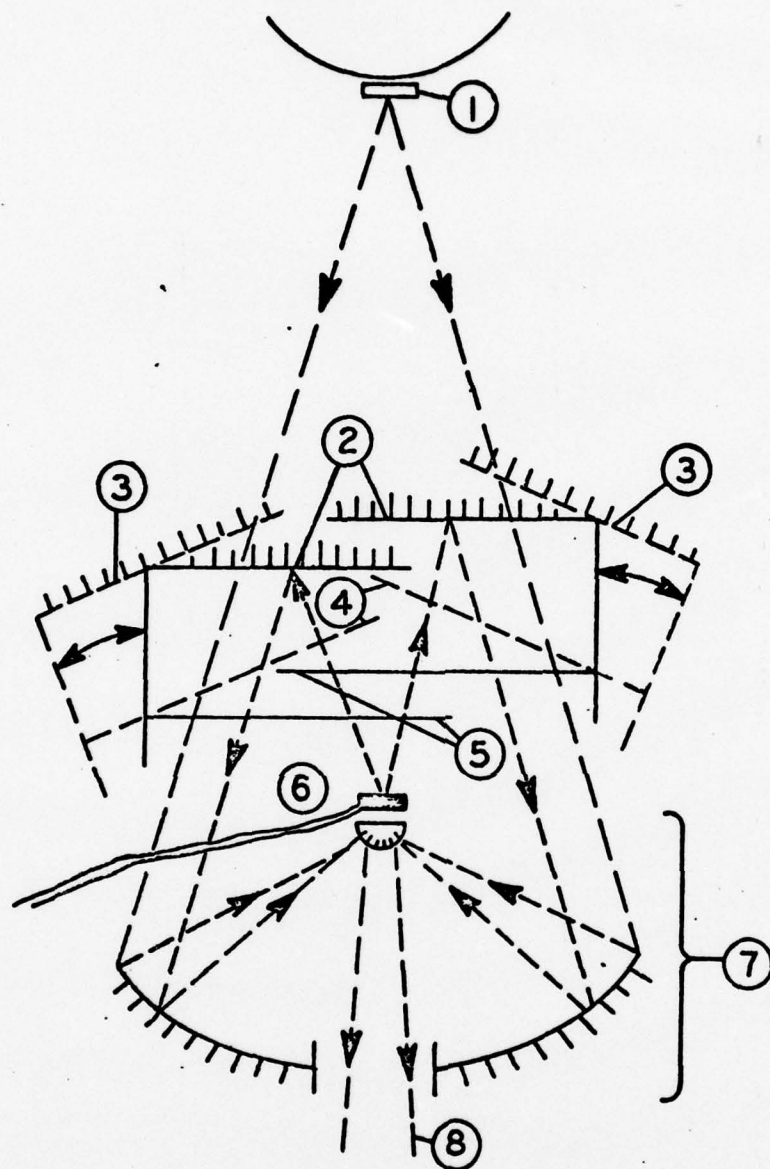
Schematic of Ball/Plate Sliding Contact
Illustrating Temperatures of Table V



- | | |
|---|---------------------------------------|
| 1. FLUID CUP | 15. ALUMINUM REFLECTOR |
| 2. FLUID | 16. BECK LENS SUPPORT |
| 3. DIAMOND HOLDER | 17. BEARING TABLE SURFACE |
| 4. DIAMOND WINDOW | 18. BEARING TABLE SUPPORT |
| 5. CONTACT REGION | 19. BECK LENS |
| 6. ROTATING BALL | 20. CHOPPER BLADE |
| 7. HOLDER | 21. ADAPTER TUBE FOR EMISSION SPECTRA |
| 8. DIAMOND HOLDER x/y ADJUSTMENT SCREW | 22. CHOPPER MOTOR |
| 9. FLUID CUP x/y ADJUSTMENT SCREW | 23. INTERFEROMETER COLLIMATING MIRROR |
| 10. FLEXIBLE SHAFT | 24. GAS COOLER |
| 11. MOTOR DRIVE | 25. REAL IMAGE OF CONTACT REGION |
| 12. COOLING WATER OUT | 26. GAS NOZZLE |
| 13. COOLING WATER IN | 27. INFRARED TRANSPARENT WINDOW |
| 14. INTERFEROMETER SOURCE COMPARTMENT COVER | |

FIGURE 6

New Micro-Interferometer Entrance Arrangement



- | | |
|-------------------------------------|---|
| 1. SOURCE | 5. REFERENCE RADIATION BLOCK-OPEN |
| 2. REFLECTING BLADES-CLOSED | 6. REFERENCE SOURCE |
| 3. REFLECTING BLADES-OPEN | 7. BECK LENS |
| 4. REFERENCE RADIATION BLOCK-CLOSED | 8. EXIT BEAM-ALTERNATINGLY SOURCE & REFERENCE |

FIGURE 7

Laboratory EHD Sliding Contact and Infrared Emission
Micro-Interferometer Entrance Arrangement

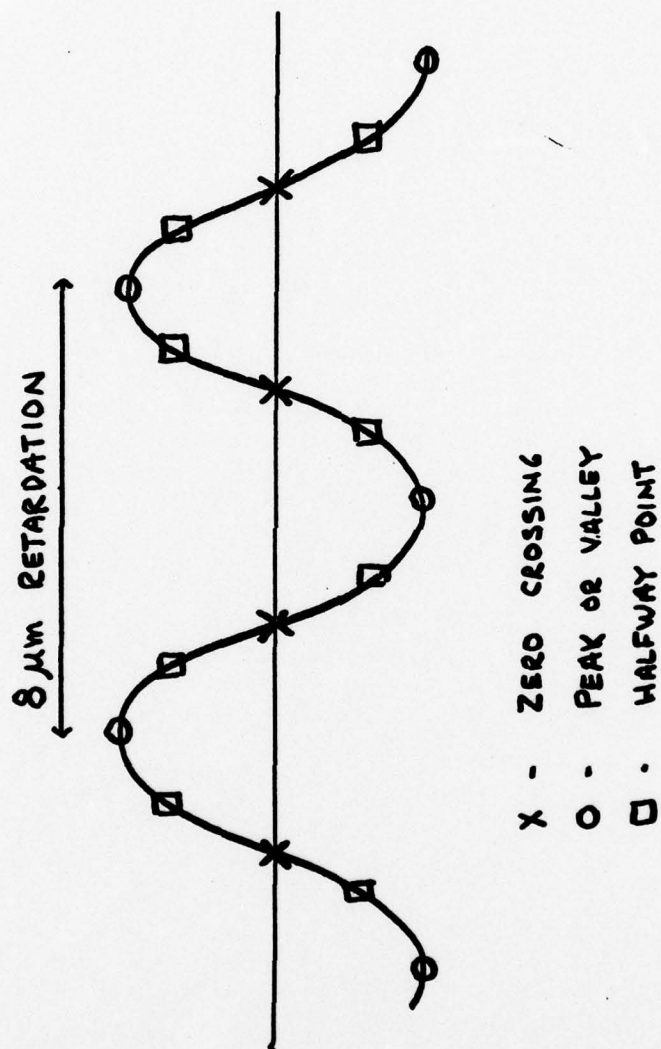


FIGURE 8

Triggering Positions for Moire' Combs Photodetector Signal

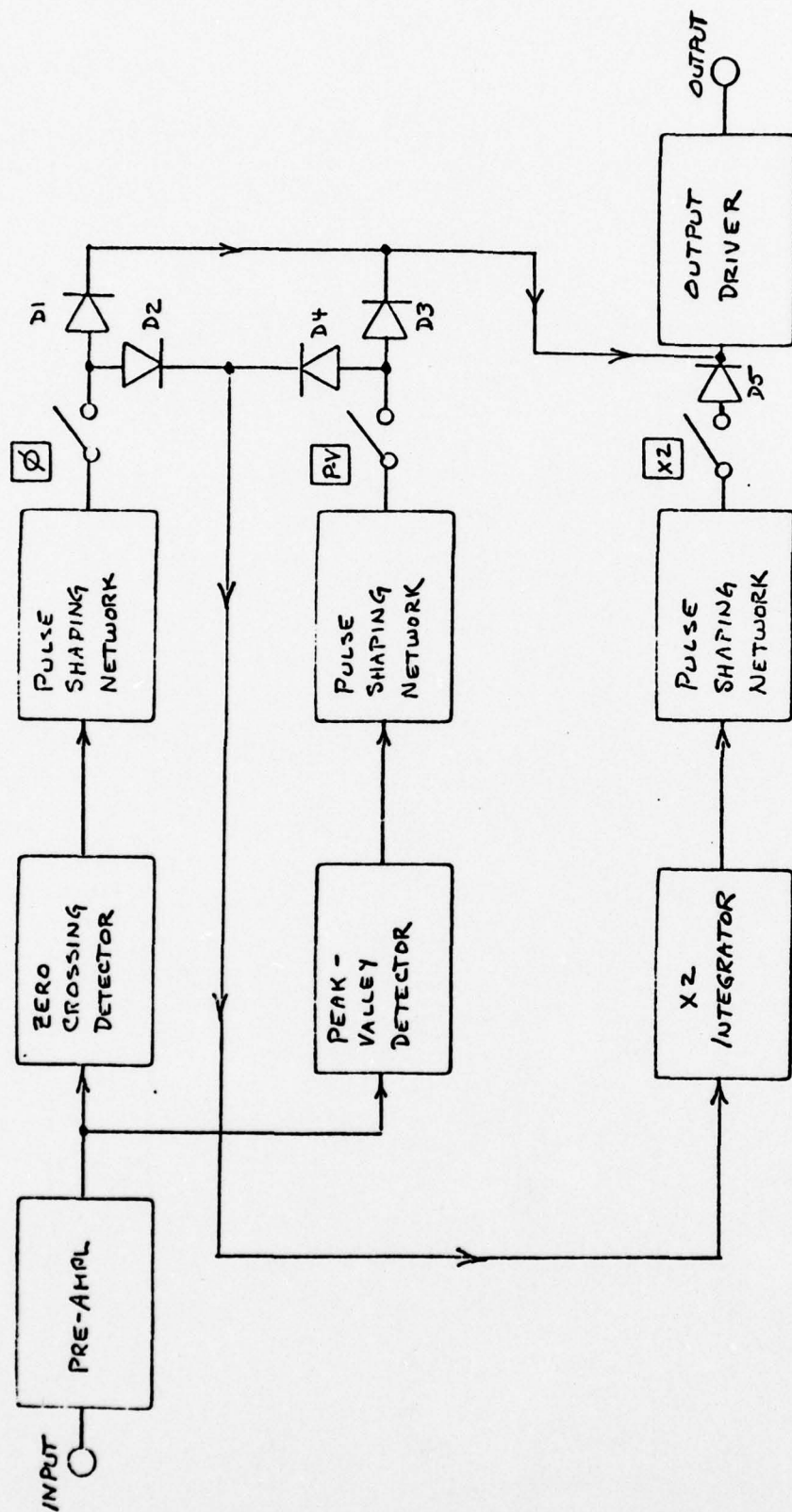


FIGURE 9
Schematic of Moire' Combs Triggering Circuitry

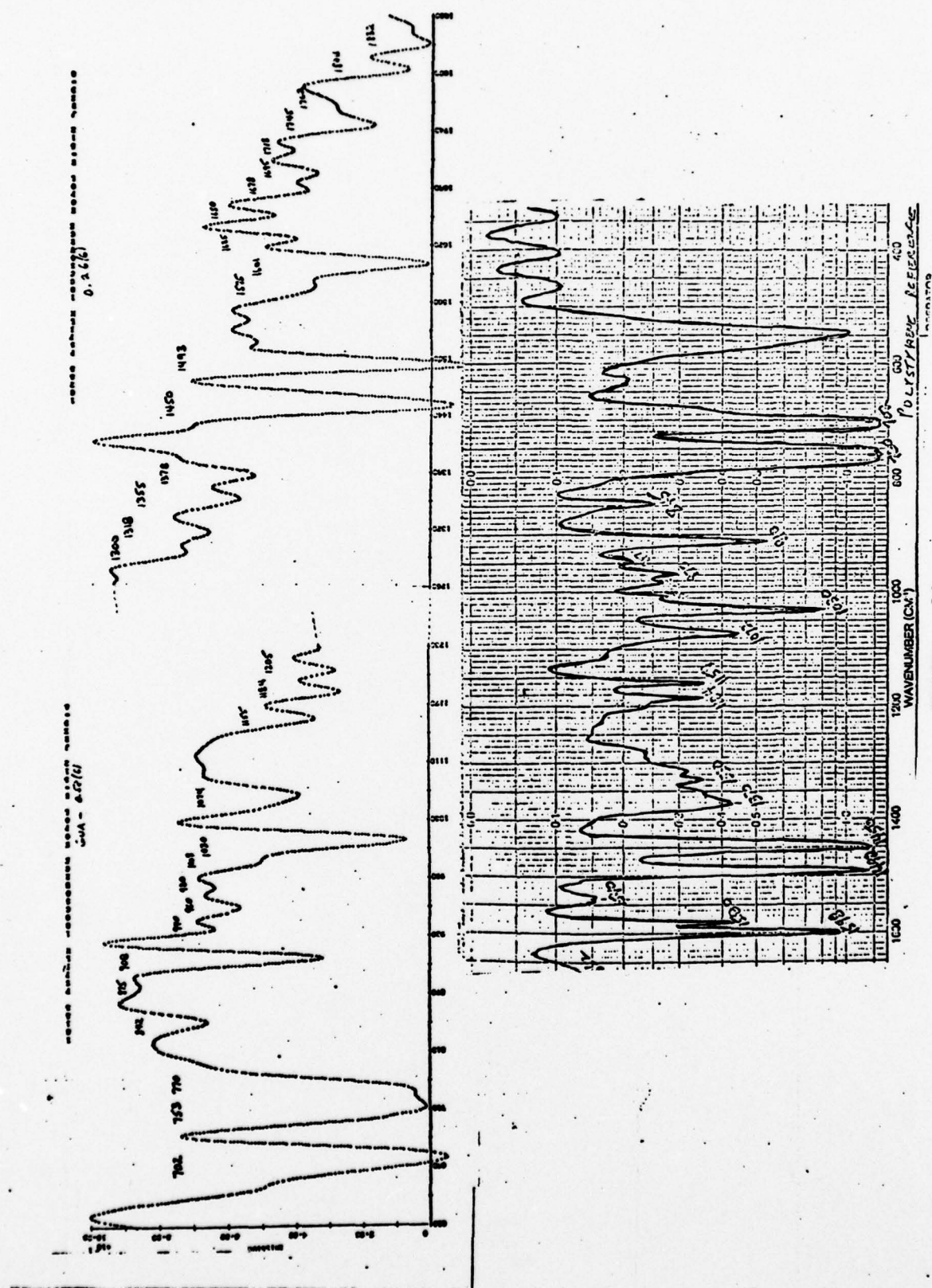


FIGURE 10

Wavenumber Calibration of Interferometer in Terms of Standard Polystyrene Spectrum
 (Note that the standard absorption spectrum is referenced, i.e., double-beam, whereas the interferometer spectrum is single-beam. The interferometer source temperature was only 100°C and the source diameter only 1 mm)

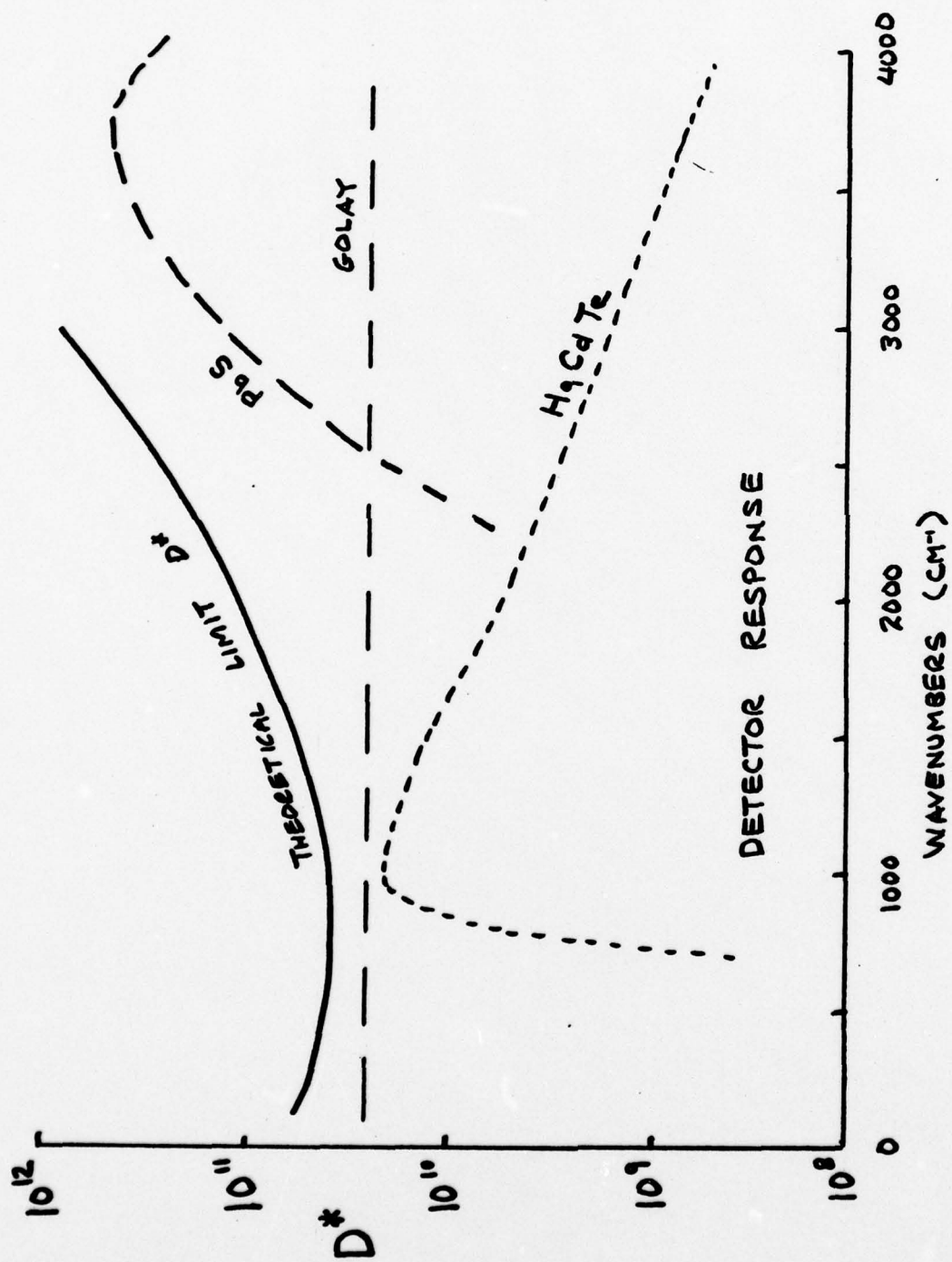


FIGURE 11

Comparison of Detectivities of Infrared Detectors

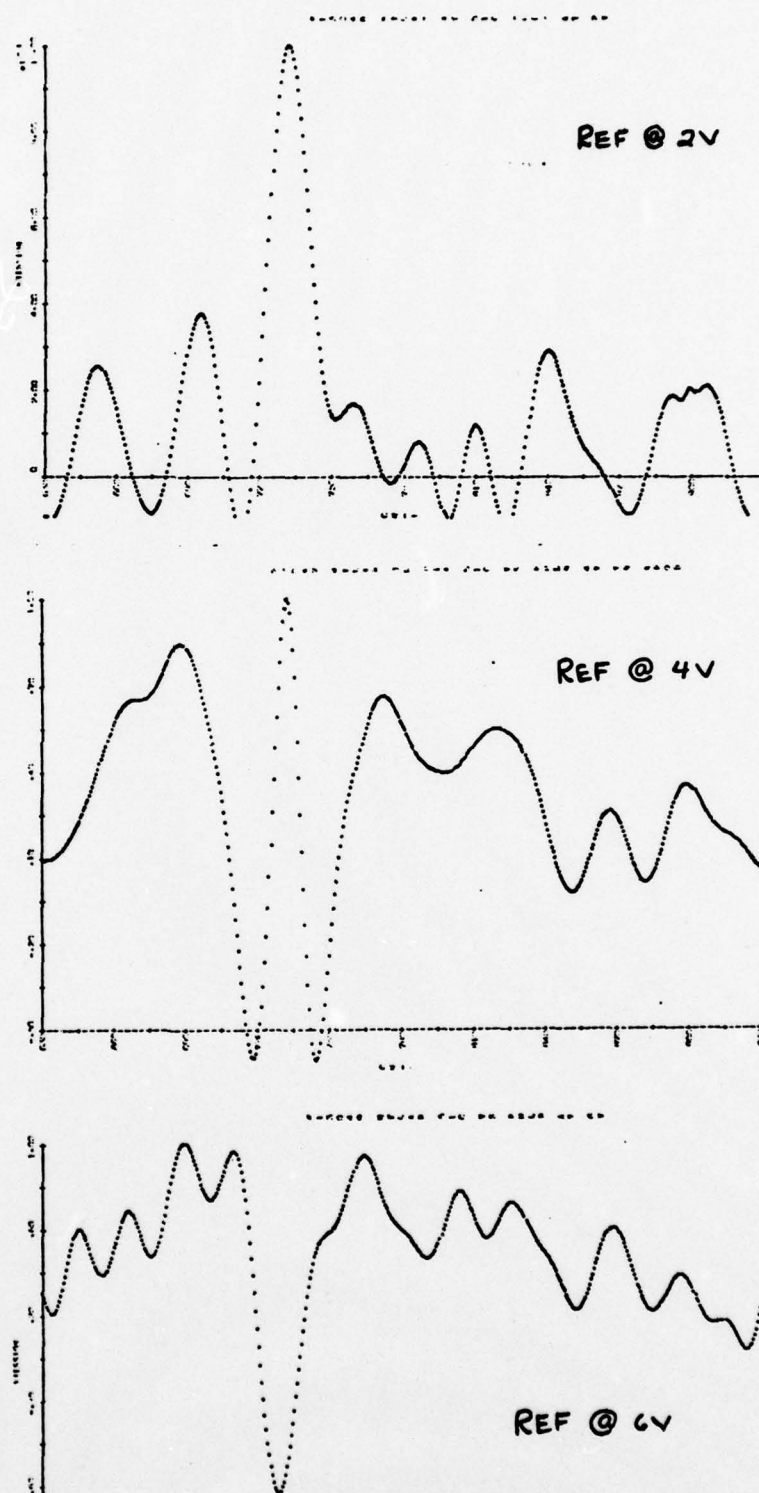


FIGURE 12

Mylar (Polyethylene Terephthalate) Film Emission Spectrum
Obtained with Different Voltages in the Reference Circuit

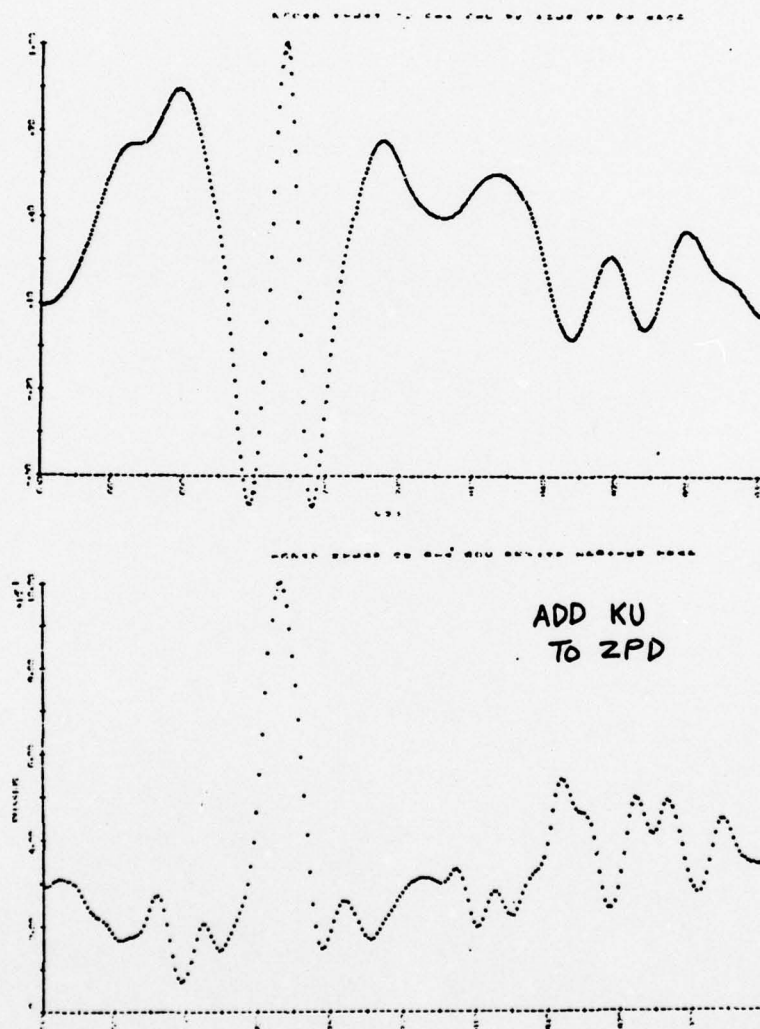
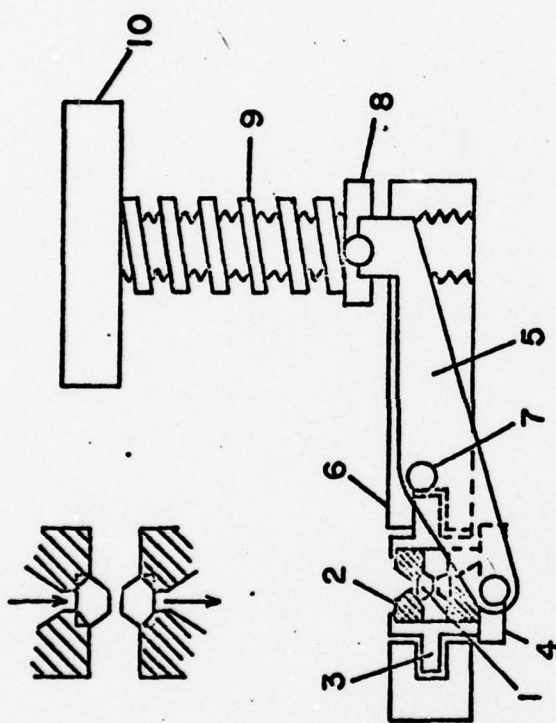


FIGURE 12 A

An Original and Its Numerically Rereferenced Emission Spectrum
of Mylar (Polyethylene Terephthalate) Film



1. DIAMOND ANVIL

2. PISTONS

3. BEARING

4. HOLDING PLATE

5. LEVER ARM

6. SUPPORTING BLOCK

7. PINION

8. PLATE

9. SPRING

10. SCREW

FIGURE 13

Schematic of Diamond Anvil Cell

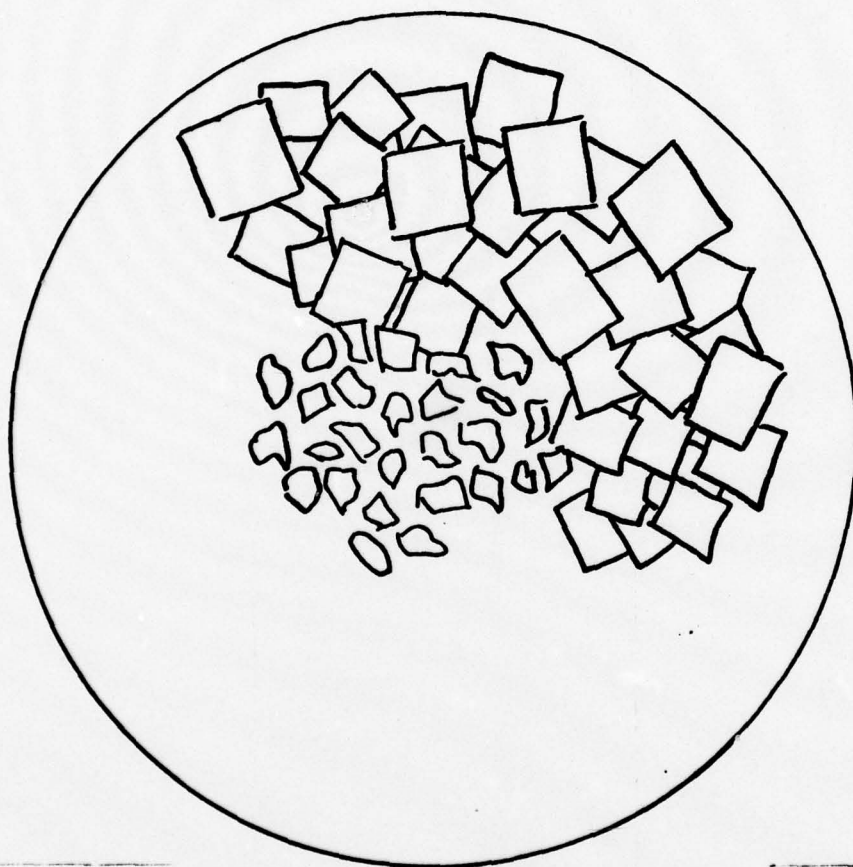


FIGURE 14

Cellular Structure Observed under the Microscope with a
Lubricant under Medium High Pressure between Crossed Polarizers

649027
41

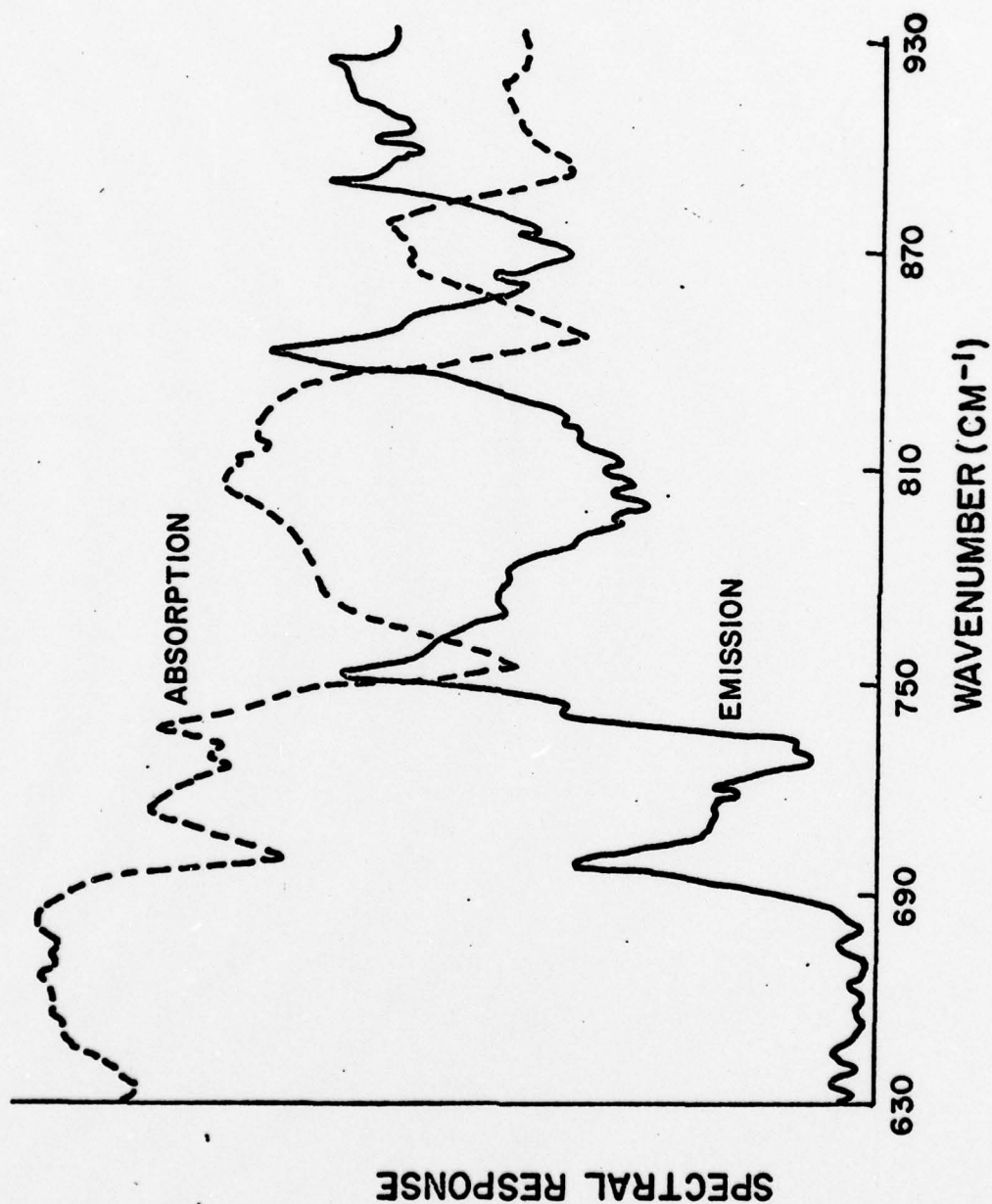


FIGURE 15

Comparison of an Emission and an Absorption Spectrum of
a Fluid Containing Monosubstituted Aromatic Hydrocarbons
(The spectra were taken in a diamond anvil cell at 165°C
and at 3 kbar pressure)

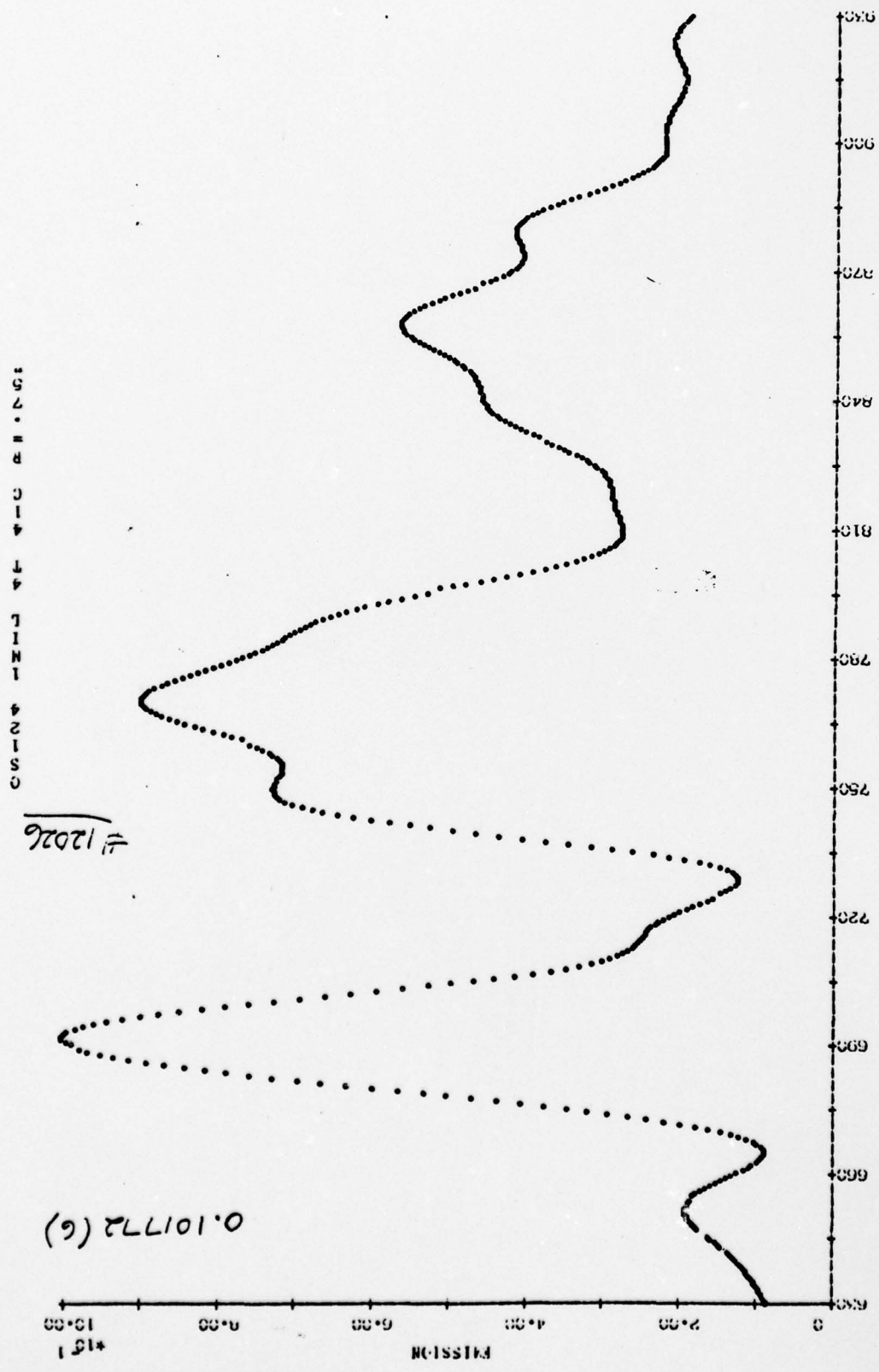
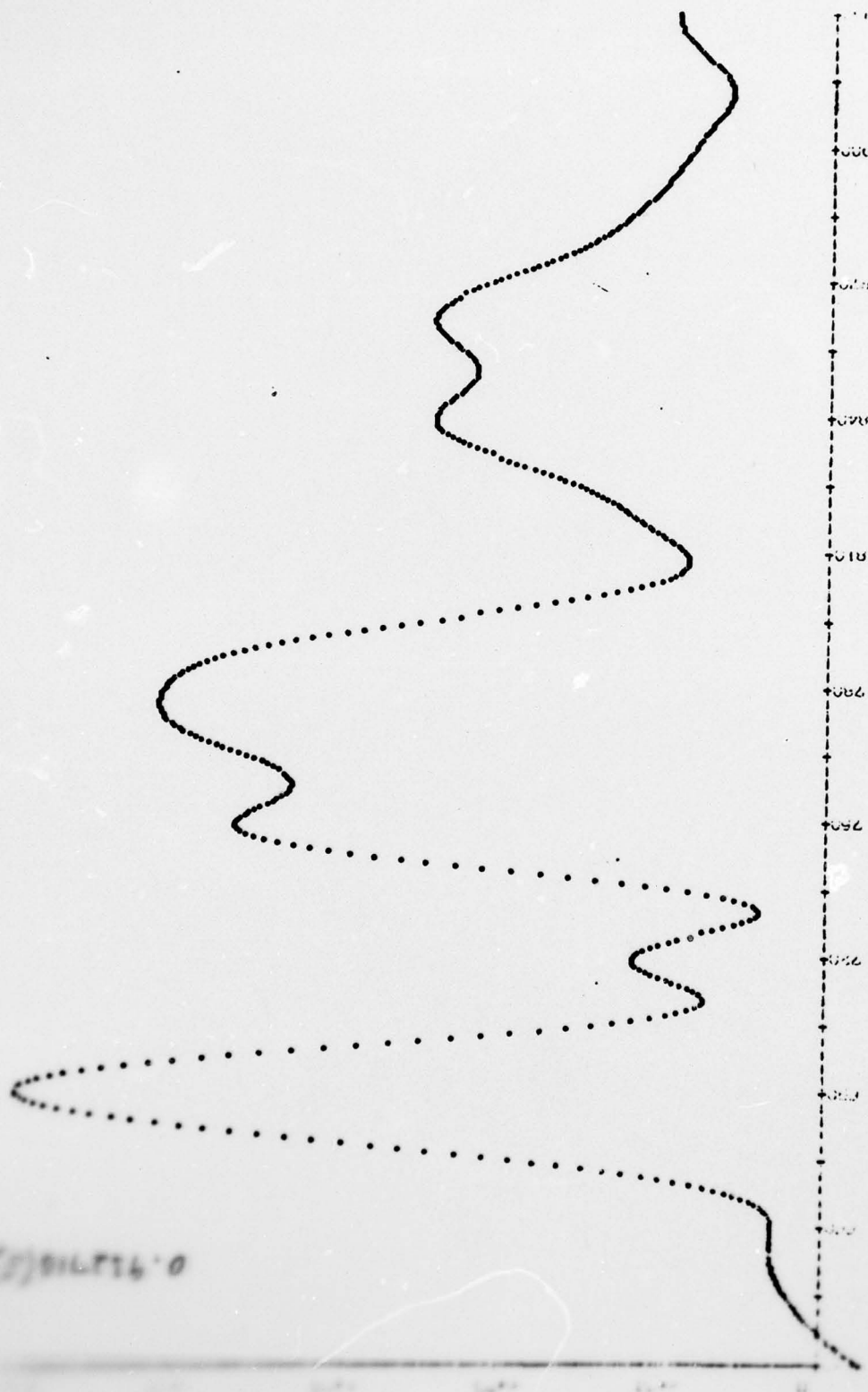


FIGURE 16
 Emission Spectrum of Polyphenyl Ether
 (5P4E or OS-124) in the Diamond Cell at
 Low Pressure (~ 2 kbar) and at 41°C
 (Aperture 1 inch)

(S) 914714-0



Emission Spectrum of Polyphenyl Ether
(5P4E or OS-124) in the Diamond Cell at
Low Pressure (~ 2 kbar) and at 42°C
(Aperture 1.5 inch)

CONCENTRATION 1.5 INCH



FIGURE 18

Emission Spectrum of Polyphenyl Ether
(5P4E or OS-124) in the Diamond Cell at
Low Pressure (~2 kbar) and at 52.5°C
(Aperture 1.5 inch)

SMR0074 50117 C27 TA CDDIMI 1 N1 42150 01/1 34021

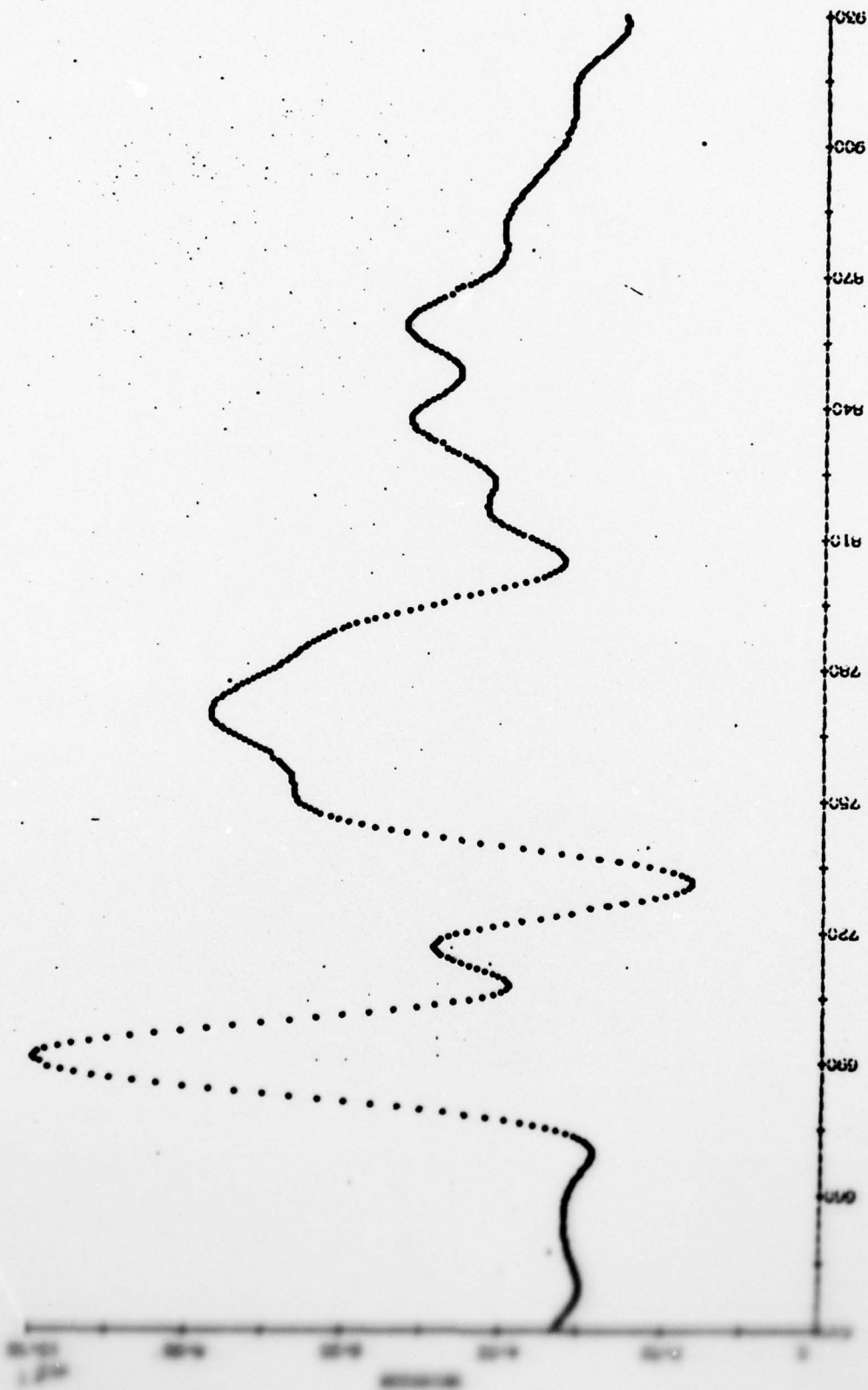


FIGURE 19

Emission Spectrum of Polyphenyl Ether
(5P4E or OS-124) in the Diamond Cell at
Low Pressure (~ 2 kbar) and at 52.5°C
Diluted 10:1 with pentaerythritol ester in the
Diamond Cell at Low Pressure (~ 2 kbar)
and at 72°C

UNITED STATES GOVERNMENT

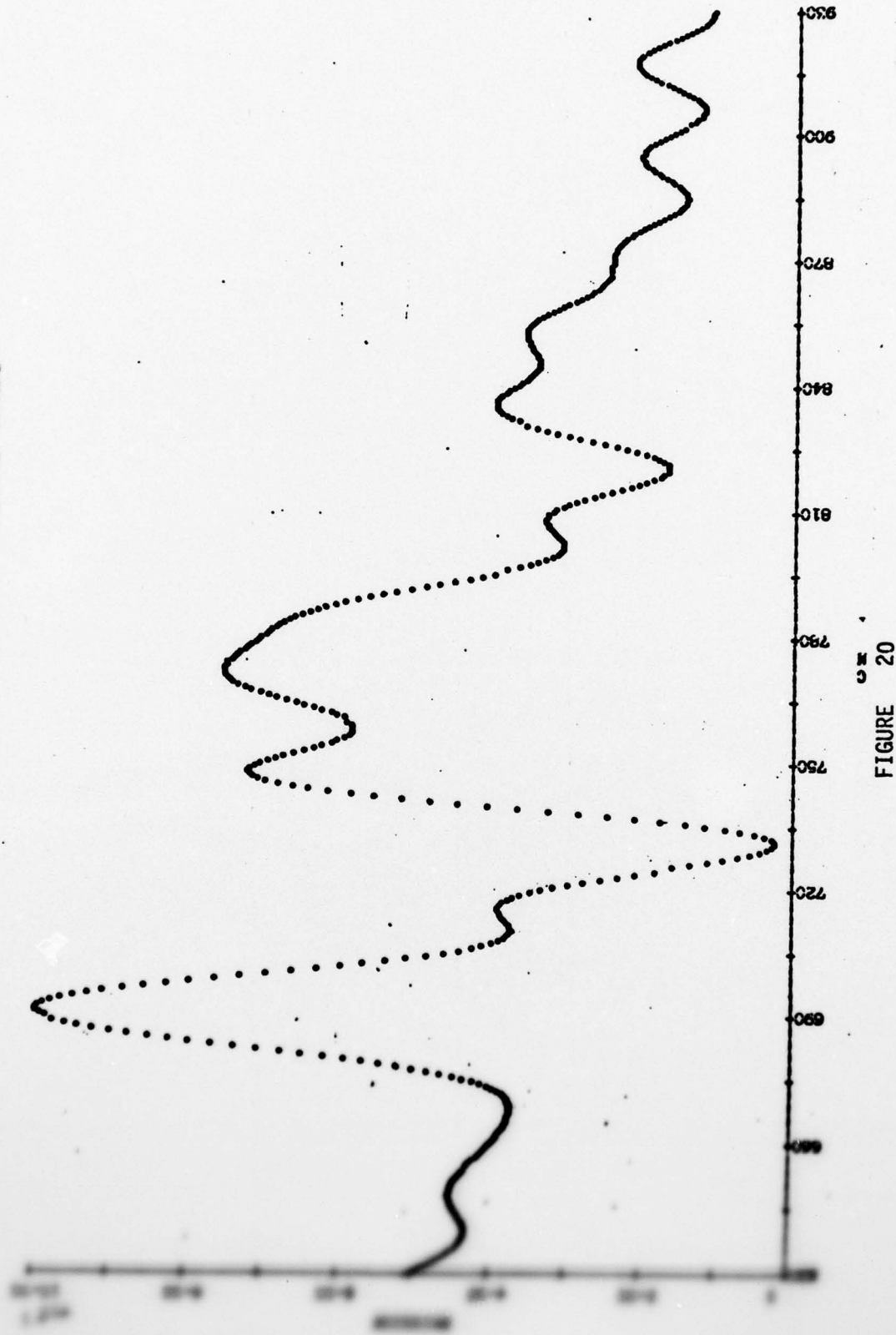


FIGURE 20

Emission Spectrum from an Operating EHD Bearing Contact
(Lubricant: OS-124, 240 rpm, 11 KG, Bath Temperature 36.5 °C)

WAVELENGTH (nm) 4000 3500 3000 2500 2000 1500 1000 500

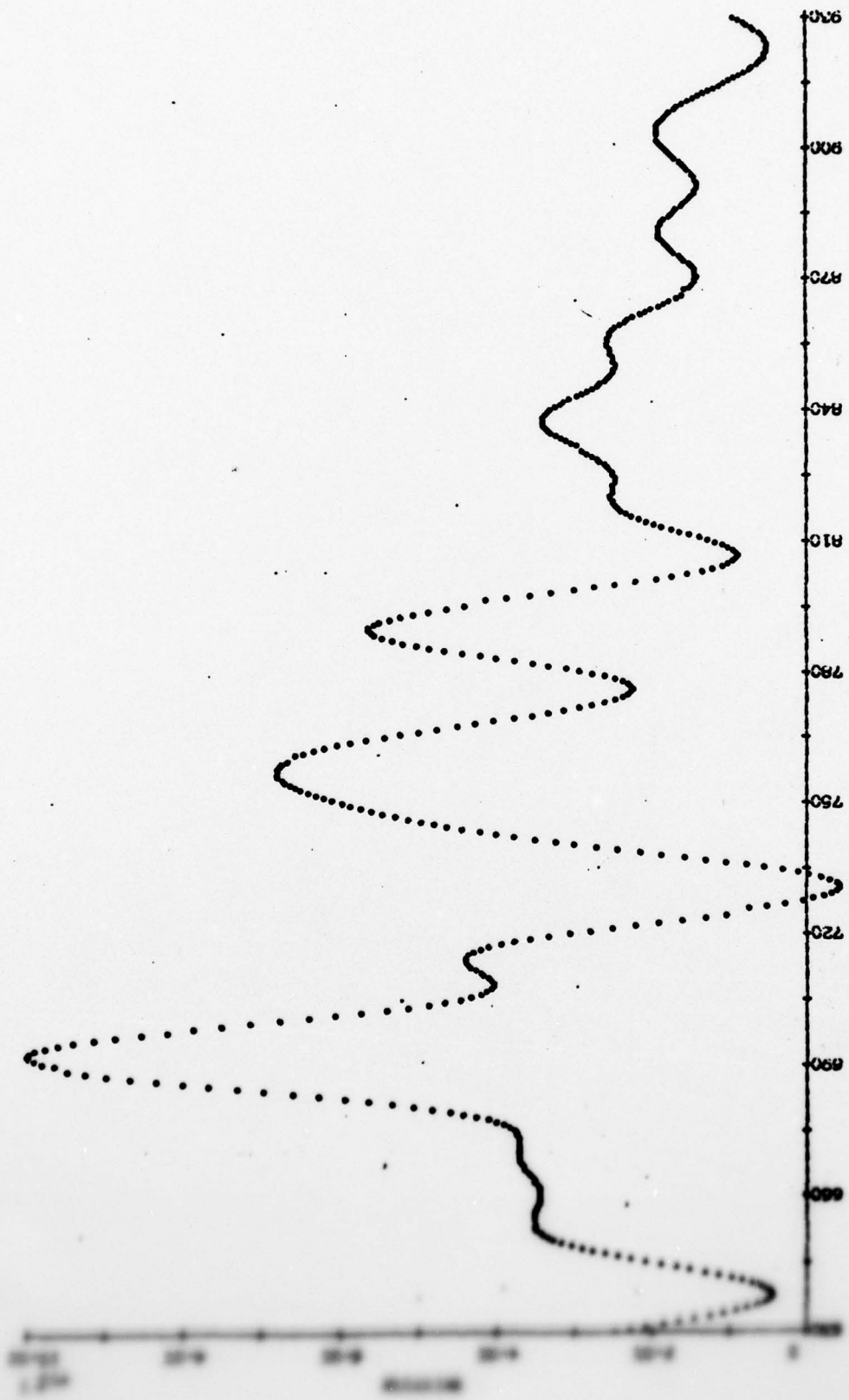


FIGURE 21

Emission Spectrum from an Operating EHD Bearing Contact
(Lubricant: OS-124, 360 rpm, 11 KG, Bath Temperature 36.5°C)

2400 RPM, BT=31°C

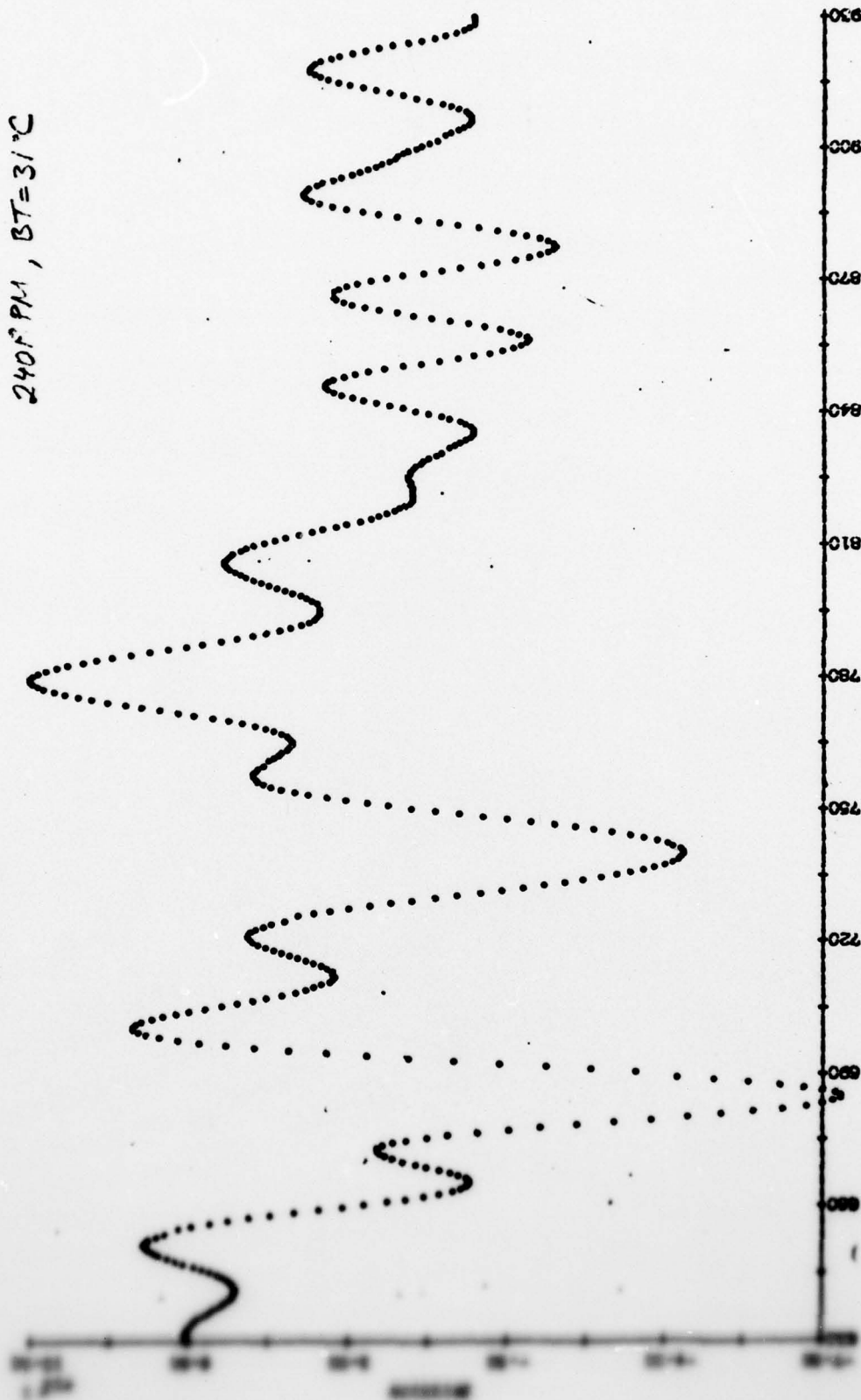


FIGURE 22

Emission Spectrum from an Operating EHD Bearing Contact
(Lubricant: OS-124, 240 rpm, 11 KG, Bath Temperature 31°C)

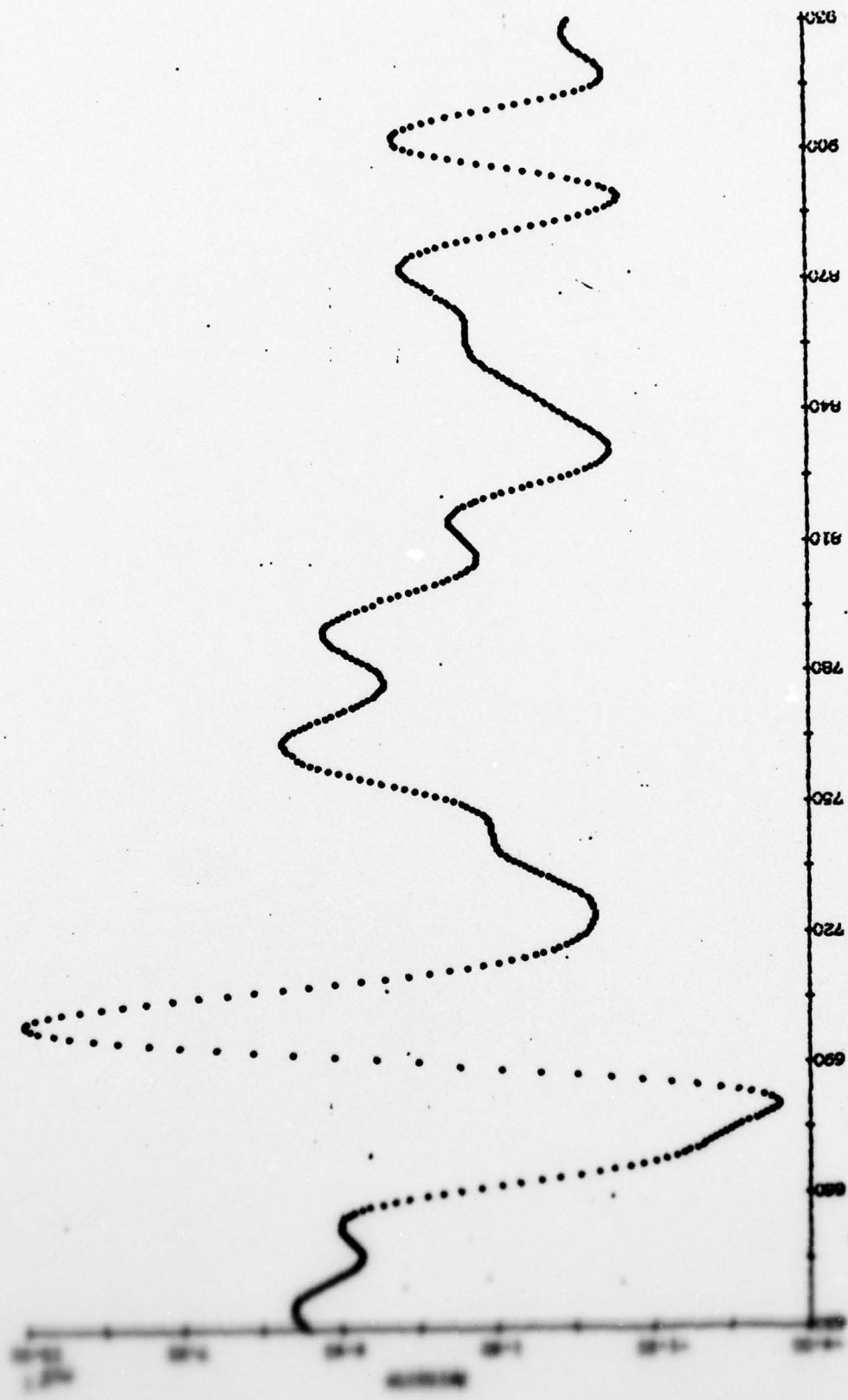


FIGURE 23

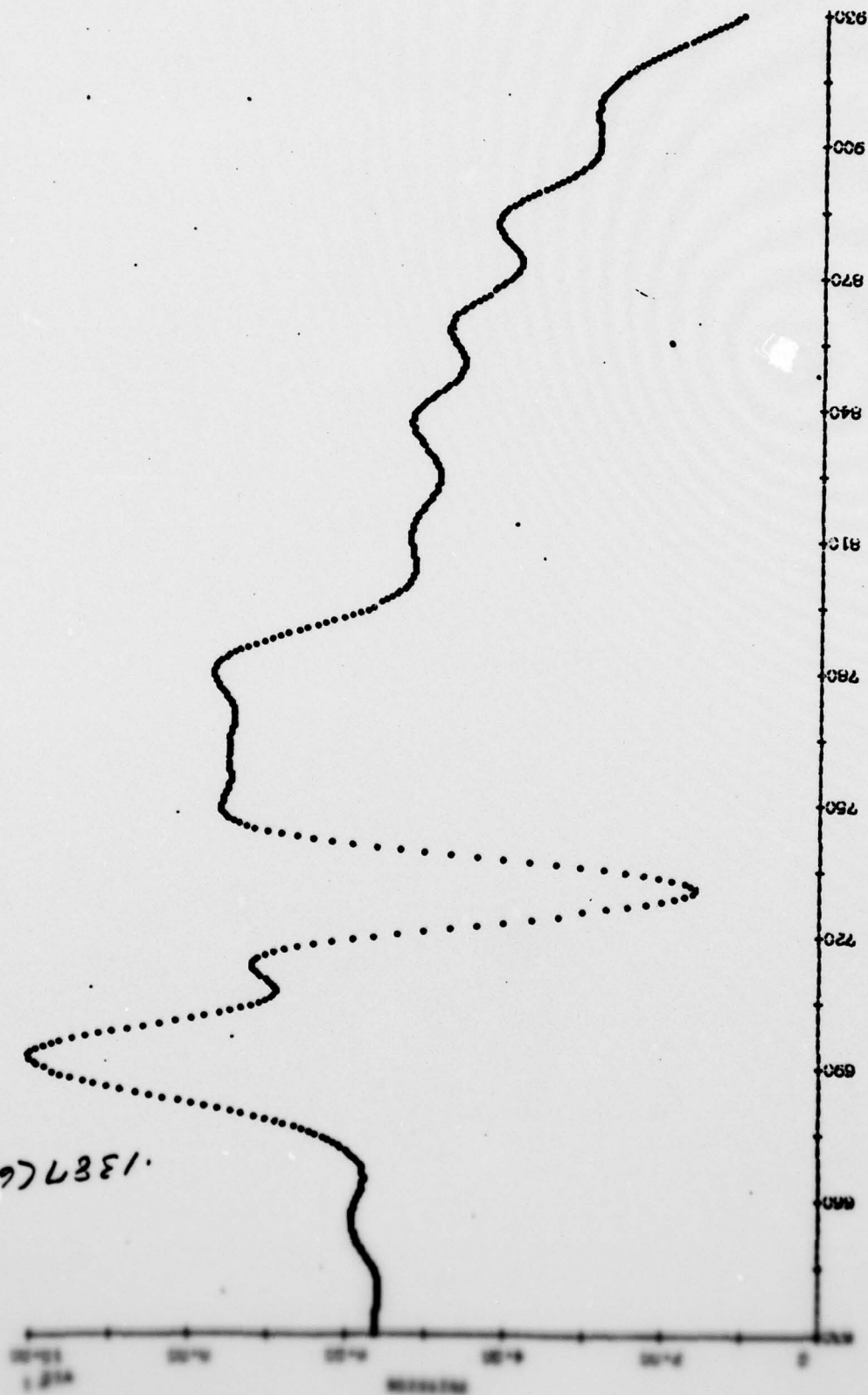
Emission Spectrum from an Operating EHD Bearing Contact
(Lubricant: OS-124, 360 rpm, 11 KG, Bath Temperature 31°C)

571959

一、

**Emission Spectrum from an Operating EHD Bearing Contact
(Lubricant: OS-124, 480 rpm, 11 KG, Bath Temperature 31°C)**

(9) 4381.



1-NC

FIGURE 25

Emission Spectrum from an Operating EHD Bearing Contact
(Lubricant: OS-124, 240 rpm, 28.5 KG, Bath Temperature 47.5°C)

10
9
8
7
6
5
4
3
2
1
0

VOLTAGE

0 2 4 6 8 10

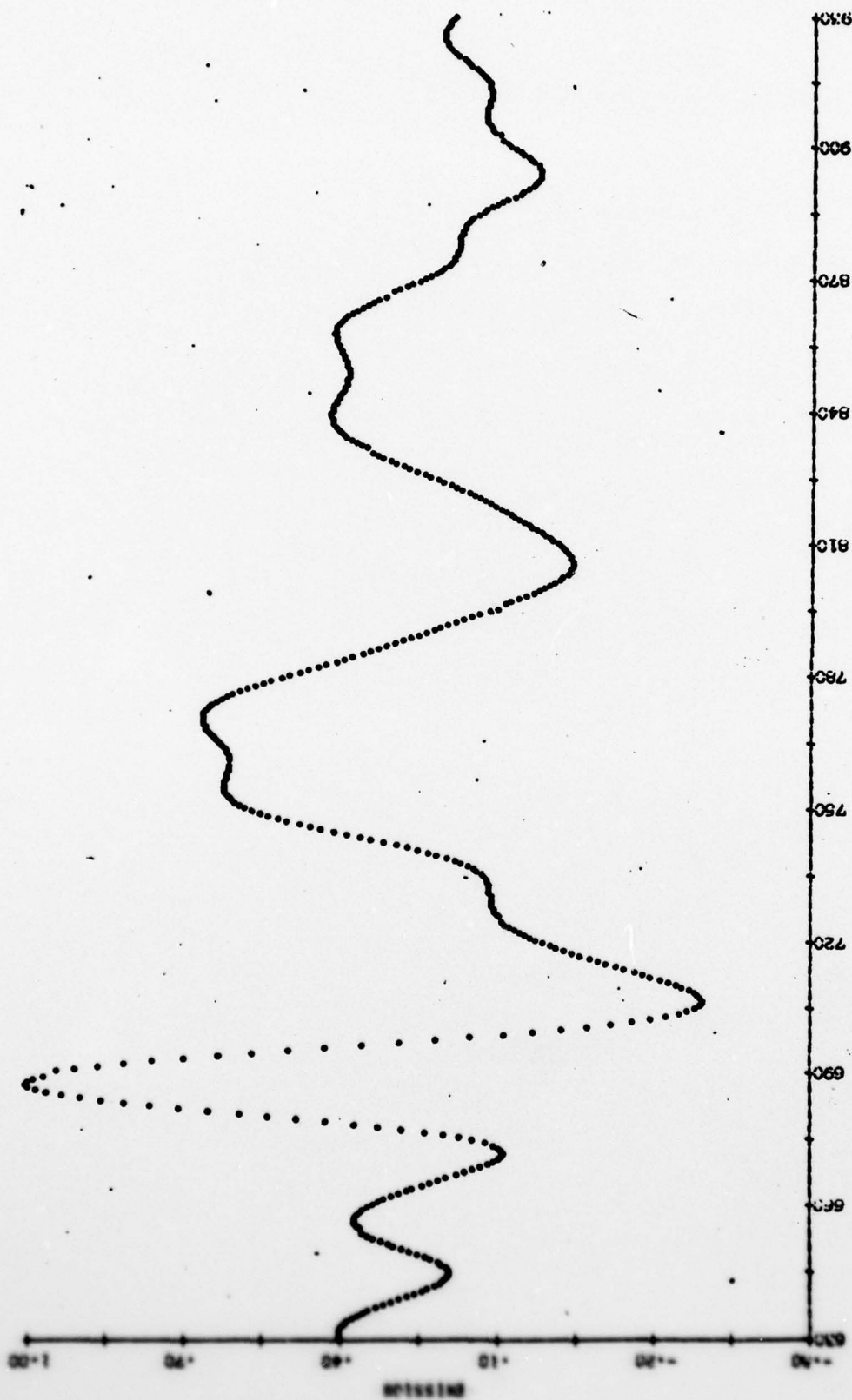
TIME

9.5 9.0 8.5 8.0 7.5 7.0 6.5 6.0 5.5 5.0 4.5 4.0 3.5 3.0 2.5 2.0 1.5 1.0 0.5 0

Emission Spectrum from an Operating EHD Bearing Contact
(Lubricant: OS-124, 360 rpm, 28.5 KG, Bath Temperature 50.5°C)

**Emission Spectrum from an Operating EHD Bearing Contact
(Lubricant: OS-124, 480 rpm, 28.5 KG, Bath Temperature 52°C)**

WAVELENGTH (nm)



LINE

FIGURE 28

Emission Spectrum from an Operating EHD Bearing Contact
(Lubricant: OS-124, 480 rpm, 11 KG, and no polarizer)

11311 LCO 21 14 1000 11 03 4 2150 66000

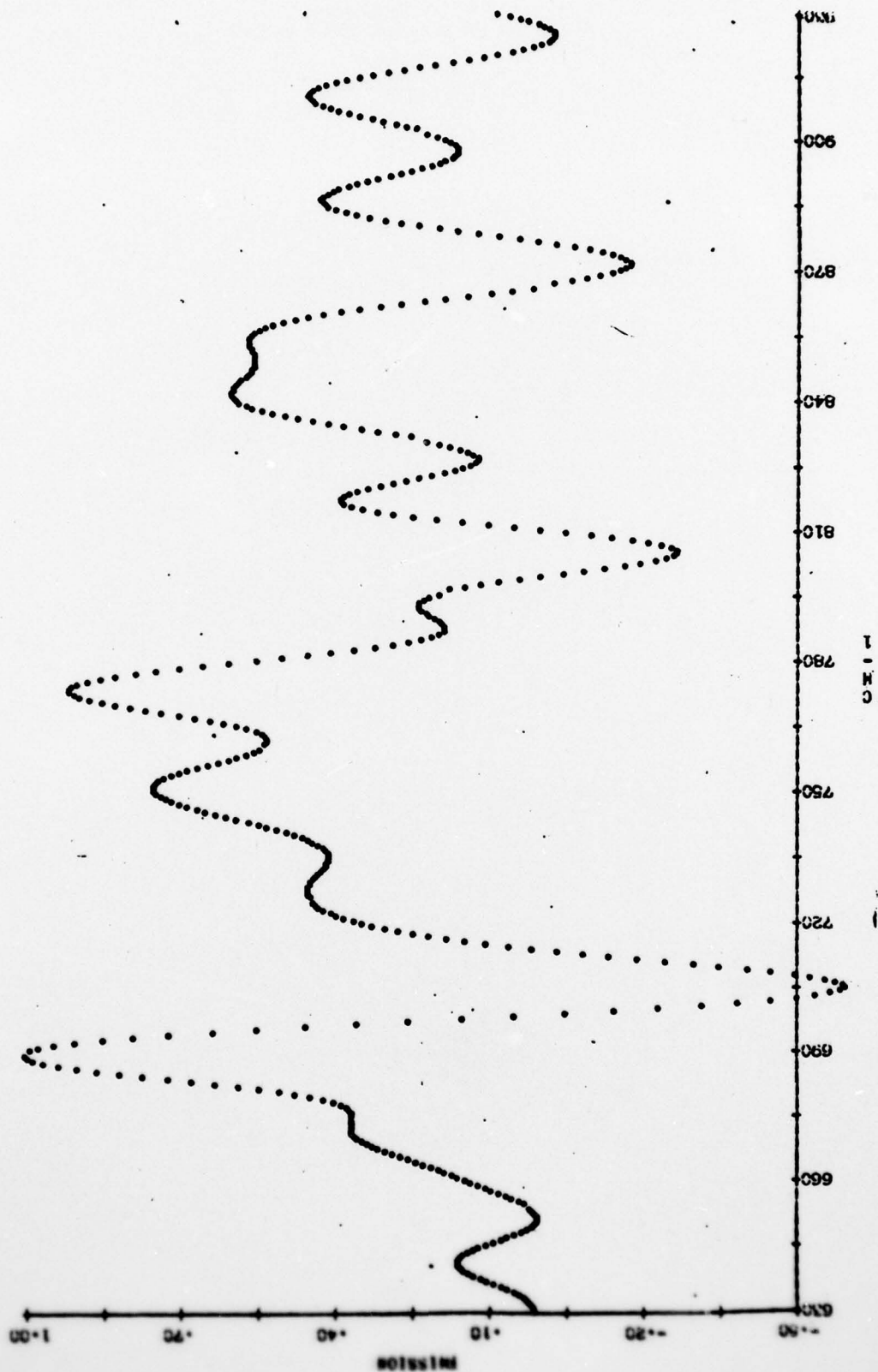
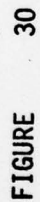


FIGURE 29

Emission Spectrum from an Operating EHD Bearing Contact
(Lubricant: OS-124, 480 rpm, 11 KG, and polarizer vertical)



**Emission Spectrum from an Operating EHD Bearing Contact
(Lubricant: OS-124, 480 rpm, 11 KG, and polarizer horizontal)**

AD-A054 290

SUNTECH INC MARCUS HOOK PA

F/G 11/8

INFRARED SPECTRA OF FLUID FILMS UNDER CONDITIONS OF INCIPIENT B--ETC(U)

DEC 77 J L LAUER

F49620-76-C-0042

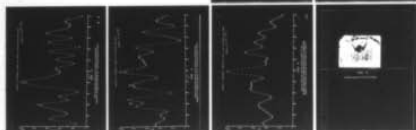
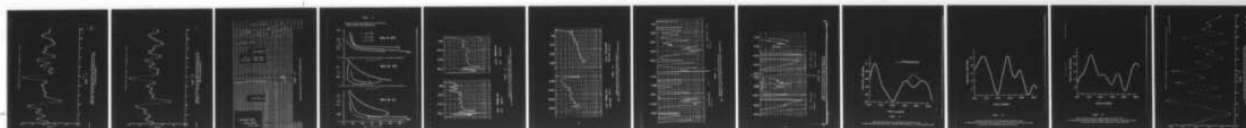
UNCLASSIFIED

AFOSR-TR-78-0190

NL

2 OF 2

AD
A054290



END
DATE
FILMED

6 -78

DDC

100 2 AVAILABLE 11 084 4 11 50 24001

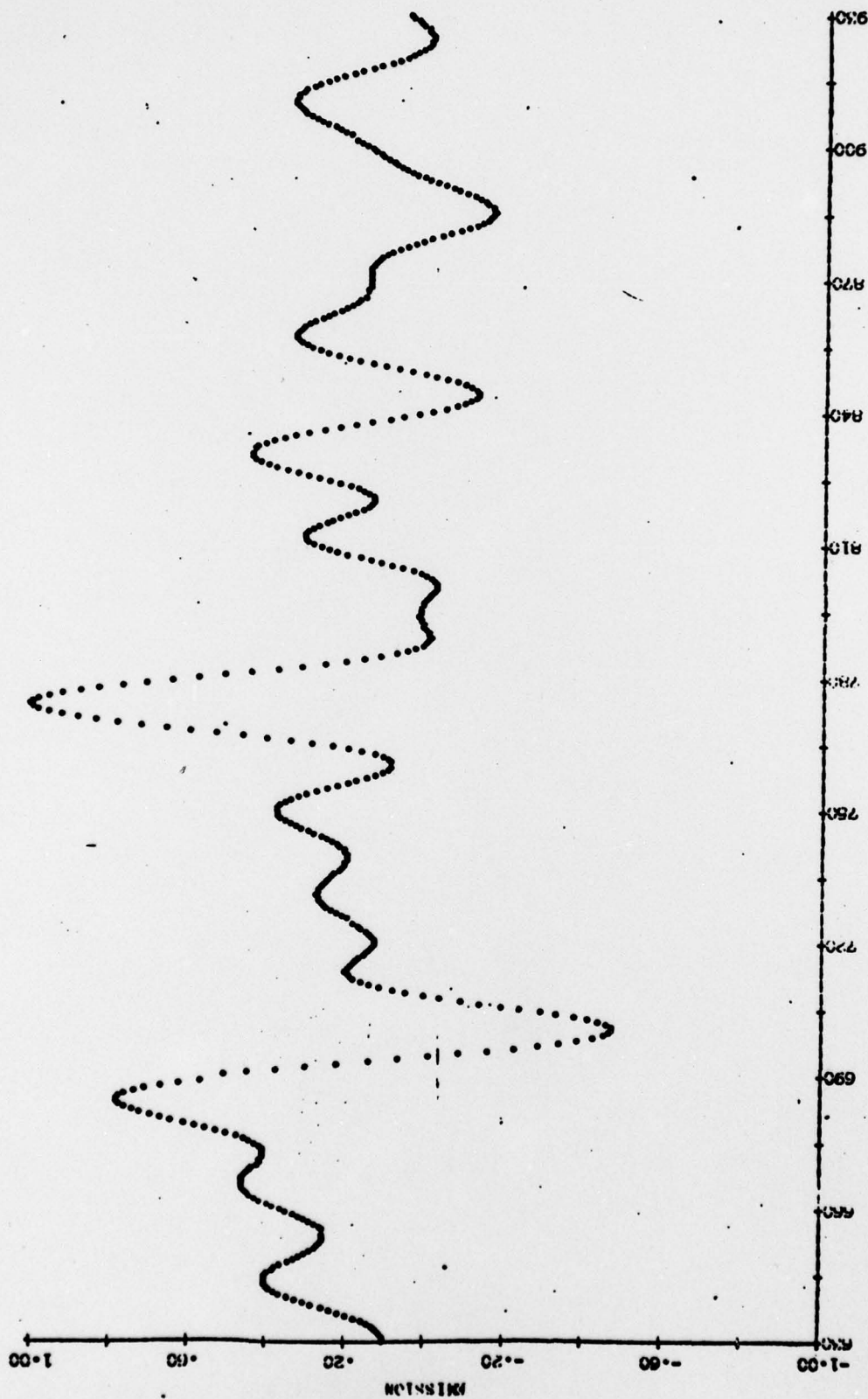


FIGURE 32

Emission Spectrum from an Operating EHD Bearing Contact
(Lubricant: OS-124, 480 rpm, 11 KG, and polarizer in
the 2 o'clock position)

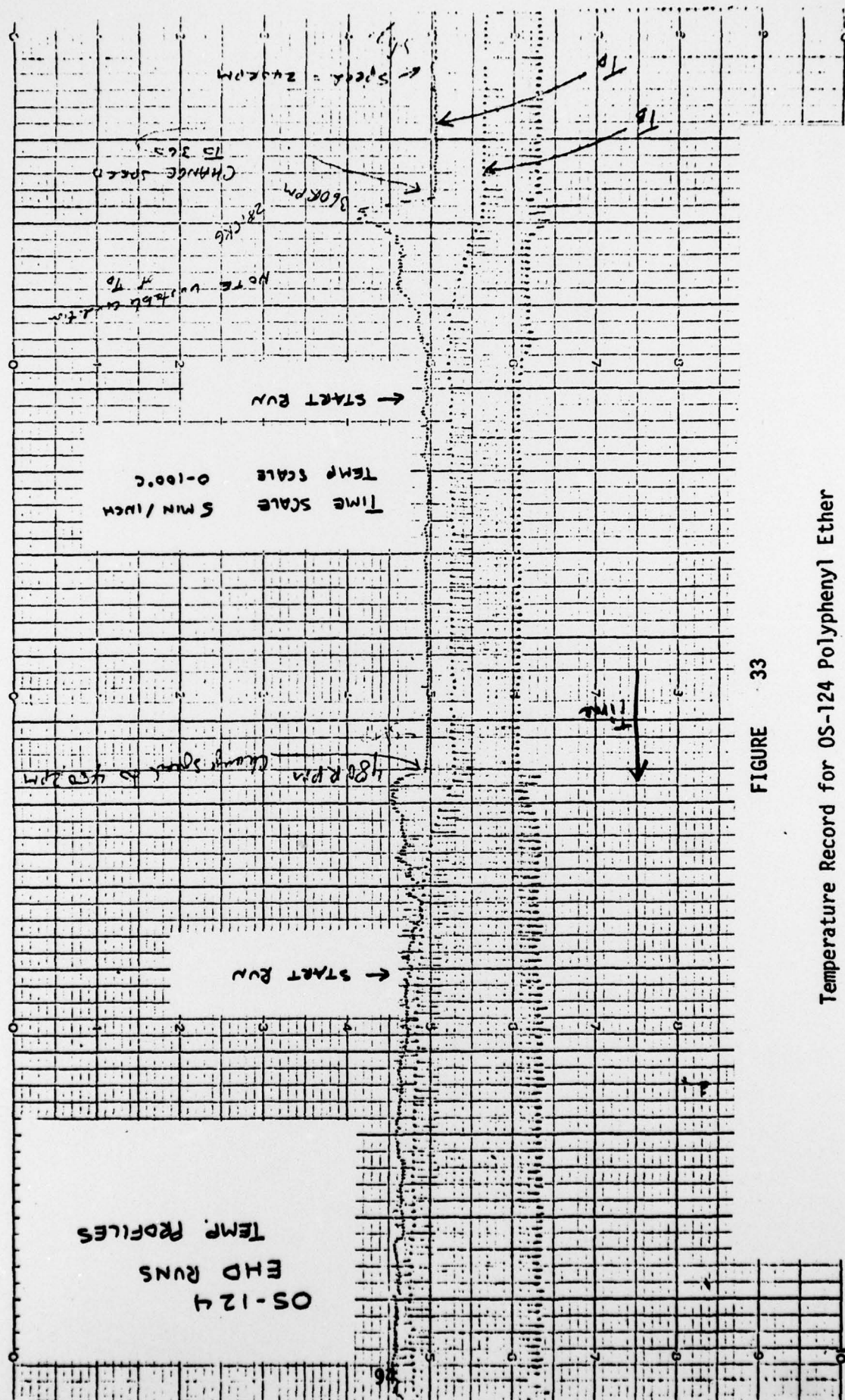
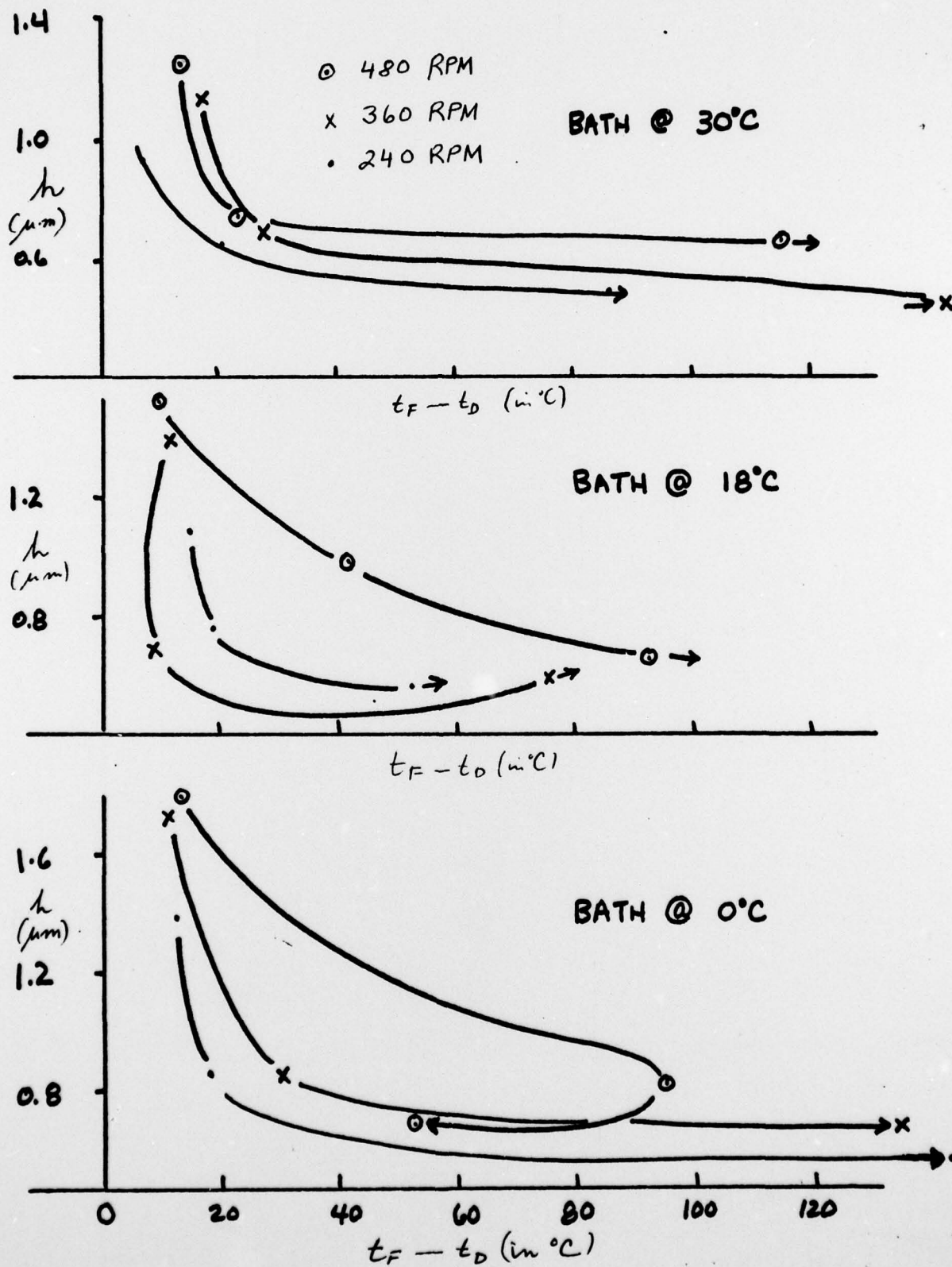


FIGURE 33

Temperature Record for OS-124 Polyphenyl Ether

FIGURE 34

Constant Speed Characteristics for OS-124 at
Varying Loads and Temperatures



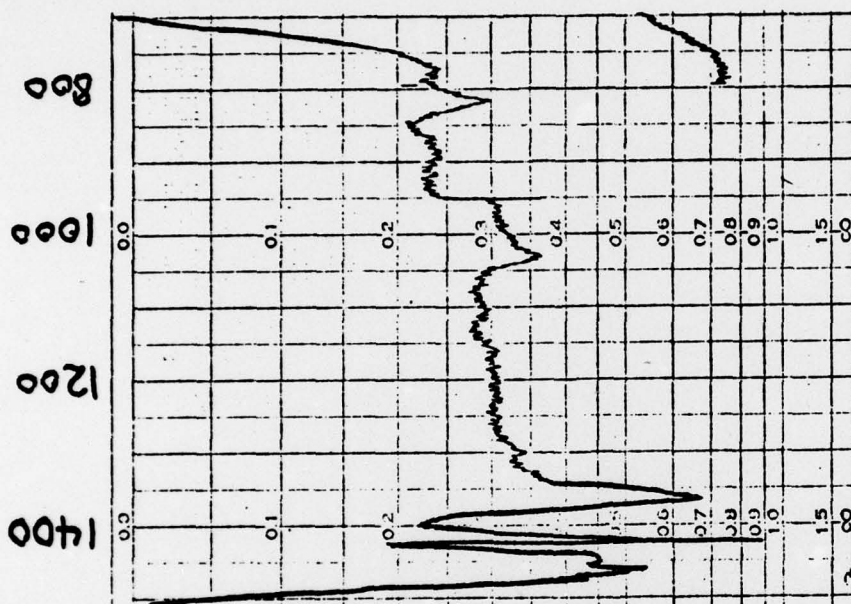
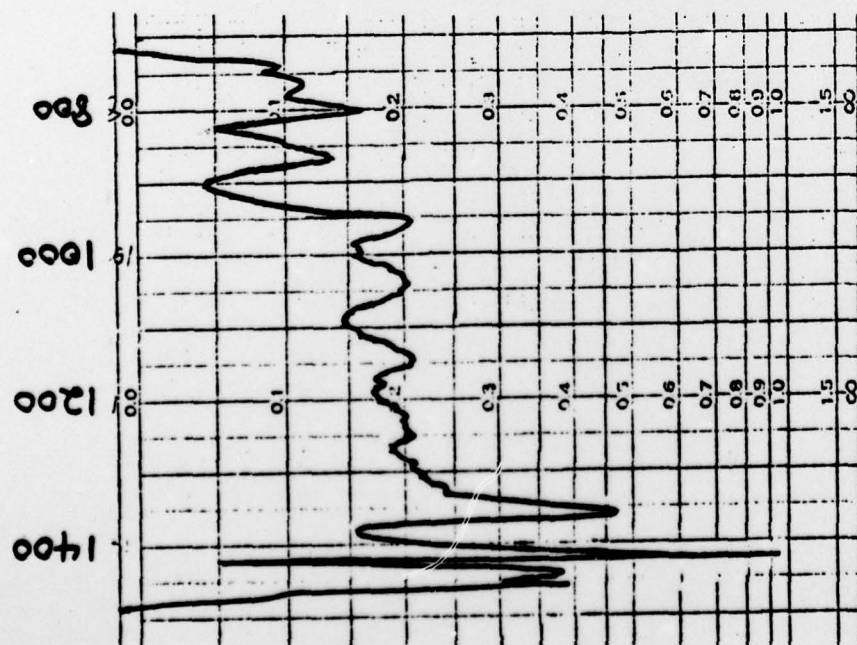
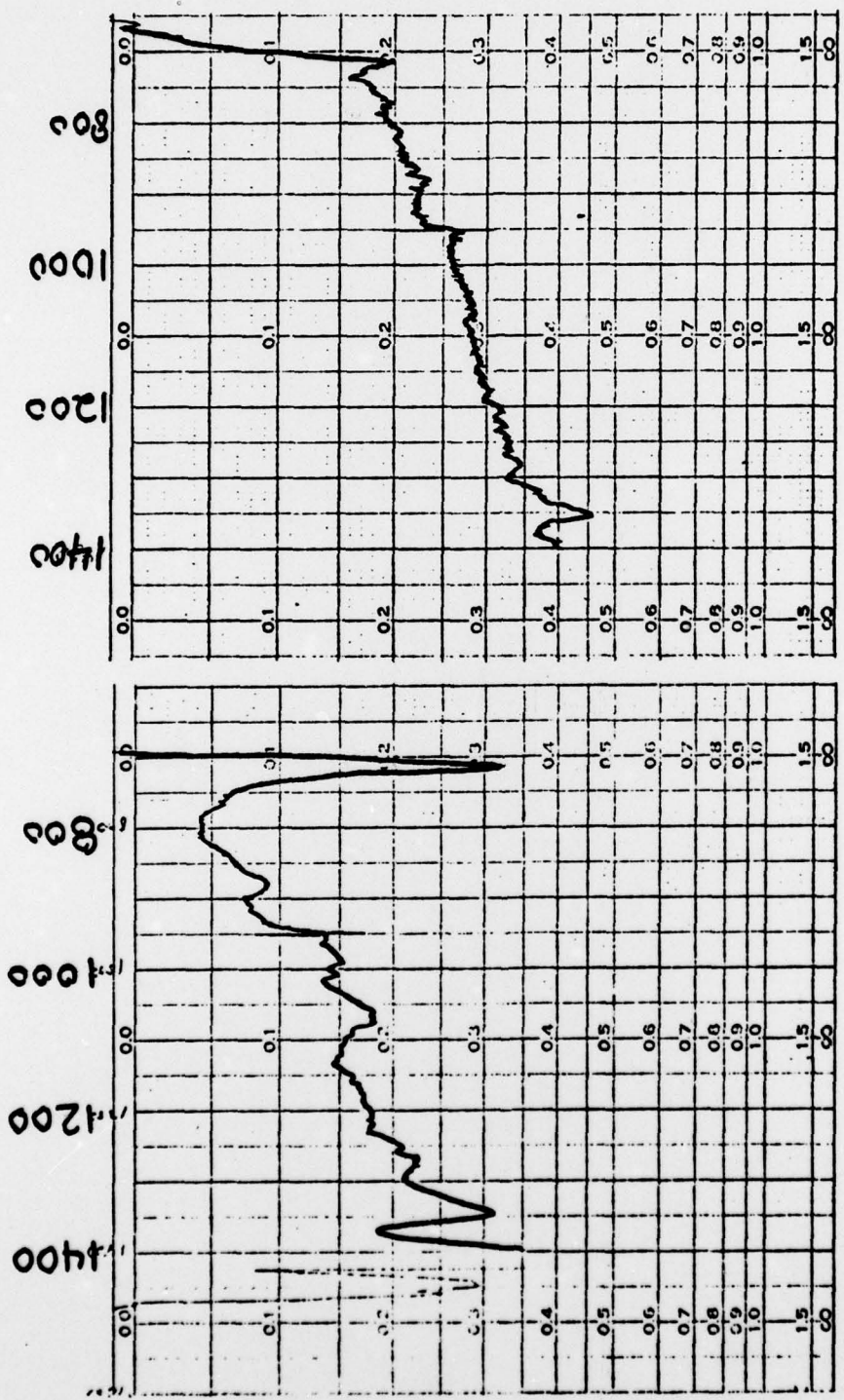


FIGURE 35

Comparison of Low and High Pressure Spectra of
N-1 Naphthene Fluid in the Diamond Cell at Ambient Temperature



LOW PRESSURE
SYN-PAR 064-1

HIGH PRESSURE
SYN-PAR 064-2

FIGURE 36

Comparison of Low and High Pressure Spectra of
XRM Synthetic Paraffin in the Diamond Cell at Ambient Temperature

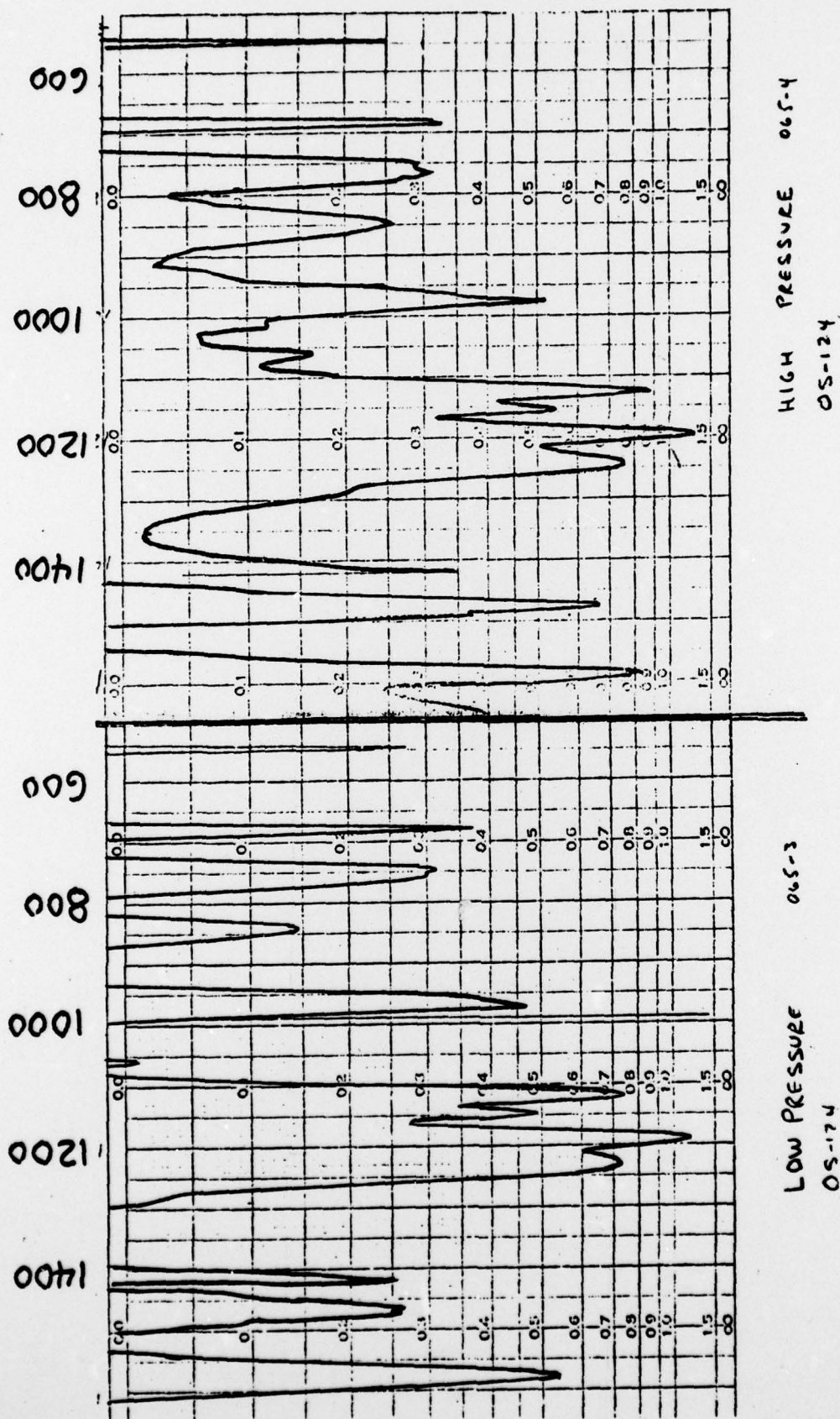
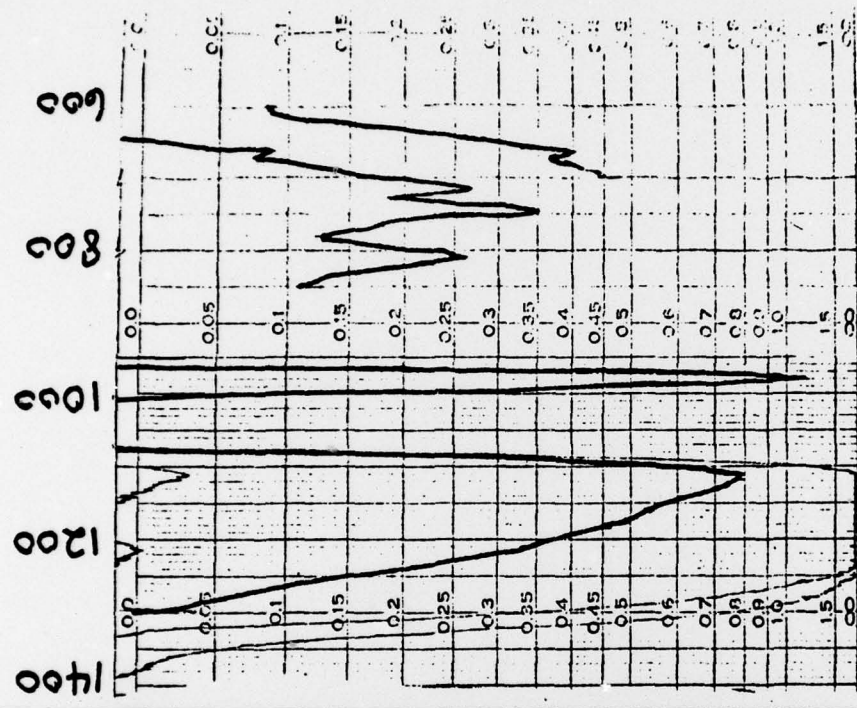


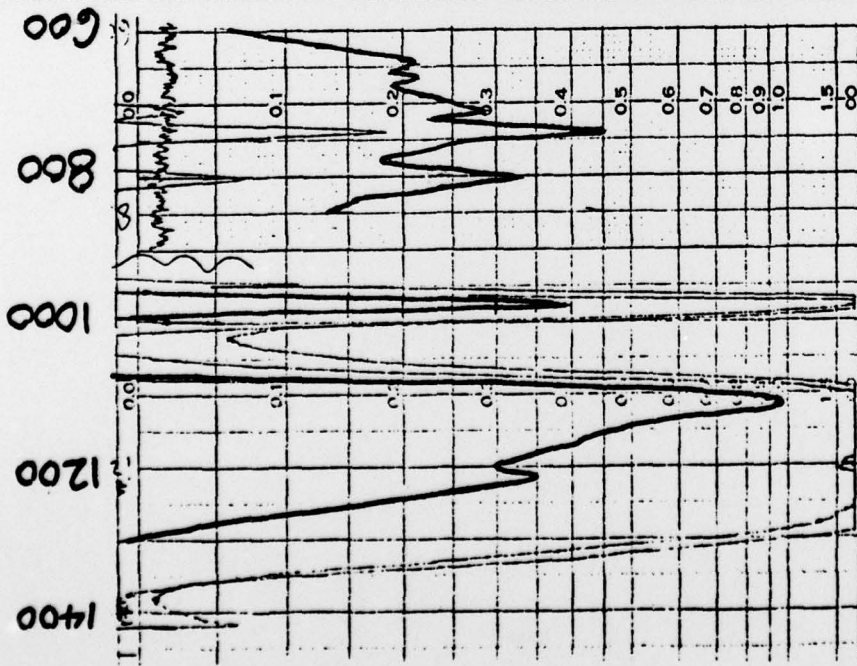
FIGURE 37

Comparison of Low and High Pressure Spectra of
5p4E Polyphenyl Ether in the Diamond Cell at Ambient Temperature



LOW PRESSURE

KRYTOX 066-1



HIGH PRESSURE

KRYTOX 066-2

FIGURE 38

Comparison of Low and High Pressure Spectra of
Krytox in the Diamond Cell at Ambient Temperature

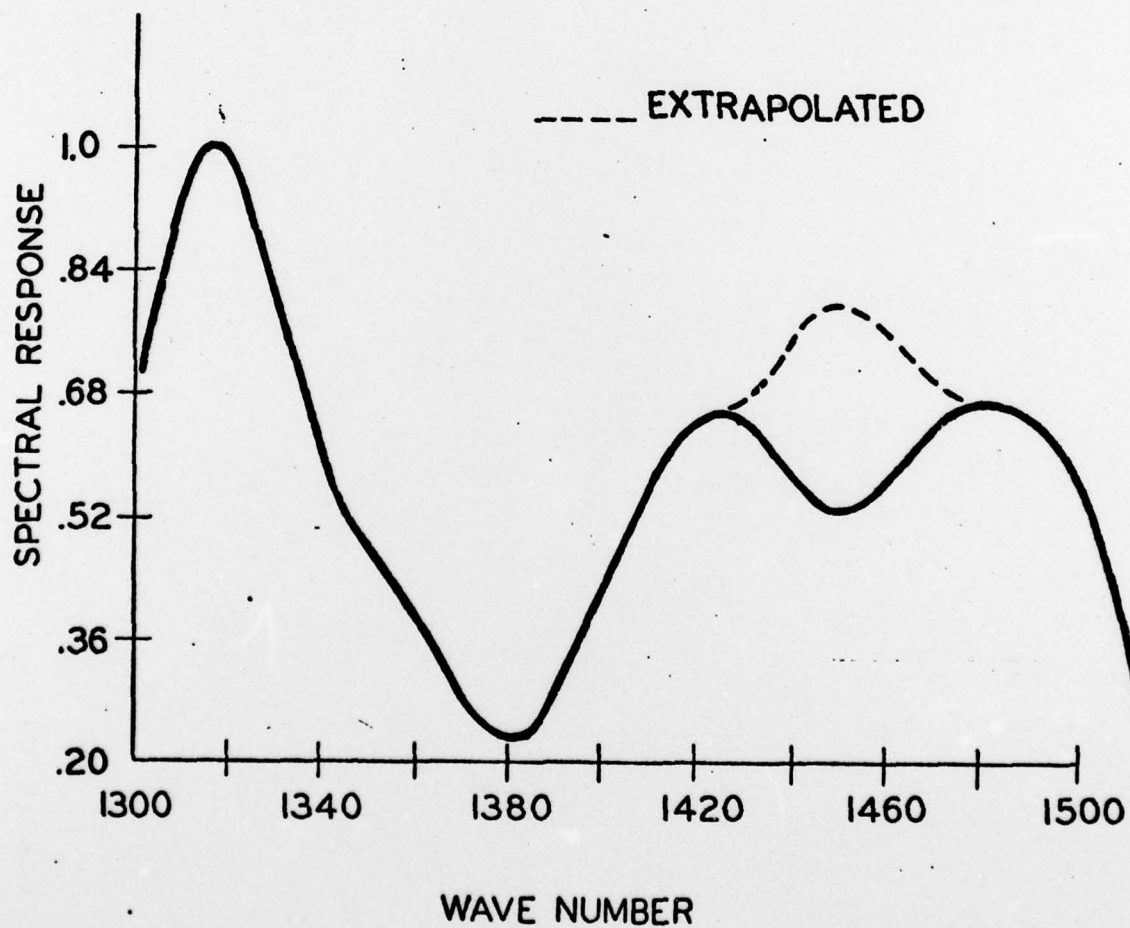


FIGURE 39

Emission Spectrum of N-1 Hydrocarbon Lubricant from
an EHD Operating Bearing Contact Showing Peak Inversion, No polarization used

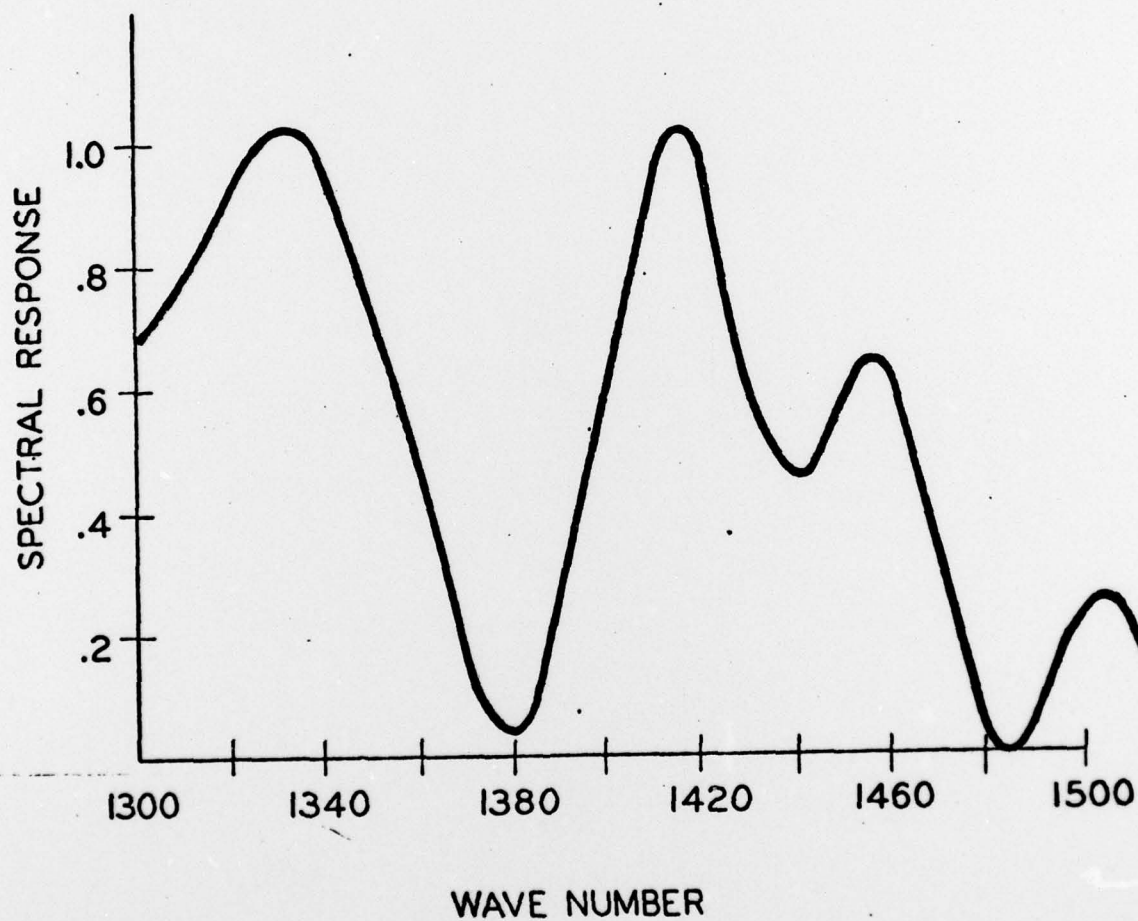


FIGURE 40

Emission Spectrum of N-1 Hydrocarbon Lubricant from
an EHD Operating Bearing Contact Showing Peak Inversion, Polarization used
in the Vertical (Conjunction Line) Position

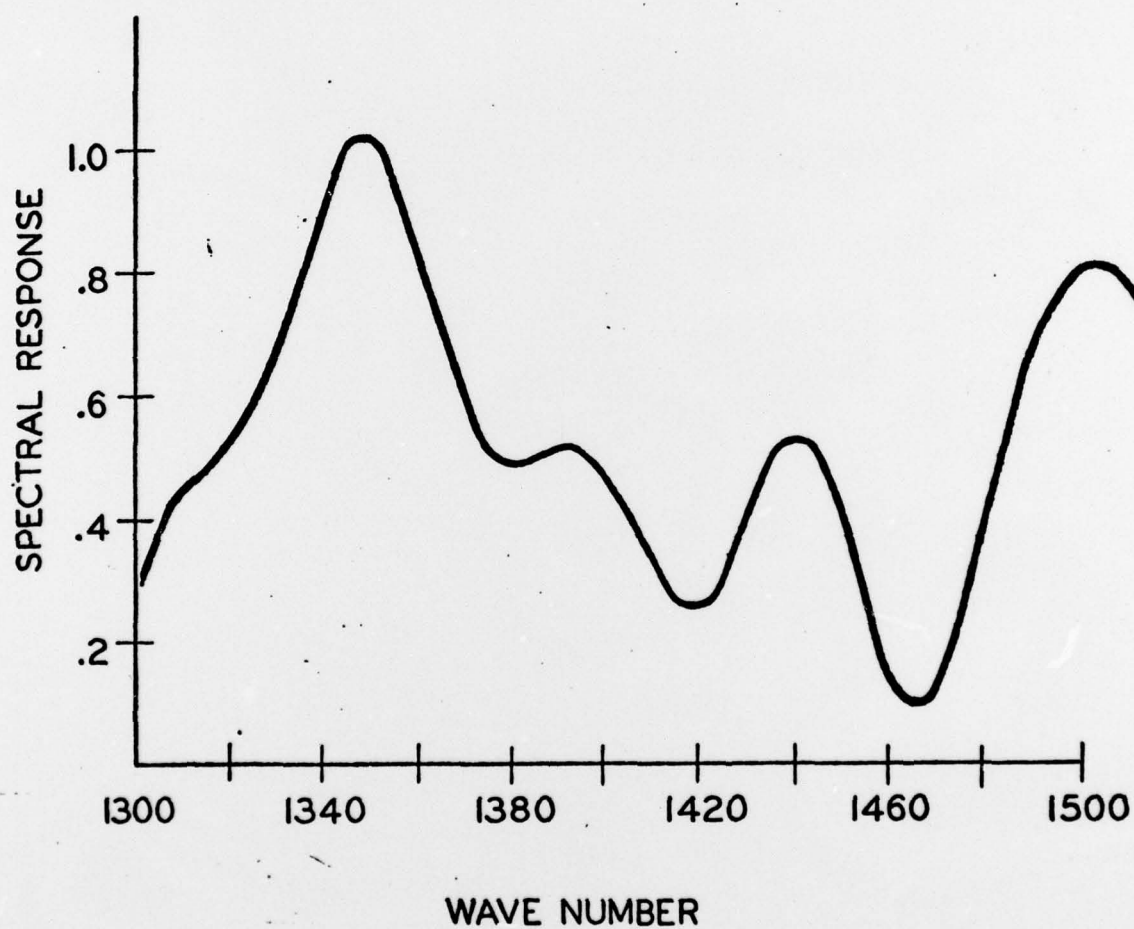
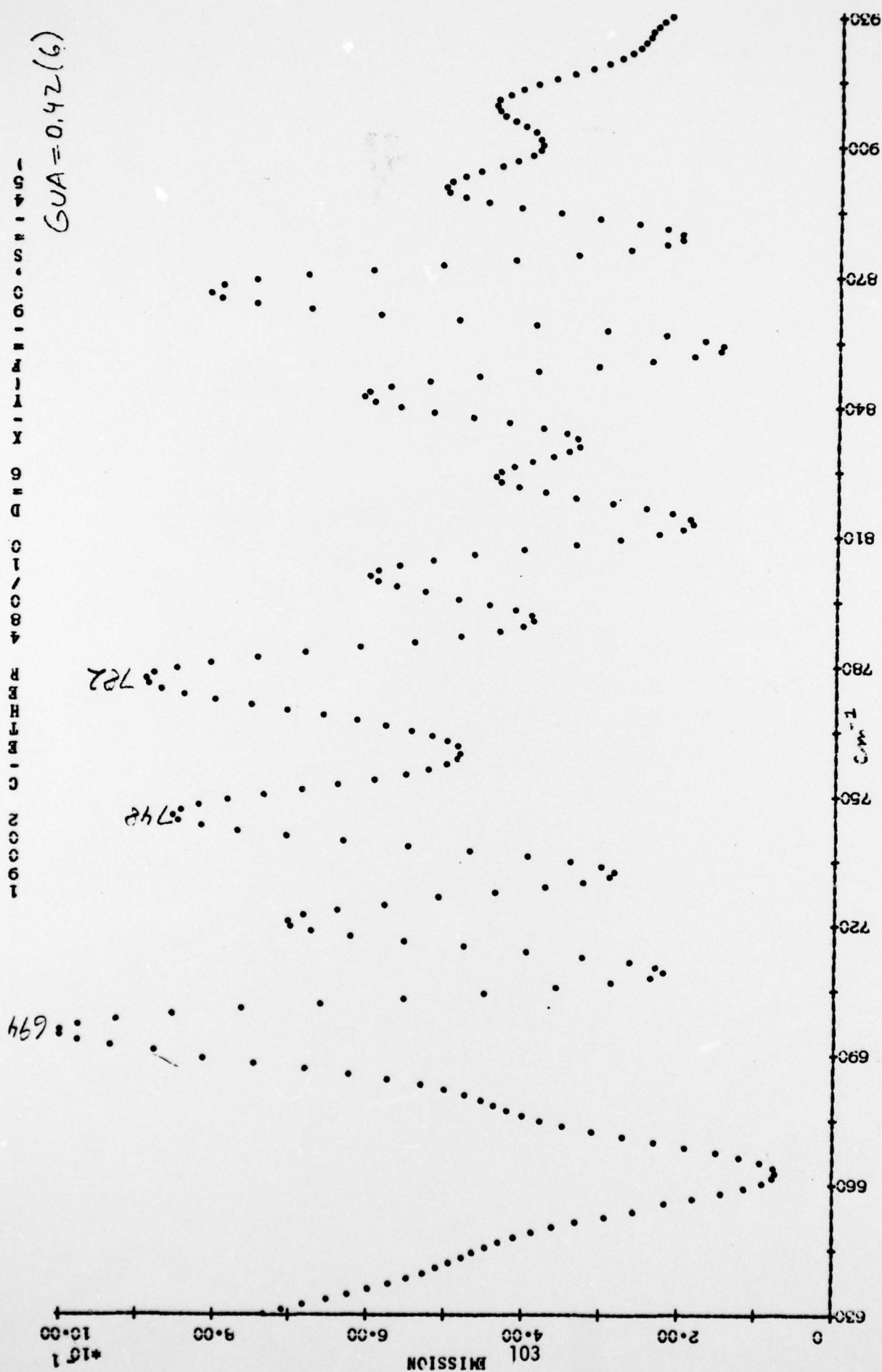


FIGURE 41

Emission Spectrum of N-1 Hydrocarbon Lubricant from
an EHD Operating Bearing Contact Showing Peak Inversion, Polarization used
in the Horizontal (across Conjunction Line) Position

$$GVA = 0.42(6)$$


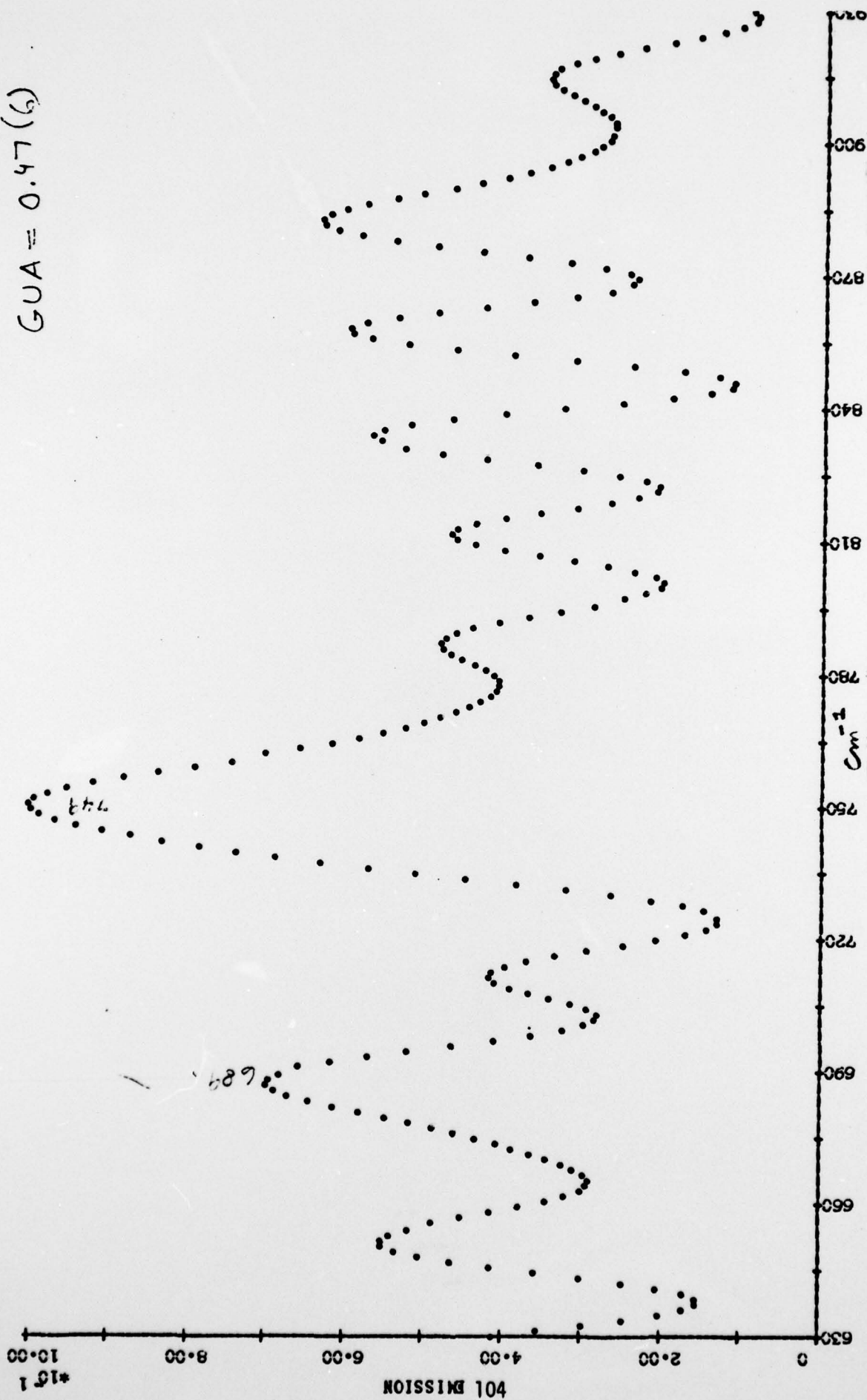
$$GUA = 0.47 (G)$$


FIGURE 43

Emission Spectrum from the Exit Portion of the Hertzian Contact of an Operating Bearing for a Substituted Aromatic Fluid

10000 5000 3000 2000 1500 1000 500 200 100 50 20 10 5 2 1

$GUA = 0.32(6)$

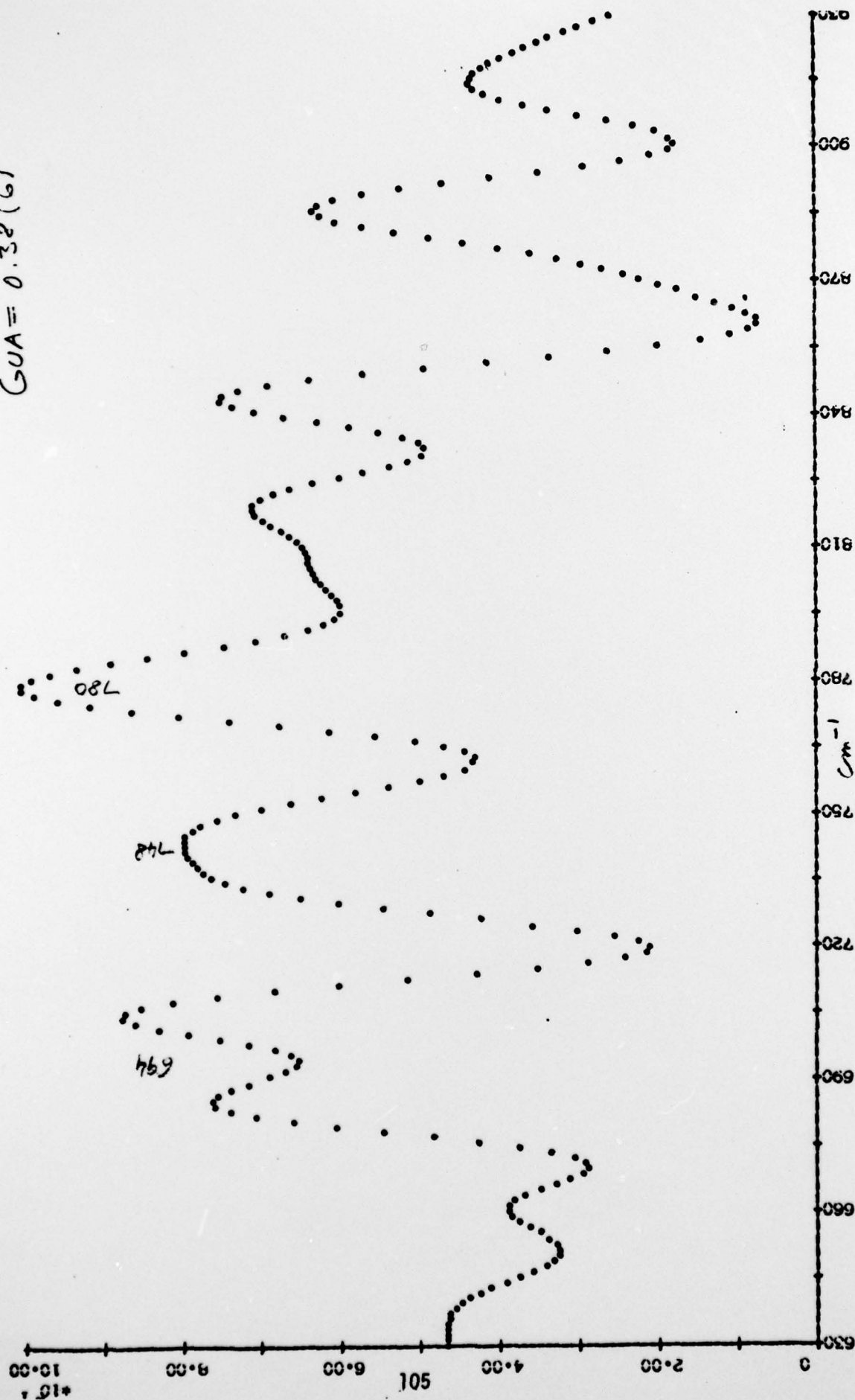


FIGURE 44

Emission Spectrum from the Inlet Portion of the Hertzian Contact of an Operating Bearing for a Substituted Aromatic Fluid

NUM 01 ROIRP I X X CDA CN/084 RHHM.C 40091

GUA = 0.101 (7)

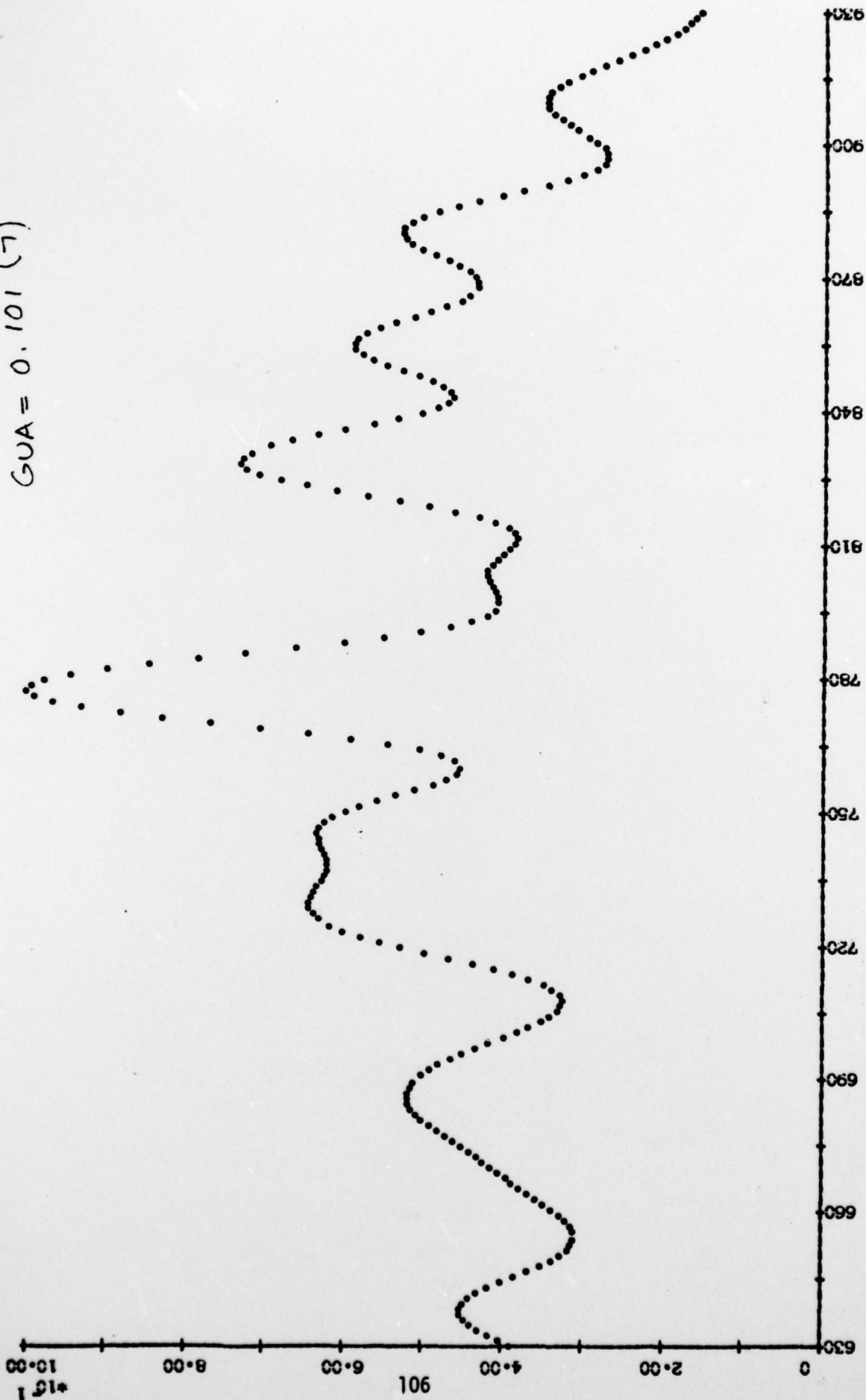


FIGURE 45

Emission Spectrum from the Central Portion of the
Hertzian Contact of an Operating Bearing for a Substituted
Aromatic Fluid under twice the Load as Used for Figure 42

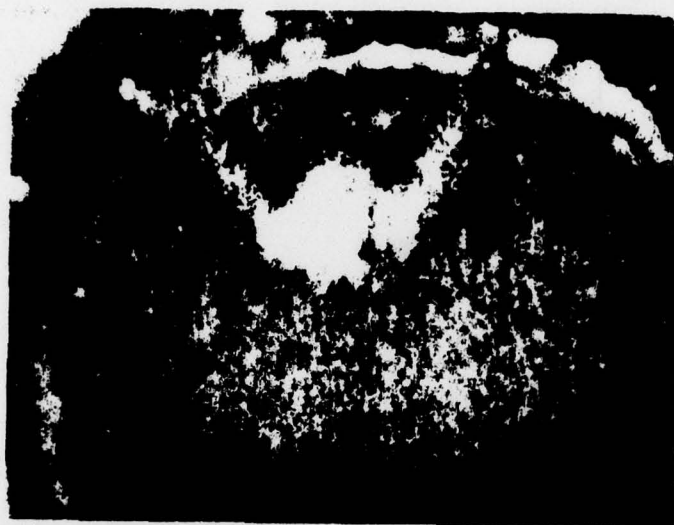


FIGURE 46

Photomicrograph of Friction Polymer